

Importance of the Electron-Phonon Interaction with the Forward Scattering Peak for Superconducting Pairing in Cuprates

Miodrag L. Kulić

*J. W. Goethe-Universität Frankfurt am Main, Theoretische Physik,
Max-von-Laue-Strasse 1, 60438 Frankfurt am Main, Germany*

(Dated: July 23, 2018)

We discuss first some basic experimental facts related to ARPES, tunnelling, optics ad neutron scattering measurements. They give evidence for the relevance of the electron-phonon interaction (EPI) in pairing mechanism of HTSC cuprates. A controllable and very efficient theory for strong correlations and their effects on EPI is discussed. The theory is based on the $1/N$ expansion method in the t-J model without using slave bosons (or fermions). The remarkable prediction is that strong correlations renormalize EPI and other charge-fluctuation properties (by including nonmagnetic impurity scattering) in such a way that the forward scattering peak (FSP) appears in the corresponding effective interactions. The existence of FSP in EPI is additionally supported by the weakly screened Madelung interaction in the ionic-metallic structure of layered cuprates. Pronounced FSP in EPI of HTSC cuprates reconciles many puzzling results, which could not be explained by the old theory with the momentum independent EPI. For instance, EPI with FSP gives that the couplings in the s- and d-wave pairing channel are of the same magnitude near and below the optimal hole doping. It is shown that FSP in the impurity scattering potential is responsible for robustness of d-wave pairing in cuprates with nonmagnetic impurities and other defects. The ARPES kink and the isotope effect in the nodal and anti-nodal points, as well as the collapse of the elastic nonmagnetic impurity scattering in the superconducting state, are explained by this theory in a consistent way. The proposed theory also explains why the nodal kink is not-shifted in the superconducting state while the anti-nodal kink is shifted by the maximal superconducting gap. It turns out that in systems with FSP in EPI besides the classical phase fluctuations there are also internal fluctuations of Cooper pairs. The latter effect is pronounced in systems with long-ranged pairing forces, thus giving rise to an additional contribution to the pseudogap behavior.

PACS numbers:

I. INTRODUCTION

In this year the physics community celebrate twenty years from the remarkable discovery of high-temperature superconductors (HTSC) by G. Bednorz and K. A. Müller. However, all of us are aware of the fact that our friend and teacher Vitalii Lazarevich Ginzburg [1] is the pioneer in this fascinating field. He was not only the first who raised this question but he also actively advocated the possibility of the room-temperature superconductors (RTSC) [2]. Moreover, he has proposed the well known excitonic mechanism of pairing in quasi 2-D structures, which, in fact, was a precursor for other studies of this important subject. Finally, HTSC were discovered in 1986 by Bednorz and Müller in rather exotic quasi-2D HTSC materials - cuprates [3]. A number of interesting approaches for reaching high critical temperature T_c were elaborated in the famous VL superconductivity-group in the I. E. Tamm department at the P. N. Lebedev Institute in Moscow. (VL is the popular name of V. L. Ginzburg - see [1].) One of the most important results, which came from the "theoretical kitchen" of the VL group, was related to a possible limit of T_c due to the electron-phonon interaction (EPI).

Regrettably, study of the pairing mechanism in cuprate superconductors was significantly influenced by prejudices related to EPI. One prejudice in the search of HTSC materials is related to the question of the up-

per limit of T_c within the phonon mechanism of pairing [4]. By assuming that the *total macroscopic longitudinal dielectric function* $\varepsilon_{tot}(\mathbf{k}, \omega = 0)$ is positive for all \mathbf{k} ($\varepsilon_{tot}(\mathbf{k}, \omega = 0) > 0$, \mathbf{k} is the momentum and ω is the frequency) the authors in Ref. [4] came to a pessimistic conclusion that EPI is able to produce only a moderate $T_c < 10$ K, since as they predicted the EPI coupling constant is limited to its maximal value $\lambda_{EPI}^{\max} < 0.5$. However, a number of experiments contradicted this statement, since the large coupling constant $\lambda_{EPI} > 1$ is realized in a number of materials. For instance $\lambda_{EPI} \approx 2.5$ in the $PbBi$ alloy (although T_c is not large), and $\lambda_{EPI} \approx 1$ with $T_c \approx 40$ K in MgB_2 . There are a number of other systems with $\lambda_{EPI} > 0.5$, such as A_3C_{60} with $\lambda_{EPI} \approx 1$ and $T_c \approx 40$ K, etc. The correct answer to this question was given by D. A. Kirzhnitz [5], a remarkable man and physicist from the Ginzburg group, who has shown that thermodynamic and lattice stability do not exclude the possibility that $\varepsilon_{tot}(\mathbf{k}, \omega = 0) < 0$. In fact a negative value of $\varepsilon_{tot}(\mathbf{k}, \omega = 0)$ is realized in a large portion of the Brillouin zone in most superconductors [6]. This important result means that the dielectric function ε_{tot} does not limit T_c in the phonon mechanism of pairing - see more in [2], [6], [7] and [8].

Concerning HTSC in cuprates one of the central questions is - what is the pairing mechanism in these materials? In the last twenty years, the scientific community was overwhelmed by all kinds of (im)possible proposed

pairing mechanisms, most of which are hardly verifiable, if at all. This trend is still continuing nowadays (although with smaller slope), in spite of the fact that the accumulated experimental results eliminate all but few. A somehow similar situation happened also in experimental physics of HTSC cuprates, where a whole spectrum of possible and impossible values of some (for pairing mechanism) relevant quantities was reported. As illustration the reader can look at (critical) analysis of experimental situation in optics done by Ivan Božović [9] - especially of the measurements of the plasma frequency ω_{pl} . The dispersion in the reported value of ω_{pl} , from 0.06 to 25 eV - almost three orders of magnitude - tells us that in some periods the science suffers from the lack of rigorousness and objectiveness.

By the end of the twenty-years era in studying HTSC materials, more or less three main directions in search for the pairing mechanism have crystallized. The *first approach*, based on *strong correlations*, was first proposed by P. W. Anderson in 1987 and followed by many others. The starting point is that the physics of cuprates is the physics of doped Mott insulator [10], which is supposed to be well described by the single-band Hubbard model (or its extensions). The promoters of this approach believe that strong electronic correlations alone are the driving mechanism behind the whole phase diagram of these materials - the antiferromagnetic phase, metallic and superconducting one. Since strong correlations belong to the strong coupling problem it is understandable that even nowadays, exactly 20 years after the discovery of HTSC, there is still no reliable theory of strong correlations in HTSC materials which is capable to describe both the normal and the superconducting state.

The *second approach* is based on pronounced *antiferromagnetic spin fluctuations* which are present in cuprates especially at very low doping - we call it the spin-fluctuation interaction approach (SFI) [12]. Later on we will argue that this phenomenological approach - which can be theoretically justified in the very weak coupling limit only - is based on two ingredients which are more in conflict than in agreement with the existing experimental results. First, the spin-fluctuation spectrum taken from the (low-frequency) NMR measurements differs from the one obtained in neutron scattering measurements - see [7], [11]. The latter is shifted to much higher energies. Second, in order to explain large T_c within the SFI approach, one has to assume an unrealistically large spin-fluctuation coupling constant $g_{sf} \approx 0.6$ eV, which implies that, the pairing coupling constant is also unrealistically large $\lambda_{sf}(\sim g_{sf}^2) > 2$. Our statement is confirmed by a number arguments. Let us mention here some of them, while others are given in Sec. II. A. For instance, such a large λ_{sf} gives much larger resistivity than the measured one. Also, g_{sf} extracted from ARPES and neutron scattering measurements is much smaller, i.e. $g_{sf} \approx 0.2$ eV what gives rather small pairing constant $\lambda_{sf} < 0.3$, see Sec. II A.

Let us stress that both of the above approaches are

based either on the Hubbard model or on its (more popular) derivative, the t-J model. Here, the central question is - do these two models show superconductivity at high temperature? The Monte-Carlo calculations on the 2D repulsive ($U > 0$) Hubbard model give *no evidence for superconductivity with a large critical temperature* [13]. On the other hand, there is a strong tendency for superconductivity (either BCS like or Berezinskii-Kosterlitz-Touless like in 2D systems) in the attractive ($U < 0$) Hubbard model for the same intensity of U . Recent numerical calculations in the t-J model [14] have shown that *there is no superconductivity in the t-J model* at temperatures characteristic for cuprates. If it exists (at all!) T_c must be very low ~ 1 K. These numerical results tells us that the lack of HTSC in the repulsive ($U > 0$) single-band Hubbard model, as well as in the t-J model, is not due to 2D-fluctuations (which at finite T suppress superconductivity with phase coherence) but it is due to the inherent ineffectiveness of strong correlations and spin fluctuations to produce HTSC in cuprates. This means also that the simple single-band Hubbard and the t-J model are insufficient to explain the pairing mechanism in cuprates, and some other ingredients must be included. Since EPI is strong in oxides it is physically plausible and justified that it should be accounted for. As we shall argue later on, the experimental support for the importance of EPI comes from optics, tunnelling, and especially from recent ARPES measurements.

Regarding the EPI one can ask whether it contributes significantly to d-wave pairing in cuprates? Surprisingly, in spite of a number of experiments in favor of EPI many of researchers believe that EPI is irrelevant and that the pairing mechanism is due to SFI and strong correlations alone - see [12]. This belief is mainly based on: (i) an incorrect stability criterion, discussed briefly above, and (ii) the fact that in cuprates d-wave pairing ($\Delta(\mathbf{k}, \omega) \approx \Delta_s(k, \omega) + \Delta_d(\omega)(\cos k_x - \cos k_y)$ with $\Delta_s < 0.1\Delta_d$) is realized with gapless regions on the Fermi surface [15], which is incompatible with EPI. So, the EPI mechanism of pairing in cuprates has been abandoned mainly because of these two (incorrect) prejudices.

In fact, there is rich experimental evidence that EPI is sufficiently large in cuprates in order to produce HTSC, i.e. the EPI coupling constant is $\lambda \gtrsim 1$. Let us quote some of them: (1) The superconductivity-induced *phonon renormalization* [7] is much larger in cuprates than in *LTSC* superconductors. This is partially due to the larger value of Δ/E_F in HTSC than in *LTSC*. (2) The *line-shape* in the phonon Raman scattering is very asymmetric (Fano line), which points to a substantial interaction of lattice vibrations with some quasiparticle continuum (electronic liquid). For instance, the phonon Raman measurements [7] on $HgBa_2Ca_3Cu_4O_{10+x}$ at $T < T_c$ give very large softening (self-energy effects) of the A_{1g} phonons with frequencies 240 and 390 cm^{-1} by 6 % and 18 %, respectively. At the same time there is a dramatic increase of the line-width immediately below T_c , while above T_c the line-shape is strongly asym-

metric. A substantial phonon renormalization was obtained in $(Cu, C)Ba_2Ca_3Cu_4O_{10+x}$ [7]. (3) The *large isotope coefficients* ($\alpha_O > 0.4$) in $YBCO$ away from the optimal doping [16] and $\alpha_O \approx 0.15 - 0.2$ in the optimally doped $La_{1.85}Sr_{0.15}CuO_4$. At the same time one has $\alpha_O \approx \alpha_{Cu}$ making $\alpha \approx 0.25 - 0.3$. This result tell us that other, besides O, ionic vibrations participate in pairing. (4) Very important evidence that EPI plays an important role in pairing comes from *tunnelling spectra* in cuprates, where the phonon-related features have been clearly seen in the $I - V$ characteristics [17]. (5) The *penetration depth* in the a-b plane of $YBCO$ is significantly increased by the substitution $O^{16} \rightarrow O^{18}$, i.e. $(\Delta\lambda_{ab}/\lambda_{ab}) = (^{18}\lambda_{ab} - ^{16}\lambda_{ab})/^{16}\lambda_{ab} = 2.8\%$ at 4 K [19]. Since $\lambda_{ab} \sim m^*$, the latter result, if confirmed, might be due to a nonadiabatic increase of the effective mass m^* . (6) The *breakthrough* in the physics of cuprates came from the recent ARPES measurements [20], [21], [23]. The latter show a number of features typical for systems with pronounced EPI and peculiar Coulomb interaction. For instance, there is a *kink* in the quasiparticle spectrum in the *nodal point* at characteristic (oxygen) phonon frequencies in the normal and superconducting state. The ARPES measurements indicate that the EPI coupling constant is of the order one, $\lambda \approx \lambda_{EPI} \sim 1$ in the nodal direction, and $\lambda_{EPI} \sim 2$ near the antinodal point. The authors of Ref. [23] even claim that they are able to resolve the fine structure in $Re\Sigma(\mathbf{k}, \omega)$ in ARPES, what results in the Eliashberg spectral function with a number of peaks at the characteristic phonon frequencies. The imaginary part of the ARPES self energy, $Im\Sigma(k, \omega)$, has a *knee-like structure* around $\omega_{ph} \sim 70\text{ meV}$, which is typical for systems with pronounced EPI [20], [21], [23]. Here, ω_{ph} is the characteristic maximal phonon energy. For $\omega > \omega_{ph}$ one has $Im\Sigma(k, \omega) \sim -\lambda_c\omega$, which is certainly due to Coulomb interaction (by including SFI too) with rather moderate $\lambda_c \lesssim 0.4$. Recent ARPES spectra in the anti-nodal point give evidence for the kink at 40 meV , while the spectral function shows a peak-dip-hump structure which is characteristic for systems with strong EPI ($\lambda_{EPI} \gtrsim 1$). Very recent ARPES spectra [24] show a *pronounced isotope effect* in the real part of the quasiparticle self-energy. These results give clear evidence that the EPI is appreciate and strongly involved in pairing and quasiparticle scattering.

On the *theoretical side* there are self-consistent *LDA* band-structure calculations which (in spite of their shortcomings) give a rather large bare EPI coupling constant $\lambda \sim 1.5$ in $La_{1.85}Sr_{0.15}CuO_4$ [25]. The tight-binding calculations of EPI in $YBCO$ gave $\lambda \approx 2$ and $T_c \approx 90\text{ K}$ [26]. The *nonadiabatic effects* due to poor metallic screening along the *c*-axis, not accounted for in [25], may additionally increase λ as pointed first in [27]. All these facts are in favor of a substantial EPI in cuprates. However, if the properties of the normal and superconducting state in cuprates are interpreted in terms of the standard EPI theory - which is well established in low-temperature superconductors (*LTSC*) - some puzzles arise. One of

them is related to the normal-state resistivity in optimally doped cuprates, which indicates that the transport coupling constant λ_{tr} is rather small, i.e. $\lambda_{tr} < \lambda/3$ according to ARPES and tunnelling measurements [7], [11]. For instance, the combined resistivity and low frequency conductivity (Drude part) measurements give $\lambda_{tr} \approx 0.3$ if the plasma frequency takes the value $\omega_{pl} \sim 1\text{ eV}$ - see more below. So, if one assumes that $\lambda_{tr} \approx \lambda$, which is the case in most *LTSC*, such a small λ can not give large T_c ($\approx 100\text{ K}$). This implies two possibilities: (a) $\lambda_{tr} \ll \lambda$ and the pairing is due to EPI, or (b) $\lambda_{tr} \simeq \lambda$ but EPI is responsible for pairing by virtue of some peculiarities in the equations describing superconductivity - for instance because of non-Migdal vertex corrections. Related to this dilemma, it is worth mentioning that a similar puzzling situation ($\lambda_{tr} \ll \lambda$) is realized in $Ba_xK_{1-x}BiO_3$ (with $T_c \simeq 30\text{ K}$), where optical measurements give $\lambda_{tr} \approx 0.1 - 0.3$ [28], while tunnelling measurements [29] give $\lambda \sim 1$. Note, in $Ba_xK_{1-x}BiO_3$ there are no magnetic fluctuations (or magnetic order) and no signs of strong electronic correlations. Therefore, EPI is favored as the pairing mechanism in $Ba_xK_{1-x}BiO_3$. It seems that in this compound long-range forces in conjunction with some nesting effects, may be responsible for this discrepancy.

According to the above discussion, the microscopic theory of EPI and pairing in cuprates must be able to explain the following three important facts: (1) why $\lambda_{tr} \ll \lambda$; (2) why d-wave pairing is realized in the presence of strong EPI; (3) why is d-wave pairing robust in presence of non-magnetic impurities and defects? Here we shall argue that the theory which is based on the existence of the *forward scattering peak* (FSP) in EPI can account for both facts. We point out that d-wave pairing in cuprates is very *robust in the presence of nonmagnetic impurities* contrary to the prediction of the standard theory. We shall argue in what follows that this robustness is again due to strong correlations which give rise also to FSP in the impurity scattering [7], [11]. The FSP in EPI and in non-magnetic impurity scattering can be due to: (i) strong electronic correlations; (ii) the presence of long-range Madelung potential in EPI, which is poorly screened for phonons vibrating along the *c*-axis; (iii) out of plain impurities and defects which are poorly screened. The concept of FSP in EPI and nonmagnetic impurity scattering potential due to strong correlations was for the first time put forward in [30], [31], [32]. This approach, which was elaborated further by the present author and his collaborators, see more in [7], [11], is essential to explain ARPES in cuprates.

This paper is organized as follows. In Sec. II we discuss direct and indirect experimental evidence for the importance of the EPI in cuprates. The recent ARPES results are discussed in more detail. Section III is devoted to the *systematic and controllable theory* of strong correlations without using the slave boson (or fermion) technique. This theory treats strong correlations in terms of Hubbard operators $X^{\alpha\beta}$ - we call it the *X-method* - which

describe the motion of the composite electrons. The latter takes care that the double occupancy at a given lattice site is excluded. The central question in strongly correlated systems is - *how to calculate the coherent part in the quasiparticle dynamics?* This was achieved within the *X-method* by using a systematic and controllable $1/N$ expansion. In Sec. IV we discuss the renormalization of EPI by strong correlations. The $1/N$ expansion indicates that strong correlations lead to FSP in EPI. We stress that this result is straightforward in the X-method, while in the slave-boson method until now there have been no reliable calculations of EPI. We point out that the X-method predicts in the t-J model, that the EPI coupling becomes long-ranged in the presence of strong correlations. As the result of this specific renormalization, the EPI coupling constant in the d-channel reaches the value of that in the s-channel for some optimal doping and below it. Furthermore, in conjunction with the residual Coulomb interaction this gives rise to d-wave pairing, since the residual Coulomb interaction is much stronger in the s-channel than in the d-channel. It is also shown that FSP appears in the nonmagnetic impurity scattering giving rise to robustness of d-wave pairing in cuprates. Section V applies the proposed theory to explanation of ARPES experiments, of the d-wave robustness in presence of impurities, of transport properties, etc. The problem of the pseudogap is discussed in Sec. VI from the point of view of the proposed theory. It turns out that the long-range EPI force gives rise to internal fluctuations of Cooper pairs, which together with phase fluctuations reduce strongly the mean-field critical temperatures.

There are numerous experimental indications on the nanoscale inhomogeneities of HTSC oxides, for instance recent STM experiments [18]. In that case the superconducting order parameter is inhomogeneous, i.e. $\Delta(\mathbf{k}, \mathbf{R})$ where \mathbf{R} is the center of mass of Cooper pairs. In this review we shall not discuss this effects, which are in our opinion play secondary role in pairing mechanism. By understanding what is going on in homogeneous systems we have a starting basis to study effects of inhomogeneities.

II. EXPERIMENTAL RESULTS IN FAVOR OF THE EPI

The experimental situation which is related to the quasiparticle scattering in the normal and superconducting state of cuprates is extensively analyzed in a number of reviews [7], [11]. Here we summarize briefly some experiments which are important for the microscopic theory of pairing in cuprates and which indicates importance of EPI in the quasiparticle scattering. Before this discussion let us analyze briefly interplay of EPI and SFI in the pairing mechanism and their relative strength by taking into account three important experimental facts: (1) T_c in cuprates is high, i.e. $T_c^{\max} \sim 160$ K; (2)

the pairing in cuprates is d-wave like, i.e. $\Delta(\mathbf{k}, \omega) \approx \Delta_s(k, \omega) + \Delta_d(\omega)(\cos k_x - \cos k_y)$ with $\Delta_s < 0.1\Delta_d$, and (3) the EPI coupling constant is rather large, $\lambda \approx 1 - 2$. Let us assume that d-wave pairing in cuprates is due to some non-phononic mechanism, for instance due to SFI. If EPI in cuprates would isotropic like in LTSC materials then it would be very detrimental for d-wave pairing as it is shown in [33] by numerical studies of interplay of SFI and EPI by the Eliashberg theory. Here we shall elucidate this important problem in a physically plausible and semi-quantitative way. In the case of dominating *isotropic* EPI in normal state, then near T_c the linearized Eliashberg equations have an approximative form

$$Z(\omega)\Delta(\mathbf{k}, \omega) = \sum_{\mathbf{q}} \int_0^{\omega_{\max}} \frac{d\Omega}{\Omega} V(\mathbf{k}, \mathbf{q}, \Omega) \Delta(\mathbf{q}, \omega) \tanh \frac{\xi(\mathbf{q})}{2T_c} \\ Z(\omega) \approx 1 + i\Gamma_{ep}. \quad (1)$$

For pure d-wave pairing one has $V(\mathbf{k}, \mathbf{q}, \omega) = V(\omega)(\cos k_x - \cos k_y)(\cos q_x - \cos q_y)$ and $\Delta(\mathbf{k}, \omega) = \Delta(\omega)(\cos k_x - \cos k_y)$ what gives the equation for T_c

$$\ln \frac{T_c}{T_{c0}} = \Psi\left(\frac{1}{2}\right) - \Psi\left(\frac{1}{2} + \frac{\Gamma_{ep}}{2\pi T_c}\right). \quad (2)$$

Here, T_{c0} is the bare critical temperature due to the SFI mechanism and Ψ is the di-gamma function. At temperatures near T_c one has $\Gamma_{ep} \approx 2\pi\lambda_{ep}T$ and the solution of Eq. (2) is

$$T_c \approx T_{c0}e^{-\lambda_{ep}}.$$

The latter result means that when $\lambda_{ep} = 1 - 2$ and $T_c^{\max} \sim 160$ K the bare T_{c0} due to SFI must be very large, i.e. $T_{c0} = (400 - 1100)$ K, what is highly unrealistic. However, this result, together with d-wave pairing in cuprates, imply that EPI in these materials must be *strongly dependent on the momentum transfer*, as it was first argued in [30]. Only in that case is EPI conform with d-wave pairing, either as its main cause or as a supporter of non-phononic mechanism such as SFI. In the following Sections we shall argue that the strongly momentum dependent EPI is the main player in cuprates providing strength of the pairing mechanism, while the residual Coulomb interaction and SFI, although weaker, trigger it to d-wave pairing.

A. Magnetic neutron scattering and spin fluctuation spectral function

In a number of papers the experimental results for the pronounced imaginary part of the susceptibility $Im\chi(\mathbf{k}, k_z, \omega)$, at the AF wave vector $\mathbf{k} = \mathbf{Q} = (\pi, \pi)$, are interpreted as a support for SFI mechanism of pairing [12]. We briefly explain the *inadequacy* of such an interpretation.

(1) The breakthrough in understanding the role of spin-fluctuations came from magnetic neutron scattering experiments on $YBa_2Cu_3O_{6+x}$ by Bourges group [34]. They showed that the spectral function $Im\chi^{(odd)}(\mathbf{k}, \omega)$ (the odd part in the bilayer system) is strongly dependent on hole doping. By varying doping there is a huge reconstruction of $Im\chi^{(odd)}(\mathbf{Q}, \omega)$ in the frequency interval which is important for superconducting pairing, say $5 \text{ meV} < \omega < (60 - 70) \text{ meV}$. On the other hand, there is only a small variation of the T_c . For instance, in underdoped $YBa_2Cu_3O_{6.92}$ one has that $Im\chi^{(odd)}(\mathbf{Q}, \omega)$ (and $S(\mathbf{Q}) = \int_0^{70} d\omega Im\chi^{(odd)}(\mathbf{Q}, \omega) \sim \lambda_{SFI} \langle \omega \rangle$) is much larger than that in the near optimally doped $YBa_2Cu_3O_{6.97}$, i.e. $S_{6.92}(\mathbf{Q}) \gg S_{6.97}(\mathbf{Q})$, although the difference in their critical temperatures T_c is very small, i.e. $T_c = 91 \text{ K}$ in $YBa_2Cu_3O_{6.92}$ and $T_c = 92.5 \text{ K}$ in $YBa_2Cu_3O_{6.97}$. The reader can convince himself directly from the Fig 1(b). Such a large reconstruction of $Im\chi^{(odd)}(\mathbf{Q}, \omega)$ but a negligible change in T_c in YBCO is a strong argument against the SFI mechanism of pairing in cuprates. Furthermore, the *anti-correlation* between the NMR spectral function $I_{\mathbf{Q}} = \lim_{\omega \rightarrow 0} Im\chi(\mathbf{Q}, \omega)/\omega$ and T_c (where $T_c \sim 1/I_{\mathbf{Q}}^{\alpha}$, $\alpha > 0$) see [7] additionally disfavors SFI models of pairing [12], i.e. the strength of pairing interaction is little affected by SFI. These results also mean that in spite of pronounced spin fluctuations around \mathbf{Q} , the pairing quasiparticle self-energy is little affected by SFI.

(2) The next very serious argument against SFI pairing mechanism is the *smallness of coupling constant g_{sf}* . Namely, the real spin-fluctuation coupling constant extracted from experiments is rather small $g_{sf} \leq 0.2 \text{ eV}$, in contrast to the large value ($g_{sf}^{(MMP)} \sim 0.6 \text{ eV}$) assumed in the SFI theory by Pines and collaborators in order to get large $T_c \sim 100 \text{ K}$. (Note that the pairing coupling in the SFI theory is $\lambda_{sf} \sim g_{sf}^2$, and for the realistic value of $g_{sf} \leq 0.2 \text{ eV}$ it would produce $\lambda_{sf} \sim 0.2$ and very small $T_c \sim 1 \text{ K}$ - see more in [7].) The large value for $g_{sf}^{(MMP)}$ gives resistivity much larger than what is observed [7]. The upper limit for $g_{sf} (\leq 0.2 \text{ eV})$ is extracted: (i) from the width of the 41 meV magnetic resonance peak in the superconducting state [35]; (ii) from the small magnetic moment ($\mu < 0.1 \mu_B$) found in the antiferromagnetic state of LSCO and YBCO. based on this fact in [36] it was estimated $\lambda_{sf} \sim 0.2$; (iii) from ARPES experiments [21] that give $\lambda_{sf} \sim 0.3$ - see also [37].

(3) The *SFI* model is in some sense a phenomenological derivative of the t-J Hamiltonian. However, recently it was shown that *there is no superconductivity in the t-J model* at temperatures characteristic for cuprates [14]. If it exists (at all!) T_c must be very low.

(4) In the *superconducting state* the magnetic fluctuations are drastically changed, as expected for the singlet pairing state, since it induces a spin gap in magnetic excitation spectrum of s-wave superconductors - see Fig. 1(c). However, the spectrum in superconducting state of cuprates is more complex due to d-wave pairing

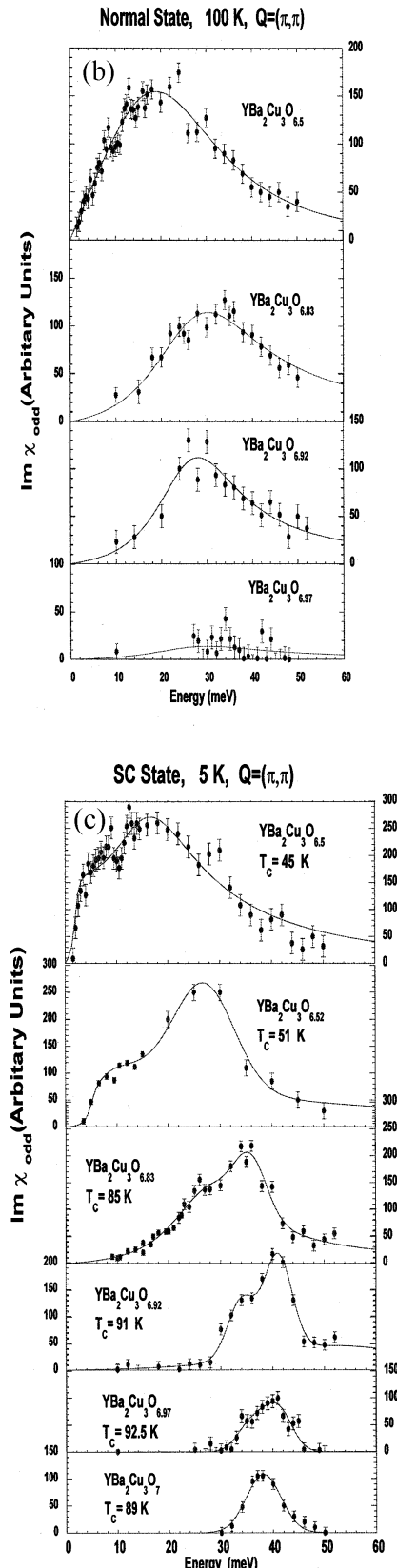


FIG. 1: Magnetic spectral function $Im\chi^{(-)}(\mathbf{k}, \omega)$: (b) for $YBa_2Cu_3O_{6+x}$ in the normal state at $T = 100 \text{ K}$ and at $Q = (\pi, \pi)$. 100 counts in the vertical scale corresponds to $\chi_{max}^{(-)} \approx 350\mu_B^2/\text{eV}$; (c) for $YBa_2Cu_3O_{6+x}$ in the superconducting state at $T = 5 \text{ K}$ and at $Q = (\pi, \pi)$. From Ref. [34].

and due to some specificities of the band structure. For instance, at $T < T_c$ the sharp peak in $Im\chi^{(odd)}(\mathbf{k}, \omega)$ is observed at $\omega_{reson} = 41$ meV and $\mathbf{k}_{2D} = (\pi/a, \pi/a)$ - the *resonance mode* - of the fully oxygenated (optimally doped) $YBa_2Cu_3O_{6+x}$ ($x \sim 1$, $T_c \approx 92$ K) - see the bottom of Fig. 1c. With increased doping, the resonance mode becomes sharper and moves to higher frequencies (scaling with T_c), while its height decreases [34] - see Fig. 1(c). In optimally doped cuprates the spectral weight of the resonance peak is only 2-5 % of the total weight. Recently there were speculations in the literature that d-wave superconductivity in cuprates might be due to the resonance mode! This claim is untenable, since this mode can not cause superconductivity simply because its intensity near T_c is vanishingly small, thus not affecting T_c at all. If the magnetic resonance would be the origin for superconductivity (and high T_c) the phase transition at T_c would be of the *first order*, contrary to the experiments showing that it is of the second order. In fact, the resonance mode is a *affected by superconductivity* but not its cause.

However, in spite of the fact that the strength of SFI is small, it can, together with other contributions of the residual Coulomb interaction, *trigger* d-wave pairing. However, the *strength of pairing is due to EPI with FSP* - see more below and in [7], [11].

B. Dynamic conductivity and resistivity

Optics measurements play very important role in studying the quasiparticle dynamics since this method probes bulk sample contrary to ARPES and tunnelling which probe tiny regions near the sample surface.

A diversity of the results on the reflectivity measurements in cuprates were reported in the past. The dynamic conductivity $\sigma(\omega)$, which is not a directly measured quantity but is derived from $R(\omega)$, was analyzed in terms of the quasiparticle self-energy $\Sigma(k, \omega)$ instead of the transport self-energy $\Sigma_{tr}(k, \omega)$. In fact $\Sigma(k, \omega) \neq \Sigma_{tr}(k, \omega)$ and this was the main reason for a number of erroneous conclusions. Here we discuss briefly the normal state $\sigma(\omega)$ in the low frequency region $\omega < 1$ eV where the *intra-band* effects dominate the quasiparticle scattering. In the low ω regime, the processing of data in the metallic state of cuprates is usually done by using the generalized Drude formula for the in-plane conductivity $\sigma(\omega) = \sigma_1(\omega) + i\sigma_2(\omega)$ [38], [39]

$$\sigma_{ii}(\omega) = \frac{\omega_{p,ii}^2}{4\pi} \frac{1}{\Gamma_{tr}(\omega, T) - i\omega m_{tr}(\omega)/m_\infty}. \quad (3)$$

$i = a, b$ enumerates the plane axis, $\omega_{p,ii}$, $\Gamma_{tr}(\omega, T)$ and $m_{tr}(\omega)$ are the plasma frequency, transport scattering rate and optical effective mass, respectively. For optimally doped HTSC systems the best fit for $\Gamma_{tr}(\omega, T)$ is given by $\Gamma_{tr}(\omega, T) \approx \max\{\alpha T, \beta\omega\}$ in a broad temperature (100 K $< T < 2000$ K) and frequency range (10

meV $< \omega < 200$ meV), where α, β are of the order one. These results tell us that the quasiparticle liquid - which is responsible for transport properties in HTSC - is not a simple weakly interacting Fermi liquid. In that respect it is a well known fact that quasiparticles interacting with phonons at finite T are not described by the standard Landau-Fermi liquid, in particular at higher temperatures $T > \Theta_D/5$, since the scattering rate is of the order of quasiparticle energy, i.e. one has $\Gamma \sim \max(\omega, T)$. Such a system is well described by the *Migdal-Eliashberg theory* whenever $\omega_D \ll E_F$ is fulfilled, which in fact treats quasiparticles beyond the original Landau quasiparticle concept. Note that even when the original Landau quasiparticle concept fails, the transport properties may be described by the Boltzmann equation, which provides a broader definition of the Landau-Fermi liquid.

As we said, in a number of articles it was *incorrectly* assumed that $\Gamma(\omega, T) \approx \Gamma_{tr}(\omega, T)$ holds in cuprates. Since the theory of EPI gives that $\Gamma(\omega, T) = \text{const}$ for $\omega > \omega_{ph,\max}$ (the maximal phonon frequency) and experiments give $\Gamma_{tr}(\omega, T) \sim \omega$ for $\omega > \omega_{ph,\max}$, it was (incorrectly) concluded that EPI in cuprates is small and can not be responsible for superconductivity and transport properties in the normal state. However, the thorough theoretical calculations of $\sigma(\omega)$ in a number of materials (including HTSC and LTSC systems) by including realistic EPI spectral function $\alpha_{tr,EPI}^2 F(\omega)$ [38], [39], [40] showed that as a rule one has: (1) $\Gamma_{tr}(\omega, T) \neq \Gamma(\omega, T)$ and (2) $\Gamma_{tr}(\omega, T) \sim \omega$ is linear in the broad region up to $\omega_{sat} \simeq -Im\Sigma_{tr}(\omega_{sat}) \gg \omega_{ph,\max}$. Such a behavior of $\Gamma_{tr}(\omega, T)$ and $\Gamma(\omega, T)$ is also realized in HTSC materials and in other metallic non-superconducting oxides; an extensive discussion is given in [7] and [8].

The main conclusion from the optics measurements is that EPI can explain the optical spectra of cuprates for $\omega < 1$ eV. Moreover, this analysis shows that the EPI coupling constant is rather large, i.e. $1 < \lambda_{EPI} \lesssim 2$. The transport spectral function $\alpha_{tr}^2(\omega)F(\omega)$ can be in principle extracted from the transport scattering rate

$$\Gamma_{tr}(\omega, T = 0) = \frac{2\pi}{\omega} \int_0^\omega d\Omega(\omega - \Omega) \alpha_{tr}^2(\Omega) F(\Omega) \quad (4)$$

- see [7], [8]. However, real measurements are performed at finite $T (> T_c)$ where $\alpha_{tr}^2(\omega)F(\omega)$ is the solution of the inhomogeneous Fredholm integral equation of the first kind. This inverse problem at finite temperatures in cuprates was studied in [38] (see also [39]), where the smeared structure of $\alpha_{tr}^2(\omega)F(\omega)$ in $YBa_2Cu_3O_{7-x}$ was obtained, in a qualitative agreement with the shape of the phonon density of states $F(\omega)$. At finite T the problem is more complex because the fine structure of $\alpha_{tr}^2(\omega)F(\omega)$ gets blurred, as the calculations in [41] confirm. The latter showed that $\alpha_{tr}^2(\omega)F(\omega)$ ends up at $\omega_{max} \approx 70 - 80$ meV, which is the maximal phonon frequency in cuprates. This result indicates strongly that the EPI in cuprates is dominant in the IR optics. Strictly speaking, this is still not a definitive proof for the EPI since the solution of the Fredholm equation of the first

kind is extremely sensitive to the input, because the unknown function ($\alpha_{tr}^2(\omega)F(\omega)$ which is a positive quantity) is under integral and smoothed by some kernel. It is known that this smoothing can miss some fine details of the solution.

We point out that if $R(\omega)$ (and $\sigma(\omega)$) are due to some other bosonic process with large frequency cutoff ω_c in the spectrum, as it is the case with SFI scattering where $\alpha_{tr}^2(\omega)F(\omega) \sim g_{sf}^2 Im\chi_s(\omega)$ and $\omega_c \approx 400$ meV, the extracted $\alpha_{tr}^2(\omega)F(\omega)$ should end up at this high ω_c . This was done in [42] for $T > T_c$, where it was found that $\alpha_{tr}^2(\omega)F(\omega)$ reaches negative values in a broad energy region 70 meV $< \omega < \omega_c$. These results rule out SFI as a dominant scattering mechanism in cuprates and favor EPI. Recent

We stress that the extraction of Γ_{tr} from $R(\omega)$ is a rather subtle procedure, since it depends on the assumed value of dielectric constant ε_∞ . For instance, if one takes $\varepsilon_\infty = 1$ then Γ_{tr}^{EP} is linear up to very high ω , while for $\varepsilon_\infty > 1$ the linearity of Γ_{tr}^{EP} saturates at lower ω . For instance, the extracted $\Gamma_{tr}^{EP}(\omega, T)$ in [43] is linear up to very high ω . Since in these papers there is no information (!) on ε_∞ , the too linear behavior might mean that the ion background and interband transitions (contained in ε_∞) are not properly taken into account in these papers. We stress again, that the behavior of $\Gamma_{tr}(\omega)$ is linear up to much higher frequencies for $\varepsilon_\infty = 1$ than for $\varepsilon_\infty \approx 4 - 5$ - the characteristic value for HTSC, giving a lot of room for inadequate interpretations of results. Note that recent ellipsometric measurements on YBCO [44] confirm the earlier results [46] that $\varepsilon_\infty \geq 4$ and that Γ_{tr}^{EP} saturates at lower frequency than it was the case in Ref. [43]. We stress again that a reliable estimate of the value and of the ω, T dependence of $\Gamma_{tr}(\omega)$ and $m(\omega)$ can be done, not from the reflectivity measurements [43], but from ellipsometric ones only [46], [44].

In concluding this part we stress two facts: (1) The large difference in the ω, T behavior of $\Gamma_{tr}^{EPI}(\omega, T)$ and $\Gamma^{EPI}(\omega, T)$ is not a specificity of cuprates but it is realized also in a number of *LTSC* materials. In fact this is a common behavior even in simple metals, such as Al or Pb where $\Gamma^{EPI}(\omega, T)$ saturates at much lower (Debay) frequency than $\Gamma_{tr}^{EPI}(\omega, T)$ and $\Gamma_{tr}^{*,EPI}(\omega, T)$ do - see more in [7], [8] and references therein. In that respect the difference between simple metals and cuprates is in the scale of phonon frequencies, i.e. $\omega_{\max}^{ph} \sim 100$ K in simple metals, while $\omega_{\max}^{ph} \sim 1000$ K in cuprates. Having in mind these well established and well understood facts, it is very surprising that even nowadays, twenty years after the discovery of cuprates, the essential and quantitative difference between Γ and Γ_{tr} is neglected in the analysis of experimental data. For instance, by neglecting the pronounced (qualitative and quantitative) difference between $\Gamma_{tr}(\omega, T)$ and $\Gamma(\omega, T)$, in the recent papers [43] were made far reaching, but unjustified, conclusions that the magnetic pairing mechanism prevails; (2) It is worth mentioning that quite similar (to cuprates) properties of $\sigma(\omega)$, $R(\omega)$ and $\rho(T)$ were

observed in experiments [46] on isotropic metallic oxides $La_{0.5}Sr_{0.5}CoO_3$ and $Ca_{0.5}Sr_{0.5}RuO_3$. We stress that in these compounds there are no signs of antiferromagnetic fluctuations (which are present in cuprates) and the peculiar behavior is probably due to the EPI.

In that respect, recent experiments related to the *optical sum-rule* with the transfer of the spectral weight from high to low frequency is an additional example of controversies in this field coming from inadequate interpretation of experimental results. We stress that the theory based on EPI can explain the transfer of spectral weight by taking into account strong the ω and T dependence of $\Gamma_{tr}^{EPI}(\omega, T)$ due to the EPI - for details see [45], [44] and [11].

The temperature behavior of *in-plane resistivity* $\rho_{a-b}(T)$ is a direct consequence of quasi-2D motion of quasiparticles and of inelastic scattering which they experience. At present, there is no consensus on the origin of linear temperature dependence of the in-plane resistivity $\rho_{a-b}(T)$ in the normal state. Many researchers (erroneously) believe that such a behavior can not be due to the EPI. The inadequacy of this claim was already demonstrated by analyzing the dynamic conductivity $\sigma(\omega)$. It is well-known that at temperatures $T > \Theta_D/5$ and for the Debay spectrum one has

$$\rho(T) \simeq 8\pi^2 \lambda_{tr}^{EP} \frac{k_B T}{\hbar \omega_p^2} = \rho' T. \quad (5)$$

In cuprates the reach and broad spectrum of $\alpha_{tr}^2(\omega)F(\omega)$ favors such a linear behavior in a broader T region. The measured transport coupling constant λ_{tr} contains in principle all scattering mechanisms, although usually some of them dominate. For instance, the proponents of SFI mechanism assume that λ_{tr} is entirely due to scattering on spin fluctuations. However, by taking into account specificities of cuprates the experimental results for the in-plane resistivity $\rho_{a-b}(T)$ can be satisfactorily explained by the EPI mechanism. From tunnelling experiments [17] one concludes that $\lambda \approx 2 - 3$ and if one assumes that $\lambda_{tr} \approx \lambda$ and $\omega_{pl} \geq (3 - 4)$ eV (the value obtained from the band-structure calculations) then Eq. (5) describes the experimental situation rather well. The plasma frequency ω_{pl} which enters Eq.(5) can be extracted from optic measurements ($\omega_{pl,ex}$), i.e. from the width of the Drude peak at small frequencies. However, since $\lambda_{tr} \approx 0.25\omega_{pl}^2$ (eV) $\rho'(\mu\Omega\text{cm}/K)$ there is an experimental constraint on λ_{tr} . This gives [46] that $\omega_{pl} \approx (2 - 2.5)$ eV and $\rho' \approx 0.6$ in the oriented YBCO films, while $\rho' \approx 0.3$ in single crystals of BSCCO. These results impose a limit on $\lambda_{tr} \approx 0.4 - 0.8$.

The above analysis implies, that in order to explain $\rho(T)$ with small λ_{tr} and high T_c (which needs large λ) by EPI it is necessary to have $\lambda_{tr} \leq (\lambda/3)$. This means that in cuprates EPI is, due to some reasons, reduced in transport properties where $\lambda_{tr} \ll \lambda$. This reduction of ω_p^2 and λ_{tr} means that the λ and λ_{tr} contain renormalization (with respect to the *LDA* results) due to various quasiparticle scattering processes and interactions, which

do not enter in the *LDA* theory. In subsequent chapters we shall argue that the strong suppression of λ_{tr} may have its origin in strong electronic correlations [30], [31], [32].

In conclusion, optics and resistivity measurements in normal state of cuprates are much more in favor of EPI than against it. However, some intriguing questions still remains to be answered: **(i)** what are the values of λ_{tr} and ω_{pl} ; **(ii)** what is the reason that $\lambda_{tr} \ll \lambda$ is realized in cuprates; **(iii)** what is the role of Coulomb scattering in $\sigma(\omega)$ and $\rho(T)$. Later on we shall argue that ARPES measurements in cuprates give evidence for a contribution of Coulomb scattering at higher frequencies, where $\Gamma(\omega) \approx \Gamma_0 + \lambda_c \omega$ for $\omega > \omega_{\max}^{ph}$ with $\lambda_c \approx 0.4$. So, in spite of the fact that EPI is suppressed in transport properties it is sufficiently strong that it dominates in the self-energy in some frequency and temperature range. It is possible that at higher temperatures Coulomb scattering dominates $\rho(T)$, which certainly does not disqualify EPI as the pairing mechanism in cuprates. For better understanding of $\rho(T)$ we need a controllable theory for Coulomb scattering in strongly correlated systems, which is at present lacking.

C. Electronic and phonon Raman scattering in cuprates

(a) *Electronic Raman scattering* in various cuprates show a remarkable correlation between the Raman cross-section $\tilde{S}_{\text{exp}}(\omega)$ and the optical conductivity $\sigma_{a-b}(\omega)$, i.e. $\tilde{S}_{\text{exp}}(\omega) \sim \sigma_{a-b}(\omega)$ [7]. Previously it was demonstrated that $\sigma_{a-b}(\omega)$ depends on the transport scattering rate $\Gamma_{tr}(\omega, T)$. We have also demonstrated that the EPI with the very broad spectral function $\alpha^2 F(\omega)$ (see Fig. 2 below) explains in a natural way the ω, T dependence of $\sigma_{a-b}(\omega)$ and $\Gamma_{tr}(\omega, T)$. Therefore, the Raman spectra in cuprates can be explained by the EPI in conjunction with strong correlations. This conclusion is supported by calculations of the Raman cross-section [47] which take into account the EPI with $\alpha^2 F(\omega)$ extracted from the tunnelling measurements on $YBa_2Cu_3O_{6+x}$ and $Bi_2Sr_2CaCu_2O_{8+x}$ [17], [7]. Quite similar (to cuprates) properties of the electronic Raman scattering (besides $\sigma(\omega)$, $R(\omega)$ and $\rho(T)$) were observed in experiments [46] on isotropic metallic oxides $La_{0.5}Sr_{0.5}CoO_3$ and $Ca_{0.5}Sr_{0.5}RuO_3$ where there are no signs of antiferromagnetic fluctuations.

(b) Two important experimental results related to the *phonon Raman scattering* give evidence for strong EPI in cuprates: (i) there is a pronounced asymmetric line-shape (of the Fano resonance) in the metallic state. For instance in $YBa_2Cu_3O_7$ two Raman modes at 115 cm^{-1} (Ba dominated mode) and at 340 cm^{-1} (O dominated mode in the CuO_2 planes) show pronounced asymmetry which is absent in $YBa_2Cu_3O_6$. This result points to the strong interaction of Raman active phonons with continuum states (quasiparticles); (ii) The phonon frequencies

for some A_{1g} and B_{1g} are strongly renormalized in the superconducting state, pointing again to the large EPI - see more in [7], [11].

D. Tunnelling spectroscopy and Eliashberg spectral function

By measuring the I-V characteristic, i.e., the tunnelling conductance $G(V) = dI/dV$, one can determine the Eliashberg spectral function $\alpha^2 F(\omega)$ which determines the pairing coupling constant $\lambda = 2 \int d\omega \alpha^2 F(\omega)/\omega$. A number of experiments [17] on tunnelling- and break-junctions in cuprates gave $\alpha^2 F(\omega)$ which is spread over a broad range of frequencies ($0 < \omega < 80\text{ meV}$) and whose maxima coincide with the maxima in the phonon density of states $F(\omega)$ - see Fig. 2. This is a rather strong proof of importance of the EPI in pairing. Moreover, most of these experiments give the range of the coupling constant $1 < \lambda < 2.5$.

Since practically all phonon modes contribute to λ - see Fig. 2, this means that on the average each particular phonon mode is moderately coupled to electrons thus keeping the lattice stable. Additionally, they have found that some low-frequency phonon modes corresponding to Cu , Sr and Ca vibrations are rather strongly coupled to electrons. The high frequency oxygen vibrations along the c -axis interact with quasiparticles appreciably too. These results confirm the importance of axial phonon modes in which the change of the Madelung energy is involved, thus supporting the idea conveyed through this article of the importance of the ionic Madelung energy in the EPI interaction of cuprates.

Recent STM experiments [18] confirmed partly the results of tunnelling measurements. They find near the anti-nodal point strong EPI with 40 meV phonons and from Fourier-transformed spectra the exclude the magnetic resonance as a possible origin.

In conclusion, the common results for tunnelling measurements in cuprates, including $Ba_{1-x}K_xBiO_3$ too [48], is that no particular mode can be singled out in the spectral function $\alpha^2 F(\omega)$ as being the only one which dominates in pairing mechanism. This important result means that the high T_c is not attributable to a particular phonon mode in the EPI mechanism, since all phonon modes contribute to λ . Having in mind that the phonon spectrum in cuprates is very broad (up to 80 meV), then the large EPI coupling constant ($\lambda \approx 2$) in cuprates is not surprising at all. We stress, that compared to neutron scattering experiments the tunnelling experiments are superior in determining the EPI spectral function $\alpha^2 F(\omega)$ - see more in [7].

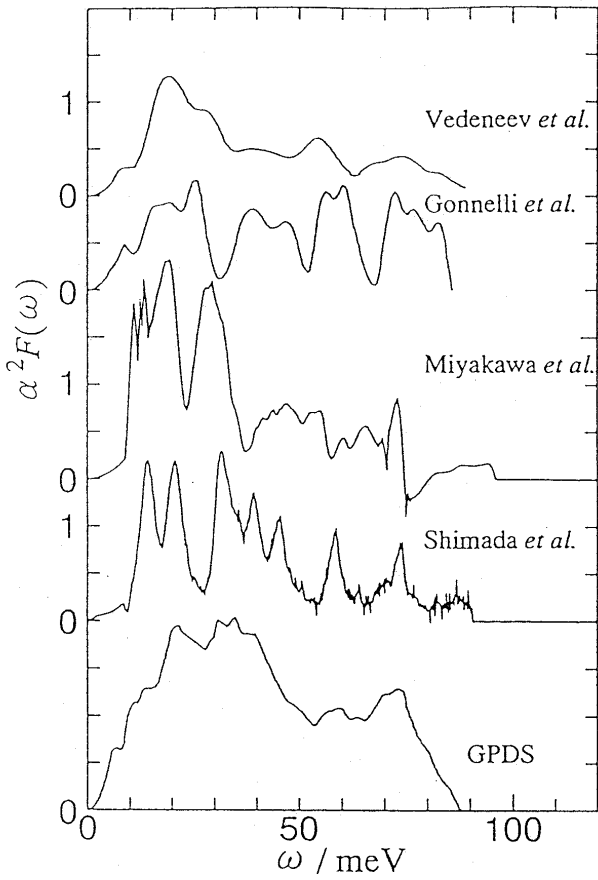


FIG. 2: The spectral function $\alpha^2 F(\omega)$ obtained from measurements of $G(V)$ by various groups on various junctions. The generalized density of states GPDS for $Bi2212$ is plotted at the bottom. From Ref. [17].

E. Isotope effect for various doping

It is well known that in the pure EPI pairing mechanism the total isotope coefficient α is given by

$$\alpha = \sum_{i,p} \alpha_i^{(p)} = - \sum_{i,p} \frac{d \ln T_c}{d \ln M_i^{(p)}}, \quad (6)$$

where $M_i^{(p)}$ is the mass of the i -th element in the p -th crystallographic position. From this formula one can deduce that the relative change of T_c , $\delta T_c/T_c$, for heavier elements is rather small - for instance it is 0.02 for $^{135}Ba \rightarrow ^{138}Ba$, 0.03 for $^{63}Cu \rightarrow ^{65}Cu$ and 0.07 for $^{138}La \rightarrow ^{139}La$. This means that measurements of α_i for heavier elements are at/or beyond the ability of experimental techniques. Therefore most isotope effect measurements were done by substituting light atoms ^{16}O by ^{18}O . In that respect one should have in mind the tunnelling experiments discussed above, which tell us that

practically all phonons contribute to the Eliashberg pairing function $\alpha^2 F(\mathbf{k}, \omega)$, and that oxygen modes give only moderate contribution to T_c . So, small oxygen isotope effect does not exclude the EPI mechanism of pairing.

Measurements of the isotope coefficients α_O (and α_{Cu}) were performed on various hole-doped and electron-doped cuprates. A brief summary of the main results is as follows [16]: (1) The O isotope coefficient α_O strongly depends on the hole concentration in the hole-doped materials; in each family of cuprates ($YBa_2Cu_3O_{7-x}$, or $La_{2-x}Sr_xCuO_4$ etc.) a small oxygen isotope effect is observed in the optimally doped (maximal T_c) samples. For instance $\alpha_O \approx 0.02 - 0.05$ in $YBa_2Cu_3O_7$ with $T_{c,\max} \approx 91 K$, $\alpha_O \approx 0.1 - 0.2$ in $La_{1.85}Sr_{0.15}CuO_4$ with $T_{c,\max} \approx 35 K$; $\alpha_O \approx 0.03 - 0.05$ in $Bi_2Sr_2CaCu_2O_8$ with $T_{c,\max} \approx 76 K$; $\alpha_O \approx 0.03$ and even negative (-0.013) in $Bi_2Sr_2Ca_2Cu_2O_{10}$ with $T_{c,\max} \approx 110 K$; the experiments on $Tl_2Ca_{n-1}BaCu_nO_{2n+4}$ ($n = 2, 3$) with $T_{c,\max} \approx 121 K$ are still unreliable and α_O is unknown; $\alpha_O < 0.05$ in the electron-doped $(Nd_{1-x}Ce_x)_2CuO_4$ with $T_{c,\max} \approx 24 K$. (2) For hole concentrations away from the optimal one, T_c decreases while α_O increases and in some cases reaches large value $\alpha_O \approx 0.5$. This holds not only for parent compounds but also for systems with substitutions, like $(Y_{1-x-y}Pr_xCa_y)Ba_2Cu_3O_7$, $Y_{1-y}Ca_yBa_2Cu_4O_4$ and $Bi_2Sr_2Ca_{1-x}Y_xCu_2O_8$. Note that the decrease of T_c is not a prerequisite for the increase in α_O . This became clear from the Cu substituted experiments $YBa_2(Cu_{1-x}Zn_x)_3O_7$ where the decrease of T_c (by increasing the Zn concentration) is followed by only a small increase of α_O . Only in the case of very low $T_c < 20 K$, α_O becomes large, i.e. $\alpha_O > 0.1$. (3) The largest α_O is obtained even in the optimally doped compounds like in systems with substitution, such as $La_{1.85}Sr_{0.15}Cu_{1-x}M_xO_4$, $M = Fe, Co$, where $\alpha_O \approx 1.3$ for $x \approx 0.4 \%$. (4) In $La_{2-x}M_xCuO_4$ there is a Cu isotope effect which is of the order of the oxygen one, i.e. $\alpha_{Cu} \approx \alpha_O$ giving $\alpha_{Cu} + \alpha_O \approx 0.25 - 0.35$ for optimally doped systems ($x = 0.15$). In the case when $x = 0.125$ with $T_c \ll T_{c,\max}$ one has $\alpha_{Cu} \approx 0.8 - 1$ with $\alpha_{Cu} + \alpha_O \approx 1.8$. The appreciate copper isotope effect in $La_{2-x}M_xCuO_4$ tells us that vibrations of other than oxygen ions could be important in giving high T_c . The latter property is more obvious from tunnelling measurements which are discussed above. (5) There is a negative Cu isotope effect in the oxygen-deficient system $YBa_2Cu_3O_{7-x}$ where α_{Cu} is between -0.14 and -0.34 if T_c lies in the $60 K$ plateau. (6) There are reports on a small negative α_O in some systems like $YSr_2Cu_3O_7$ with $\alpha_O \approx -0.02$ and in $BSCCO-2223$ ($T_c = 110 K$) where $\alpha_O \approx -0.013$ etc. However, the systems with negative α_O present considerable experimental difficulties, as it is pointed out in [16].

The above enumerated results, despite experimental difficulties, tell us that the EPI interaction is involved in the pairing mechanism of cuprates and that the relation of T_c to ionic masses is highly nontrivial and non-BCS-like. By assuming that the experimental results on

the isotope effect reflect an intrinsic property of cuprates one can rise a question: which theory can explain these results? Since at present there is no consensus on the pairing mechanism in HTSC materials there is also no definite theory for the isotope effect. Besides the calculation of the coupling constant λ any microscopic theory of pairing is confronted also with the following questions: **(a)** why is the isotope effect small in optimally doped systems and **(b)** why α increases rapidly by further under(over)doping of the system? The answer to this question is additionally complicated by the quasi-2D structure of cuprates and the closeness of these materials to the Mott-Hubbard isolator. It is known that the later gives rise to the smallness of the phase stiffness K_s^0 of the superconducting order parameter $\Delta = |\Delta| e^{i\varphi}$. In 2D superconductors the energy increase due to phase fluctuations in the conduction plane is given by [49]

$$F_{\text{phase}}(\varphi, T) = \frac{1}{2} K_s^0 \int d^2x (\nabla \varphi)^2, \quad (7)$$

where $K_s^0 = \hbar^2 n_s(T)/4m^*$ is the 2D stiffness, n_s is the 2D superconducting charge density and $m^* \approx 2m_e$ is the effective mass. In the case of the Berezinskii-Kosterlitz-Thouless transition (vortex-antivortex unbinding) one has $T_c = (\pi/2)K_s(T_c)$, where K_s is the renormalized stiffness. In that case the isotope effect is completely different from the prediction of the BCS theory. In that respect the very careful experiments on isotope effect of the *penetration depth* in the a-b plane of YBCO show a significant increase upon the substitution $O^{16} \rightarrow O^{18}$, i.e. $(\Delta\lambda_{ab}/\lambda_{ab}) = ({}^{18}\lambda_{ab} - {}^{16}\lambda_{ab})/{}^{16}\lambda_{ab} = 2.8\%$ at 4 K [19]. Since $\lambda_{ab} \sim m^*$ this could mean that there is a nonadiabatic increase of the effective mass m^* .

F. Angle-resolved photoemission spectroscopy in cuprates

ARPES is nowadays a leading spectroscopy method in the solid state physics [21]. The method consists in shining light (photons) with energies between 20 – 1000 eV on the sample and by detecting momentum (\mathbf{k})- and energy(ω)-distribution of the outgoing electrons. The resolution of ARPES has been significantly increased in the last decade with the energy resolution of $\Delta E \approx 2$ meV (for photon energies ~ 20 eV) and angular resolution of $\Delta\theta \approx 0.2^\circ$. The ARPES method is surface sensitive technique, since the average escape depth (l_{esc}) of the outgoing electrons is of the order of $l_{\text{esc}} \sim 10$ Å, of course depending on the energy of incoming photons. Therefore, very good surfaces are needed in order that the results be representative of bulk samples. In that respect the most reliable studies were done on the bilayer $Bi_2Sr_2CaCu_2O_8$ (*Bi2212*) and its single layer counterpart $Bi_2Sr_2CuO_6$ (*Bi2201*), since these materials contain weakly coupled BiO planes with the longest inter-plane separation in the cuprates. This results in a *natural cleavage* plane making these materials superior to

others in ARPES experiments. After a drastic improvement of sample quality in other families of HTSC materials, the ARPES technique has became a central method in theoretical considerations. Potentially, it gives valuable information on the quasiparticle Green's function, i.e. on the quasiparticle spectrum and life-time effects. The ARPES can indirectly give information on the momentum and energy dependence of the pairing potential. Furthermore, the electronic spectrum of the (above mentioned) cuprates is highly *quasi-2D* which allows an unambiguous determination of the initial state momentum from the measured final state momentum, since the component parallel to the surface is conserved in photoemission. In this case the ARPES probes (under some favorable conditions) directly the single particle spectral function $A(\mathbf{k}, \omega)$. In the following we discuss only those ARPES experiments which give evidence for the importance of the EPI in cuprates - see more in [21].

The *photoemission* measures a nonlinear response function of the electron system, and under some conditions it is analyzed in the so-called *three-step model*, where the total photoemission intensity $I_{\text{tot}}(\mathbf{k}, \omega) \approx I \cdot I_2 \cdot I_3$ is the product of three independent terms: **(1)** I - describes optical excitation of the electron in the bulk; **(2)** I_2 - the scattering probability of the travelling electrons; **(3)** I_3 - the transmission probability through the surface potential barrier. The central quantity in the three-step model is $I(\mathbf{k}, \omega)$ and it turns out that it can be written in the form for $\mathbf{k} = \mathbf{k}_{\parallel}$ [21]

$$I(\mathbf{k}, \omega) \simeq I_0(\mathbf{k}, v) f(\omega) A(\mathbf{k}, \omega)$$

$$I_0(\mathbf{k}, v) \sim |\langle \psi_f | \mathbf{p} \mathbf{A} | \psi_i \rangle|^2$$

$$A(\mathbf{k}, \omega) = -\frac{1}{\pi} \frac{\Sigma_2(\mathbf{k}, \omega)}{[\omega - \xi(\mathbf{k}) - \Sigma_1(\mathbf{k}, \omega)]^2 + \Sigma_2^2(\mathbf{k}, \omega)} \quad (8)$$

Here, $\langle \psi_f | \mathbf{p} \mathbf{A} | \psi_i \rangle$ is the dipole matrix element which depends on \mathbf{k} , polarization and energy v of the incoming photons. The knowledge of the matrix element is of a great importance and its calculation from first principles was done carefully in [22]. $f(\omega) = 1/(1 + \exp\{\omega/T\})$ is the Fermi function, $A(\mathbf{k}, \omega) = -\text{Im}G(\mathbf{k}, \omega)/\pi$, $G(\mathbf{k}, \omega)$ and $\Sigma(\mathbf{k}, \omega) = \Sigma_1(\mathbf{k}, \omega) + i\Sigma_2(\mathbf{k}, \omega)$ are the spectral function, the quasiparticle Green's function and the self-energy, respectively.

In some period of the HTSC era there were a number of controversial ARPES results and interpretations, due to bad samples and to the euphoria with exotic theories. For instance, a number of (now well) established results were *questioned* in the first ARPES measurements, such as: the shape of the Fermi surface, which is correctly predicted by the LDA band-structure calculations; bilayer splitting in *Bi2212*, etc.

We summarize here some important ARPES results which were obtained recently, first in the *normal state* [21]: **(1_N)** There is a well defined Fermi surface in the

metallic state - with the topology predicted by the LDA but the bands are narrower than the LDA ones; (2_N) the spectral lines are broad with $|\Sigma_2(\mathbf{k}, \omega)| \sim \omega$ (or $\sim T$ for $T > \omega$); (3_N) there is a bilayer band splitting in *Bi2212* (at least in the over-doped state); (4_N) at temperatures $T_c < T < T^*$ and in the under-doped cuprates there is a d-wave like pseudo-gap $\Delta_{pg}(\mathbf{k}) \sim \Delta_{pg,0}(\cos k_x - \cos k_y)$ in the quasiparticle spectrum; (5_N) the pseudo-gap $\Delta_{pg,0}$ increases by lowering doping; (6_N) the ARPES self-energy gives clear evidence that the EPI interaction, with the *characteristic phonon* energy ω_{ph} , is rather strong. At $T > T_c$ there are *kinks* in the quasiparticle dispersion $\omega(\xi_{\mathbf{k}})$ in the *nodal* direction (along the $(0, 0) - (\pi, \pi)$ line) at $\omega_{ph}^{(70)} \sim (60 - 70) \text{ meV}$ [20], see Fig. 3, and near the *anti-nodal point* $(\pi, 0)$ at 40 meV [23] - see Fig. 3. (7_N) The holes couple practically to the whole spectrum of phonons. For instance, at least three group of phonons (interacting with holes) were extracted recently from the ARPES self-energy in *La_{2-x}Sr_xCuO₄* [50]. (8_N) The EPI coupling constant which is obtained by comparing the slope $d\omega/d\xi_{\mathbf{k}}$ of the quasiparticle energy $\omega(\xi_{\mathbf{k}})$ at very small $|\xi_{\mathbf{k}}| \ll \omega_{ph}$ and $|\xi_{\mathbf{k}}| \gg \omega_{ph}$ gives $\lambda_{epi} \approx 1 - 2$, while the Coulomb part is $\lambda_c \approx 0.4$. (9_N) Recent ARPES spectra in the optimally doped *Bi2212* near the nodal and anti-nodal point [24] show a pronounced isotope effect in the real part of the quasiparticle self-energy, thus pointing out the important role of the EPI.

The corresponding ARPES results in the *superconducting state* are the following [21]: (1_S) there is an anisotropic superconducting gap in most HTSC compounds, which is predominately d-wave like, i.e. $\Delta_{sc}(\mathbf{k}) \sim \Delta_0(\cos k_x - \cos k_y)$ with $2\Delta_0/T_c \approx 5 - 6$; (2_S) there are dramatic changes in the spectral shapes near the anti-nodal point $(\pi, 0)$, i.e. a *sharp quasiparticle peak* develops at the lowest binding energy followed by a dip and a broader hump, giving rise to the so called *peak-dip-hump structure*; (3_S) the kink in the quasiparticle energy around the nodal-point and at $(60 - 70) \text{ meV}$ is surprisingly *not-shifted* in the superconducting state. To remind the reader, in the standard Eliashberg theory the kink should be shifted to $\omega_{ph} + \Delta_0$ at any point at the Fermi surface. (4_S) the anti-nodal kink at $\omega_{ph}^{(40)} \sim 40 \text{ meV}$ is shifted in the superconducting state by Δ_0 , i.e. $\omega_{ph}^{(40)} \rightarrow \omega_{ph}^{(40)} + \Delta_0 = (65 - 70) \text{ meV}$ since $\Delta_0 = (25 - 30) \text{ meV}$. In the following sections we shall argue that all these properties can be explained by EPI with FSP and the coupling constant $\lambda > 1$.

III. THEORY OF STRONG CORRELATIONS WITHOUT SLAVE BOSONS

The well established fact is that *strong electronic correlations* are pronounced in cuprates. However, the LDA theory fails to capture effects of strong correlations by treating them as a local perturbation only. This is an unrealistic approximation for cuprates, where strong corre-

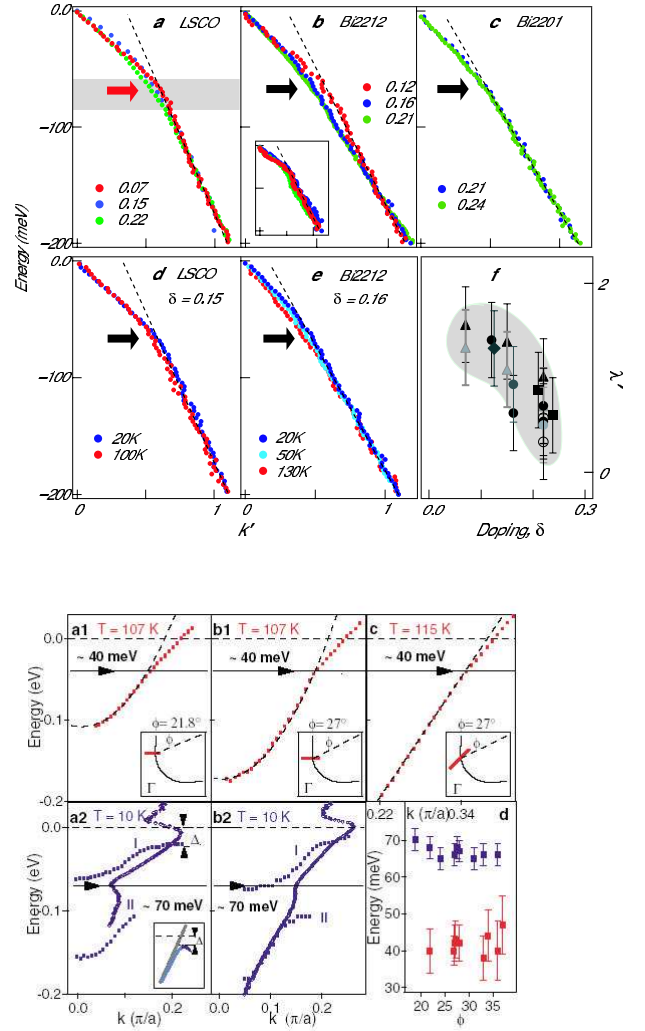


FIG. 3: (Top) Quasiparticle dispersion of *Bi2212*, *Bi2201* and *LSCO* along the *nodal* direction, plotted vs the momentum k for (a) – (c) different dopings, and (d) – (e) different T ; black arrows indicate the kink energy; the red arrow indicates the energy of the $q = (\pi, 0)$ oxygen stretching phonon mode; inset of (e) - T -dependent Σ' for optimally doped *Bi2212*; (f) - doping dependence of λ' along $(0, 0) - (\pi, \pi)$ for the different HTSC oxides. From Ref. [20]. (Bottom) Quasiparticle dispersion $E(k)$ in the normal state (a1, b1, c), at 107 K and 115 K, along various directions ϕ around the *anti-nodal* point. The kink at $E = 40 \text{ meV}$ is shown by the horizontal arrow. (a2 and b2) is $E(k)$ in the superconducting state at 10 K with the shifted kink to 70 meV. (d) kink positions as a function of ϕ in the anti-nodal region. From Ref. [23].

lations introduce non-locality in charge interactions. One of the shortcomings of the LDA is that in the half-filled case (with $n = 1$ and one particle per lattice site) it predicts metallic state only, thus missing the existence of the *Mott insulating state*. In the latter, particles are localized at lattice sites independently of the (non)existence of the *AF*. This localization is due to the large Coulomb repul-

sion U at given lattice site, i.e. $U \gg W$ where W is the band width. Some properties in the metallic state can not be described by the simple canonical Landau-Fermi liquid concept. For instance, recent ARPES photoemission measurements on the hole-doped samples show a well defined Fermi surface in the one-particle energy spectrum, which contains $1 - \delta$ electrons in the Fermi volume (δ is the hole concentration), but the band width is $(2 - 3)$ times smaller than the *LDA* band structure calculations predict [21]. The " $1 - \delta$ " behavior of the Fermi volume is consistent with the Luttinger theorem. However, experimental data on the dynamic conductivity (spectral weight of the Drude peak), Hall measurements etc. indicate that in transport properties a low density of hole-like charge carriers (which is proportional to δ) participates predominantly. These carriers experience strong scattering and their inverse lifetime is proportional to the temperature (at $T > T_c$) as we discussed earlier. It is worth mentioning here that the local moments on the *Cu* sites, which are localized in the parent *AF* compound, are counted as a part of the Fermi surface area when the system is doped by small concentration of holes in the metallic state. The latter fact gives rise to a *large Fermi surface* which scales with the number (per site) of electrons $1 - \delta$. At the same time the conductivity sum-rule is proportional to the number of doped holes δ , at least in underdoped systems, i.e., $\int_0^{\omega_c} d\omega \sigma_1(\omega) \sim \delta$ instead of $1 - \delta$ as in the canonical Landau-Fermi liquid. These two properties tell us that in cuprates we deal with a *correlated state*, and the latter must be due to the specific electronic structure of cuprates. The common ingredient of all cuprates is the presence of *Cu* atoms. In order to account for the absence of Cu^{3+} ionic configuration (the charge transfer $Cu^{2+} \rightarrow Cu^{3+}$ costs large energy $U \sim 10$ eV, i.e. the occupation of the *Cu* site with two holes with opposite spins is unfavorable) P. W. Anderson proposed in his remarkable paper [51] the Hubbard model as the basic model for quasiparticle properties in these compounds. For some parameter values it can be derived from the (minimal) microscopic *three-band model* in some parameter regime. Besides the hopping t_{pd} between the *d*-orbital of *Cu* and *p*-orbital of *O* ions (as well as t_{pp} between *O* ions) - the Emery model, it contains also the strong Coulomb interaction U_{Cu} on the *Cu* ions as well as interaction between *p*- and *d*-electrons. The main two parameters are $U_{Cu} \sim (6 - 10)$ eV and the charge transfer energy $\Delta_{pd} \equiv \epsilon_d^0 - \epsilon_p^0 \sim (2.5 - 4)$ eV, where ϵ_d^0 , ϵ_p^0 are bare energies of the *d*- and *p* levels, respectively. In cuprates the case $U_{Cu} \gg \Delta_{pd}$ is realized, i.e. they belong to the class of *charge transfer materials*. This allows us to project the complicated three-band Hamiltonian onto the low-energy sector, and to obtain an effective single-band Hubbard Hamiltonian with an effective hopping parameter t and the effective repulsion $U_{eff} \approx \Delta_{pd}$. It turns out that the case $U_{eff} \gg t$ is realized, if $\Delta_{pd} \gg t = t_{pd}^2/\Delta_{pd}$. In fact in HTSC cuprates the latter is not quite realized and probably the slightly weaker condition $\Delta_{pd} > t$ is more appropriate.

Since $t_{pd} \approx 1.3$ eV and $\Delta_{pd} \approx (2 - 3)$ eV. Nevertheless, there is a widespread believe that the suitable effective and minimal Hamiltonian, i.e. the toy model for *low-energy physics of cuprates*, is based on the Hubbard model which additionally comprises the long-range Coulomb interaction \hat{V}_C and EPI \hat{V}_{EPI} - see [7]

$$\hat{H} = - \sum_{i,j,\sigma} t_{ij} c_{i\sigma}^\dagger c_{j\sigma} + U_{eff} \sum_i n_{i\uparrow} n_{i\downarrow} + \hat{V}_C + \hat{V}_{EPI}. \quad (9)$$

Some experiments imply that the effective repulsion should be of the order of $U_{eff} \approx 4$ eV, while the nearest neighbor and next-nearest neighbor hopping t and t' , respectively are estimated to be $t = 0.3 - 0.5$ eV and t'/t equal -0.15 in *LSCO* and -0.45 in *YBCO*. Since $(U_{eff}/t) \gg 1$ the above Hamiltonian is again in the regime of strong electronic correlations, where the double occupancy of a given lattice site is strongly suppressed, i.e. $\langle n_{i\uparrow} n_{i\downarrow} \rangle \ll 1$. The latter restricts charge fluctuations of electrons (holes) on a given lattice site, since $n_i = 0, 1$ is allowed only, while processes with $n_i = 2$ are (practically) forbidden. Note, that in (standard) weakly correlated metals all charge fluctuation processes ($n_i = 0, 1, 2$) are allowed, since $U \ll W$ in these systems. Due to suppression of double occupancy one expects that the screening properties in cuprates are strongly affected - this will be demonstrated below. From the Hamiltonian in Eq. (9), which is the 2D model for the low-energy physics in the *CuO₂* plane, comes out that in the *undoped* system there is one particle per lattice - the so called half-filled case (in the band language) with $\langle n_i \rangle = 1$. It is an insulator because of large U and even antiferromagnetic insulator at $T = 0$ K. The effective exchange interaction (with $J = 4t^2/U$) between spins is Heisenberg-like. By doping the system with holes (the hole concentration is $\delta (< 1)$) means that particles are taken out from the system in which case there is on the average $\langle n_i \rangle = 1 - \delta$ particles per lattice site. Above some (small) critical doping δ_c (which is of the order 0.01 in doped cuprates) the *AF* order vanishes and the system becomes a strongly correlated metal. For some *optimal* doping $\delta_{op} (\sim 0.1)$ the system is metallic with a large Fermi surface and can exhibit even high- T_c superconductivity in the presence of the EPI, as it will demonstrated below. The latter interaction and its interplay with strong correlations is the central subject in the following sections.

A. Strong correlations in the t-J model in terms of Hubbard operators $X^{\alpha\beta}$

Since $U_{eff} \gg t$ one can let with a good accuracy $U_{eff} \rightarrow \infty$, i.e. the system is in the *strongly correlated regime* where the doubly occupancy $n_i = 2$ is excluded. One of the ways to cope with such strong correlations is to introduce the Hubbard operators $X^{\alpha\beta}$ which automatically take into account the exclusion of double occupancy. The creation and annihilation Hubbard operators $\hat{X}_i^{\sigma 0}$ and $\hat{X}_i^{0\sigma} = (\hat{X}_i^{\sigma 0})^\dagger$, with $\hat{X}_i^{\sigma 0} =$

$c_{i\sigma}^\dagger (1 - n_{i,-\sigma})$, are fermion-like and they fulfill the condition that $n_{i,\sigma} + n_{i,-\sigma} \leq 1$ on each lattice site. The latter means that there is no more than one electron (hole) per lattice site, i.e. the double occupancy is forbidden. The bosonic-like Hubbard operators $\hat{X}_i^{\sigma_1\sigma_2} = \hat{X}_i^{\sigma_1 0} \hat{X}_i^{0\sigma_2}$ (with $\sigma_1 \neq \sigma_2$) describe spin fluctuations at the i -th site. Here, the spin projection parameter $\sigma = \uparrow, \downarrow$ ($-\sigma = \downarrow, \uparrow$) and the operator $\hat{X}_i^{\sigma\sigma}$ has the meaning of the electron (hole) number on the i -th site. In the following we shall use the convention that when $\hat{X}_i^{\sigma\sigma} | 1 \rangle = 1 | 1 \rangle$ there is a fermionic particle (electron) on the i -th site, while for $\hat{X}_i^{\sigma\sigma} | 0 \rangle = 0 | 0 \rangle$ the site is empty, i.e. there is a hole on it. It is useful to introduce the hole number operator $\hat{X}_i^{00} = \hat{X}_i^{0\sigma} \hat{X}_i^{\sigma 0}$, i.e. if $\hat{X}_i^{00} | 0 \rangle = 1 | 0 \rangle$ the i -th site is empty, i.e. there is one hole on it, while for $\hat{X}_i^{00} | 1 \rangle = 0 | 1 \rangle$ it is occupied by an electron and there is no hole. These operators fulfill the *non-canonical* commutation relations

$$[\hat{X}_i^{\alpha\beta}, \hat{X}_j^{\gamma\lambda}]_\pm = \delta_{ij} [\delta_{\gamma\beta} \hat{X}_i^{\alpha\lambda} \pm \delta_{\alpha\lambda} \hat{X}_i^{\gamma\beta}]. \quad (10)$$

Here, $\alpha, \beta, \gamma, \lambda = 0, \sigma$ and δ_{ij} is the Kronecker symbol. The (anti)commutation relations in Eq. (10) are rather different from the canonical Fermi and Bose (anti)commutation relations. Since $U_{\text{eff}} = \infty$ the double occupancy is excluded, i.e. $\hat{n}_{i\uparrow} \hat{n}_{i\downarrow} | \psi \rangle = (\hat{X}_i^{22} | \uparrow\downarrow \rangle) = 0$, and by construction the $\hat{X}^{\alpha\beta}$ operators satisfy the *local constraint* (the completeness relation)

$$\hat{X}_i^{00} + \sum_{\sigma=1}^N \hat{X}_i^{\sigma\sigma} = 1. \quad (11)$$

This condition tells us that at a given lattice site there is either one hole ($\hat{X}_i^{00} | \text{hole} \rangle = 1 | \text{hole} \rangle$) or one electron ($\hat{X}_i^{\sigma\sigma} | \text{elec} \rangle = 1 | \text{elec} \rangle$). Note, if Eq. (11) is obeyed, then both commutation and anticommutation relations hold also in Eq. (10) at the same lattice site, which is due to the projection properties of Hubbard operators $\hat{X}^{\alpha\beta} \hat{X}^{\gamma\mu} = \delta_{\beta\gamma} \hat{X}^{\alpha\mu}$.

For further purposes, i.e. for studying low-energy excitations in a controllable way, the number of spin projections is *generalized* to be N , i.e. $\sigma = 1, 2, \dots, N$. By projecting out the double occupied (high energy) states from the Hamiltonian in Eq. (9) one obtains the generalized t-J model [11]

$$\begin{aligned} \hat{H}_{t-J} &= \hat{H}_t + \hat{H}_J = - \sum_{i,j} t_{ij} \hat{X}_i^{00} \hat{X}_j^{00} \\ &+ \sum_{i,j} J_{ij} (\hat{\mathbf{S}}_i \cdot \hat{\mathbf{S}}_j - \frac{1}{4} \hat{n}_i \hat{n}_j) + \hat{H}_3. \end{aligned} \quad (12)$$

The first term describes electron hopping by ensuring that the double occupancy is excluded. The second term describes the Heisenberg-like exchange energy

of almost-localized electrons. \hat{H}_3 contains three-site hopping which is believed not to be important and is usually omitted. For effects related to charge fluctuation processes it is plausible to omit it, while for spin-fluctuation processes this approximation may be questionable. The spin and number operators are given by $\hat{\mathbf{S}} = \hat{X}_i^{\bar{\sigma} 0} (\vec{\sigma})_{\bar{\sigma} 1 \bar{\sigma} 2} \hat{X}_i^{0 \bar{\sigma} 2}$; $\hat{n}_i = \hat{X}_i^{\bar{\sigma} \bar{\sigma}}$ where summation over bar indices is assumed [11].

The rather "awkward" commutation relations of $\hat{X}^{\alpha\beta}$ were one of the reason that most researchers in the field prefer to use some representations of the Hubbard operators $\hat{X}^{\alpha\beta}(\hat{f}, \hat{b})$ in terms of fermion and boson operators \hat{f}, \hat{b} , respectively. For instance, in the very popular *slave-boson representation* one has $\hat{X}_i^{0\sigma} = \hat{f}_{i,\sigma} \hat{b}_i^\dagger$ with the constraint $\hat{b}_i^\dagger \hat{b}_i + \sum_{\sigma=1}^N \hat{f}_{i,\sigma}^\dagger \hat{f}_{i,\sigma} = 1$ where \hat{f}_σ destroys a spinon with spin σ and \hat{b}^\dagger creates a holon. Since \hat{f}_σ, \hat{b} obey the canonical Fermi and Bose commutation rules it is, at first glance, very convenient to use this approach since for these operators well-elaborated many-body techniques (Feynman diagrams) exist. However, the constraint makes the spinon and the slave boson strongly coupled, and a naive decoupling of the equations of motion is risky, especially in dimensions $d \geq 2$, sometimes giving fictitious results. Therefore, the present author and his collaborators decided to work directly with the Hubbard operators, thus always keeping the composite object (bound spinon and holon in the language of SB). However, the central question in this approach is - *how to study the quasiparticle dynamic in absence of the canonical Fermi and Bose commutation rules?* The way out was found in the very elegant Baym-Kadanoff technique in obtaining Dyson equations, the method which is independent on the operator algebra - see more in [7] and references therein. Applied to strong correlations we call it the *X-method*. It turns out that the method is very efficient and one can formulate very elegant and controllable $1/N$ expansion which also allows us to study the EPI interaction in a consistent way. We stress that until now there has been no transparent and efficient way to treat the EPI within the slave-boson method.

The basic idea behind the *X-method* [52] is that the Dyson's equation for the electron Green's function can be effectively obtained by introducing the *external potential* $u^{\sigma_1\sigma_2}(1)$ (source) with the Hamiltonian \hat{H}_s

$$\begin{aligned} \int \hat{H}_s d\tau &= \int \sum_{\sigma_1, \sigma_2} u^{\sigma_1\sigma_2}(1) \hat{X}^{\sigma_1\sigma_2}(1) d1 \\ &\equiv u^{\bar{\sigma}_1\bar{\sigma}_2}(\bar{1}) \hat{X}^{\bar{\sigma}_1\bar{\sigma}_2}(\bar{1}) \end{aligned} \quad (13)$$

Here, $1 \equiv (1, \tau)$ and $\int (..) d1 \equiv \int (..) d\tau \sum_1$ and τ is the Matsubara time. In the following, integration over the bared variables $(\bar{1}, \bar{2}, ..)$ and a summation over bared spin variable $(\bar{\sigma}, ..)$ is understood. The sources $u^{\sigma_1\sigma_2}(1)$ are useful in generating higher correlation functions entering the self-energy. The electronic Green's function is defined

by [7], [52]

$$G^{\sigma_1\sigma_2}(1, 2) = \frac{-\langle \hat{T}(\hat{S}\hat{X}^{0\sigma_1}(1)\hat{X}^{\sigma_2 0}(2)) \rangle}{\langle \hat{T}\hat{S} \rangle}, \quad (14)$$

where \hat{T} is the time-ordering operator and $\hat{S} = \hat{T} \exp\{-\int \hat{H}_s(1) d1\}$. We define the *quasiparticle Green's* $g^{\sigma_1\sigma_2}$ and the *Hubbard spectral weight* $Q^{\sigma_1\sigma_2}$

$$g^{\sigma_1\sigma_2}(1, 2) = G^{\sigma_1\sigma_2}(1, 2)Q^{-1, \sigma_2\sigma_2}(2)$$

$$Q^{\sigma_1\sigma_2}(1) = \delta^{\sigma_1\sigma_2}\langle \hat{X}^{00}(1) \rangle + \langle \hat{X}^{\sigma_1\sigma_2}(1) \rangle. \quad (15)$$

It is useful to define the vertex functions

$$\gamma_{\sigma_3\sigma_4}^{\sigma_1\sigma_2}(1, 2; 3) = -\frac{\delta g^{-1, \sigma_1\sigma_2}(1, 2)}{\delta u^{\sigma_3\sigma_4}(3)} \quad (16)$$

which in what follows play very important role in the quasiparticle dynamics. It turns out that the self-energy Σ_g (note $g^{-1} = g_0^{-1} - \Sigma_g$ - [7]) can be expressed via the *charge vertex* $\gamma_c(1, 2; 3) \equiv \gamma_{\sigma\sigma}^{\sigma\sigma}(1, 2; 3)$ and the *spin vertex* $\gamma_s(1, 2; 3) \equiv \gamma_{\sigma\sigma}^{\bar{\sigma}\sigma}(1, 2; 3)$. In the paramagnetic state one has $g^{\sigma_1\sigma_2} = \delta^{\sigma_1\sigma_2}g$, $Q^{\sigma_1\sigma_2} = \delta^{\sigma_1\sigma_2}Q$ and $\Sigma^{\sigma_1\sigma_2} = \delta^{\sigma_1\sigma_2}\Sigma_g$

$$\Sigma_g(1-2) = -\frac{t_0(1-2)}{N}Q(1)$$

$$+ \delta(1-2)\frac{J_0(1-\bar{1})}{N} \langle \hat{X}^{\sigma\sigma}(\bar{1}) \rangle$$

$$- \frac{t_0(1-\bar{1})}{N}g(\bar{1}-\bar{2})\gamma_c(\bar{2}, 2; 1)$$

$$+ \frac{t_2(1, \bar{1}, \bar{3})}{N}g(\bar{1}-\bar{2})\gamma_s(\bar{2}, 2; \bar{3}) + \Sigma_Q(1-2), \quad (17)$$

where $t_2(1, 2, 3) = \delta(1-2)t_0(1-3) - \delta(1-3)J_0(1-2)$. The notation $t_0(1-2)$ (and $J_0(1-2)$) means $t_0(1-2) = t_{0,ij_2}\delta(\tau_1 - \tau_2)$. The first two terms in Eq. (17) represent the effective (reduced) kinetic energy of quasiparticles in the lower Hubbard band. As we shall see below they give rise to the quasiparticle *band narrowing* and to the *shift* of the band center, respectively. The third and fourth terms describe the kinematic and dynamic interaction of quasiparticles with charge and spin fluctuations, respectively, while the term $\Sigma_Q(1, 2)$ takes into account the counterflow of surrounding quasiparticles which takes place because of the local constraint (absence of double occupancy). Σ depends on the vertex functions $\gamma_c(1, 2; 3)$ and $\gamma_s(1, 2; 3)$ and it does not contain a small expansion parameter, like the interaction energy in weakly interacting systems, because the hopping parameter t describes at the same time the kinetic energy and *kinematic interaction* of quasiparticles. This means that there is no

controllable perturbation technique for Σ_g , due to the lack of a small parameter. In the past various decoupling procedures and mean-field like techniques were utilized, such as the steepest descent method in the path integral technique, etc. However, to the author's best knowledge, all decoupling techniques are not only non-systematic and uncontrollable, but moreover they suffer from inability to extract the coherent part of the quasiparticle spectrum. As we shall argue in what follows the coherent quasiparticle band-width (in the case $J = 0$) is proportional to δ , i.e. $W_{qp} \sim \delta \cdot t$. All decoupling technique obtain the band-width $W_d \sim (1 - \alpha \cdot \delta) \cdot t$ [53], with $\alpha \cdot \delta$ finite in the limit $\delta \rightarrow 0$. So obtained W_d is in fact the total band-width for coherent and incoherent quasiparticle motions, i.e. $W_d = W_{qp} + W_{inc}$. Thus the decoupling techniques are inappropriate in studying the coherent quasiparticle motion.

What is then the advantage of the *X-method* and the self-energy in Eq. (17)? This method allows formulation of a controllable $1/N$ expansion for Σ_g by including also the EPI, as shown below. For that purpose it is necessary to generalize the local constraint condition [52]

$$\hat{X}_i^{00} + \sum_{\sigma=1}^N \hat{X}_i^{\sigma\sigma} = \frac{N}{2}, \quad (18)$$

where $N/2$ replaces the unity in Eq. (11). Only in this case the $1/N$ expansion is systematic. It is apparent from Eq. (18) that for $N = 2$ it coincides with Eq. (11) and has the meaning that at most half of all spin states at a given lattice site can be occupied. The particle spectral function $A(\mathbf{k}, \omega) = -\text{Im}G(\mathbf{k}, \omega)/\pi$ must obey the generalized Hubbard sum rule which respects the new local constraint in Eq. (18)

$$\int d\omega A(\mathbf{k}, \omega) = \frac{1 + (N-1)\delta}{2}.$$

The $N > 2$ generalization of the local constraint allows us to make a *controllable* $1/N$ expansion of the self-energy with respect to the small quantity $1/N$ (when $N \gg 1$). Physically this procedure means that we are selecting a class of diagrams in the self-energy and response functions which might be important in some parameter regime. In [30], [31], [32] it was shown that there is a systematic $1/N$ expansion for vertices γ_c and γ_s as well as for other functions

$$g = g_0 + g_1/N + \dots, \quad (19)$$

$$Q = Nq_0 + Q_1 + Q_2/N \dots,$$

$$\Sigma = \Sigma_0 + \Sigma_1/N + \dots$$

etc.

1. The main results of the X-method

The first nontrivial terms in *leading O(1)-order* are Σ_0 and g_0 - for details see in [7], [30], [31], [32], which in fact

describe the *coherent part* of the quasiparticle self-energy and the Green's function

$$\begin{aligned} g_0(\mathbf{k}, \omega) &\equiv G_0(\mathbf{k}, \omega)/Q_0 = \frac{1}{\omega - (\epsilon_0(\mathbf{k}) - \mu)}, \\ \epsilon_0(\mathbf{k}) &= \epsilon_c - q_0 t_0(\mathbf{k}) - \frac{1}{N_L} \sum_{\mathbf{p}} J_0(\mathbf{k} + \mathbf{p}) n_F(\mathbf{p}), \\ \epsilon_c &= \frac{1}{N_L} \sum_{\mathbf{p}} t_0(\mathbf{p}) n_F(\mathbf{p}), \\ Q_0 &= \langle \hat{X}_i^{00} \rangle = N q_0 = N \frac{\delta}{2}. \end{aligned} \quad (20)$$

where N_L is the number of lattice site, $\epsilon_0(\mathbf{k})$ is the *quasiparticle energy* for the coherent motion and ϵ_c is the *level shift*. Here, $t_0(\mathbf{k})$ and $J_0(\mathbf{k})$ are Fourier transforms of $t_{0,ij}$ and $J_{0,ij}$, respectively. For $t = t'$ one has $t_0(\mathbf{k}) = 2t_0(\cos k_x + \cos k_y) + 2t' \cos k_x \cos k_y$ and $J_0(\mathbf{k}) = 2J_0(\cos k_x + \cos k_y)$, since the lattice constant is let $a = 1$. Since $Q_0(\sim N\delta)$ this means that the *quasiparticle residuum* vanishes at vanishing of doping ($\delta \rightarrow 0$). This is physically plausible since for $\delta \rightarrow 0$ the coherent motion in the t-J model is blocked. The chemical potential μ is obtained from the condition $1 - \delta = 2 \sum_{\mathbf{p}} n_F(\mathbf{p})$ which gives large Fermi surface, see discussion below. Note that Σ_Q in Eq. (17) is of the $O(1/N)$ order.

We summarize the main results obtained by the *X-method* to the leading $O(1)$ order and compare them with the corresponding ones in the slave boson (*SB*)-method [30], [31], [32]: (1) up to the $O(1)$ order, $g_0(\mathbf{k}, \omega)$ describes the *coherent motion* of quasiparticles in the metallic state, whose contribution to the total spectral weight of the particle Green's function $G_0(\mathbf{k}, \omega)$ is $Q_0 = N\delta/2$, i.e. $G_0(\mathbf{k}, \omega) = Q_0 g_0(\mathbf{k}, \omega)$ to the leading order, so we dealing with a Landau-Fermi liquid. This means that the quasiparticle residuum (and the metallic state) vanishes for zero doping $\delta = 0$ and the system is in the Mott insulating state. The quasiparticle energy is dominated by the exchange parameter if $J_0 > \delta t_0$, i.e. for very low doping, since in cuprates ($J_0/t_0 < 1/3$). For $J_0 = 0$ there is *band narrowing* since $\delta < 1$ and the quasiparticle band-width is proportional to δ , i.e. $W = z \cdot \delta \cdot t_0$. These results are identical to the corresponding ones in the *SB* method. This does not mean that the next leading terms coincide in both methods. This is actually not the case for a number of quantities (response functions). This is understandable since the *X*-method keeps the composite object (correlated motion of spinon and holon), while in the *SB* method they are decoupled. Only after invoking the existence of gauge fields (also fictitious particles) one can keep spinon and holon together in the *SB* model, if at all. (2) The *X*-method respects the local constraint at each lattice site in every step of calculations, which guarantees the correct study of response functions. (3) In the (important) paper [54] - which is based on the theory elaborated in [30], [31], [32], it was shown that there is large discrepancy in approximate calculations within the *SB* and *X* methods. For instance, in the superconducting state the anomalous self-energy

(which is of $O(1/N)$ -order in the $1/N$ expansion) of the *X*- and *SB* methods *differ substantially*. As a result, the *SB* method erroneously predicts *superconductivity* due to the kinematic interaction in the *t-J* model (for $J = 0$) with large T_c , while the *X*-method gives extremely small T_c (≈ 0) [54]. The reason for this discrepancy is that the calculations done within the *SB* method miss a class of compensating diagrams, which are in contrast taken into account automatically within the *X* method. So, although the two approaches yield some similar results in leading $O(1)$ order their implementation in the next leading $O(1/N)$ order show that they are indeed different - see discussion below. Note that the $1/N$ expansion in the *X*-method is well-defined and transparent. (4) The renormalization of the EPI coupling constant by strong correlations is different in the two approaches even in the large N -limit, as shown below; (5) The optical conductivity $\sigma_1(\omega, \mathbf{q} = 0) \equiv \sigma_1(\omega)$ and the optics sum-rule exhibit very interesting behavior as a function of doping concentration

$$\int_0^{\omega_c} d\omega \sigma(\omega) = \frac{\pi}{4} \delta \cdot N e^2 a^2 \epsilon_c. \quad (21)$$

It is seen that the optics sum-rule is proportional to the number of holes δ , instead of $n = 1 - \delta$ as it would be in the weakly interacting case [7]. Here a is the lattice constant. (6) Note, that the volume below the Fermi surface in the case of strong correlations scales with $n = 1 - \delta$, i.e. the *Fermi surface is large* like in the conventional Fermi liquid. The above analysis clearly shows significant difference ((5) vs (6)) in response functions of strongly correlated systems and the canonical Landau-Fermi liquid.

IV. THE FORWARD SCATTERING PEAK IN THE EPI OF CUPRATES

The EPI coupling constant in *LTSC* materials is calculated by the local-density functional (*LDA*) method. The latter is suitable for ground state properties of crystals and it is based on an effective electronic crystal potential V_g . Since in principle V_g differs significantly from $\Sigma_0(\mathbf{k}, \omega = 0)$ (the many body effective potential - see [7]) then the *LDA* coupling constant $g_{EP}^{(LDA)}$ can be also very different from the real coupling constant g_{EP} . Strictly speaking the EPI does not have meaning in the *LDA* method - see discussion in [7], because the latter treats ground state properties of materials, while the EPI is due to excited states and inelastic processes in the system. We shall not deal with this problem here - see [7].

A. LDA method for the EPI in cuprates

The *LDA* method considers electrons in the ground state (there is a generalization to finite T), whose energy can be calculated by knowing the spectrum $\{\epsilon_k\}$ of the

Kohn-Sham (Schrödinger like) equation

$$[\frac{\hat{\mathbf{p}}^2}{2m} + V_g(\mathbf{r})]\psi_k(\mathbf{r}) = \epsilon_k \psi_k(\mathbf{r}), \quad (22)$$

which depends on the *effective one-particle potential*

$$V_g(\mathbf{r}) = V_{ei}(\mathbf{r}) + V_H(\mathbf{r}) + V_{XC}(\mathbf{r}). \quad (23)$$

Here, V_{ei} is the electron-lattice potential, V_H is the Hartree term and V_{XC} describes exchange-correlation effects - see [7]. Because the EPI depends on the excited states (above the ground state) of the system, this means that in principle the LDA method can not describe it - see [7]. However, by using an analogy with the microscopic Migdal-Eliashberg theory one can define the EPI coupling constant $g^{(Mig)} = g\Gamma_c/\varepsilon$ also in the LDA theory, see [7]. It reads

$$\begin{aligned} g_{\alpha, ll'}^{(LDA)}(\mathbf{k}, \mathbf{k}') &= \sum_n g_{\alpha, nll'}^{(LDA)}(\mathbf{k}, \mathbf{k}') \\ &= \langle \psi_{\mathbf{k}l} | \sum_n \frac{\delta V_g(\mathbf{r})}{\delta R_{n\alpha}} | \psi_{\mathbf{k}'l'} \rangle, \end{aligned} \quad (24)$$

where n means summation over the lattice sites, $\alpha = x, y, z$ and the wave function $\psi_{\mathbf{k}l}$ is the solution of the Kohn-Sham equation. Formally one has $\delta V_g/\delta \mathbf{R}_n = \Gamma_{LDA} \varepsilon_e^{-1} \nabla V_{ei}$. Even in such a simplified approach it is difficult to calculate $g_{\alpha, ll'}^{(LDA)} = g_{\alpha, n}^{RMTA} + g_{\alpha, n}^{nonloc}$ because it contains the *short-range (local) coupling*

$$g_{\alpha, n}^{RMTA} \sim g_{\alpha, n}^{RMTA}(\mathbf{k}, \mathbf{k}') \sim \langle Y_{lm} | \hat{r}_\alpha | Y_{l'm'} \rangle \quad (25)$$

with $\Delta l = 1$, and the *long-range coupling*

$$g_{\alpha, n}^{nonloc}(\mathbf{k}, \mathbf{k}') \sim \langle Y_{lm} | (\mathbf{R}_n^0 - \mathbf{R}_m^0)_\alpha | Y_{l'm'} \rangle \quad (26)$$

with $\Delta l = 0$. In most calculations the local term $g_{\alpha, n}^{RMTA}$ is calculated only, which is justified in simple metals only but not in the HTSC oxides. In cuprates the local term gives a very small EPI coupling $\lambda^{RMTA} \sim 0.1$, which is apparently much smaller than the experimental value $\lambda > 1$, and which gives rise to a pessimistically small T_c [55]. The small λ^{RMTA} was also one of the reasons for discarding the EPI as pairing mechanism in HTSC oxides. At the beginning of the HTSC era the electron-phonon spectral function $\alpha^2 F(\omega)$ was calculated for the case $La_{2-x}Sr_xCuO_4$ in [58] by using the first-principles band structure calculations and the nonorthogonal tight-binding theory of lattice dynamics. The value $\lambda = 2.6$ was obtained and with the assumed $\mu^* = 0.13$ this gave $T_c = 36 K$. However, these calculations also predicted a lattice instability for the oxygen breathing mode in $La_{1.85}Sr_{0.15}CuO_4$ that has never been observed. Moreover, the same method was applied to $YBa_2Cu_3O_7$ in [58] where it was found $\lambda = 0.5$, which at best provides $T_c = (19 - 30) K$. In fact the calculations in [58] did

not take into account the Madelung coupling (i.e. they neglected the matrix elements with $\Delta l = 0$).

However, because of the weak screening of the ionic (long-range) Madelung coupling in HTSC oxides - especially for vibrations along the *c*-axis - it is necessary to include the nonlocal term $g_{\alpha, n}^{nonloc}$. This task was achieved within the LDA approach by the Pickett's group [25], where the EPI coupling for $La_{2-x}M_xCuO_4$ is calculated within the *frozen phonon* method for $\mathbf{q} = 0$ modes. By extrapolating the result for $\mathbf{q} = 0$ to finite q they obtained $\lambda = 1.37$ and $\omega_{\log} \approx 400 K$, and for $\mu^* = 0.1$ they predicted that $T_c = 49 K$ ($T_c \approx \omega_{\log} \exp\{-1/[(\lambda/(1 + \lambda)) - \mu^*]\}$). The justification of this procedure was questioned in [7] were smaller λ was obtained. For more details see Ref. [7] and references therein. Next, some calculations, based on the tight-binding parametrization of the band structure in $YBa_2Cu_3O_7$, gave rather large EPI coupling $\lambda \approx 2$ and $T_c = 90 K$ [26].

We point out, that model calculations which take into account the long-range ionic Madelung potential appropriately [56], [57] also gave rather large coupling constant $\lambda \sim 2$, which additionally hints to the importance of long-range forces in the EPI - see [7] and references therein..

Since in HTSC oxides the plasma frequency along the *c*-axis, ω_{pl}^c , is of the order (or even less) of some characteristic *c*-axis vibration modes, it is necessary to include the *nonadiabatic effects* in the EPI coupling constant, i.e. its frequency dependence $g_{\alpha, n} \sim g^0/\varepsilon_{cc}(\omega)$. This non-adiabaticity was partly accounted for by the Falter group [27] by calculating the electronic dielectric function along the *c*-axis $\varepsilon_{cc}(\mathbf{k}, \omega)$ in the RPA approximation. The result was that $g_{\alpha, n}$ increased appreciably beyond its (well screened) metallic part, which gave a large increase of the EPI coupling not only in the phonon modes but also in the plasmon one. This question deserves much more attention than what it received in the past.

The electron band structure and the Fermi surface can be satisfactorily described by the tight binding model, which is characterized with various hopping parameters t_{ij} and the local atomic (ionic) levels ϵ_i . Accordingly, there are two kinds of the EPI coupling. The *covalent part* of the EPI is due to strong *covalency* of the *Cu* and *O* orbital in the CuO_2 planes. In this case, the EPI coupling constant is characterized by the parameter ("field") $E^{cov} \sim \partial t_{p-d}/\partial R \sim q_{cov} t_{p-d}$, where t_{p-d} is the hopping integral between $Cu(d_{x^2-y^2})$ and $O(p_{x,y})$ orbital and the length q_{cov}^{-1} characterizes the spacial exponential fall-off of the hopping integral t_{p-d} . As the phonon Raman scattering shows, the covalent EPI is unable to explain the strong phonon renormalization (the self-energy features) in the B_{1g} mode in $YBa_2Cu_3O_7$ by superconductivity, since in this mode the *O*-ions vibrate along the *c* - *axis* in opposite directions and for this mode $\partial t_{p-d}/\partial R$ is zero in the first order in the phonon displacement. Therefore, the EPI in this mode is certainly due to the *ionic contribution* which comes from the change in Madelung energy, as it was first proposed

in [56], [57]. Namely, the Madelung interaction creates an electric field perpendicular to the CuO_2 planes, which is due to the surrounding ions that form an asymmetric environment. In that case the site energies ϵ_i^0 contain the matrix element $\epsilon^{ion} = \langle \psi_i | V(\mathbf{r}) | \psi_i \rangle$, where $|\psi_i\rangle$ is the atomic wave function at the i -th site, while the potential $V(\mathbf{r})$ steams from the surrounding ions. In the simple and transition metals the surrounding ions are well screened and therefore the change of ϵ^{ion} in the presence of phonons is negligible, in contrast to cuprates which are almost *ionic compounds*, in particular along the c -axis where the change of ϵ^{ion} is appreciable and characterized by the field strength $E^{ion} = V_M/d_n$. Here, V_M is the characteristic Madelung potential due to the surrounding ions and d_n is the distance between the neighboring ions. Immediately after the discovery of cuprates it was assumed in many papers [58] that the covalent part dominates the EPI in these materials. However, the calculation that considered only the covalent effects [58] gave a rather small T_c ($\sim 10\text{-}20$ K in $YBCO$, and $20\text{-}30$ K in $La_{1.85}Sr_{0.15}CuO_4$). It turns out that in cuprates the opposite inequality $E^{ion} \gg E^{cov}$ is realized for most c -axis phonon modes in spite of the fact that $q_{cov} > 1/d_n$ - see more in [7] and references therein. This is supported by detailed theoretical studies of $YBCO$ [57], where the change in the *ionic Madelung energy* due to the out of plane oxygen vibration in the B_{1g} mode is calculated. Similar to $YBCO$, the large superconductivity-induced phonon self-energy effects in $HgBa_2Ca_3Cu_4O_{10+x}$ and in $(Cu, C)Ba_2Ca_3Cu_4O_{10+x}$ for the A_{1g} modes are also due to the ionic (Madelung) coupling. In these modes oxygen ions move also along the c -axis and the ionicity of the structure is involved in the EPI. This type of *long-range EPI* is absent in usual isotropic metals (*LTSC* superconductors), where the large Coulomb screening makes EPI local. Similar ideas were recently incorporated into the Eliashberg equations in [59]. The weak screening along the c -axis, which is due to the very small hopping integral for carrier motion, is reflected in the very small plasma frequency $\omega_p^{(c)}$ along this axis. Since for some optical phonon modes one has $\omega_{ph} > \omega_p^{(c)}$, nonadiabatic effects in the screening are important. The latter can give rise to much larger EPI coupling constant for this modes [27]. These ideas are also supported by the recent ARPES measurements on the single-layer $Bi_2Sr_2CuO_6$ ($Bi2201$) where the coupling of electrons with phonons in the region $30\text{--}60$ meV in the overdoped compound is significantly reduced compared to the optimally doped case. This can be explained by the larger electronic screening along the c -axis in overdoped compound.

To summarize, ARPES, electron and phonon Raman scattering measurements in the normal and superconducting state of cuprates gave the following important results: (a) phonons interact strongly with the electronic continuum, i.e. EPI is substantial; (b) the ionic contribution (the Madelung energy) to EPI interaction for c -axis phonon modes gives substantial contribution to the (large) EPI coupling constant ($\lambda > 1$).

B. Renormalization of the electron-phonon interaction by strong correlations

Based on the above discussion the minimal (toy) model Hamiltonian for HTSC cuprates contains besides the t-J terms also the electron-phonon interaction

$$\begin{aligned} \hat{H} &= \hat{H}_{tJ} + \sum_{i,\sigma} \epsilon_{a,i}^0 \hat{X}_i^{\sigma\sigma} + \hat{H}_{ph} \\ &+ \hat{H}_{EP}^{ion} + \hat{H}_{EP}^{cov} + \hat{V}_{LC}, \\ \hat{H}_{EP}^{ion} &= \sum_{i,\sigma} \hat{\Phi}_i (\hat{X}_i^{\sigma\sigma} - \langle \hat{X}_i^{\sigma\sigma} \rangle), \\ \hat{H}_{EP}^{cov} &= -\frac{1}{N} \sum_{i,j,\sigma} \frac{\partial t_{0,ij}}{\partial (\mathbf{R}_i^0 - \mathbf{R}_j^0)} (\hat{\mathbf{u}}_i - \hat{\mathbf{u}}_j) \hat{X}_i^{\sigma 0} \hat{X}_j^{0\sigma}. \end{aligned} \quad (27)$$

where \hat{H}_{EP}^{ion} , \hat{H}_{EP}^{cov} are the ionic and covalent contribution to the EPI, respectively. We consider first the ionic term where $\hat{\Phi}_i(\hat{\mathbf{u}}_{L,\kappa})$ describes the change of the atomic energy $\epsilon_{a,i}^0$ due to the change of long-range Madelung energy in the presence of phonon displacements $\hat{\mathbf{u}}_{L,\kappa}$ of other atoms. L and κ enumerate unit lattice vectors and atoms in the unit cell, respectively. Note that the theory is formulated for the general nonlinear form of $\hat{\Phi}_i(\hat{\mathbf{u}}_{L,\kappa})$ dependence, and the following analysis holds in principle also for an anharmonic EPI. The term proportional to $\langle \hat{X}_i^{\sigma\sigma} \rangle$ in Eq. (27) is introduced in order to have $\langle \hat{\Phi}_i \rangle = 0$ in the equilibrium state. We stress that the X-method allows controllable calculation of the covalent contribution [11]. In contrast, the treatment of EPI by the *SB* method is complicated and not well defined, giving sometimes wrong results - see more in [7].

After technically lengthy calculations, which are performed in [30], [31], the expression for the ionic contribution to the EPI part (frequency-dependent) of the self-energy reads

$$\begin{aligned} \Sigma_{EP}^{(dyn)}(1, 2) &= -V_{EP}(\bar{1}, \bar{2}) \gamma_c(1, \bar{3}; \bar{1}) g_0(\bar{3}, \bar{4}) \gamma_c(\bar{4}, 2; \bar{2}) \\ V_{EP}(1, 2) &= \varepsilon_e^{-1}(1 - \bar{1}) V_{EP}^0(\bar{1} - \bar{2}) \varepsilon_e^{-1}(\bar{2} - 2) \\ V_{EP}^0(1 - 2) &= -\langle T\hat{\Phi}(1)\hat{\Phi}(2) \rangle \end{aligned} \quad (28)$$

The propagator $V_{EP}^0(1 - 2)$ (which includes also the coupling constant) of the bare EPI comprises in principle also the anharmonic contribution. From Eq. (28) it is seen that in strongly correlated systems the ionic part of the EPI is proportional to the square of the *three-point charge vertex* $\gamma_c(1, 2; 3)$ (due to correlations). The self-energy is given by

$$\Sigma_{EP}^{(dyn)}(\mathbf{k}, \omega) = \int_0^\infty d\Omega \langle \alpha^2 F(\mathbf{k}, \mathbf{k}', \Omega) \rangle_{\mathbf{k}'} R(\omega, \Omega)$$

$$R(\omega, \Omega) = -2\pi i(n_B(\Omega) + \frac{1}{2})$$

$$+ \psi(\frac{1}{2} + i\frac{\Omega - \omega}{2\pi T}) - \psi(\frac{1}{2} - i\frac{\Omega + \omega}{2\pi T}) \quad (29)$$

where the (momentum-dependent) Eliashberg spectral function $\alpha^2 F(\mathbf{k}, \mathbf{k}', \omega)$ is defined below, $n_B(\Omega)$ is the Bose function and $\psi(x)$ is the di-gamma function - [7], [30], [31].

C. Forward scattering peak in the charge vertex γ_c

The three-point *charge vertex* $\gamma_c(1, 2; 3)$ plays an important role in renormalization of all charge processes, such as EPI in Eq. (28), Coulomb scattering and the scattering on non-magnetic impurities. $\gamma_c(1, 2; 3)$ (and its Fourier transform $\gamma_c(\mathbf{k}, q)$, $q = (\mathbf{q}, iq_n)$, $q_n = 2\pi n T$) was calculated in the $t - J$ model in leading $O(1)$ order [30], [31], [32], [7]. It is the solution of the following linear integral equation

$$\gamma_c(1, 2; 3) = \delta(1 - 2)\delta(1 - 3)$$

$$+ t_0(1 - 2)g_0(1 - \bar{1})g_0(\bar{2} - 1^+)\gamma_c(\bar{1}, \bar{2}; 3)$$

$$+ \delta(1 - 2)t_0(1 - \bar{1})g_0(\bar{1} - \bar{2})g_0(\bar{3} - 1)\gamma_c(\bar{2}, \bar{3}; 3)$$

$$- J_0(1 - 2)g_0(1 - \bar{1})g_0(\bar{2} - 2)\gamma_c(\bar{1}, \bar{2}; 3) \quad (30)$$

The (charge) vertex function $\gamma_c(\mathbf{k}, q)$ describes a specific screening of the charge potential due to strong correlations. In the presence of an external perturbation (u) there is a *change of the band-width*, as well as the *change of the local chemical potential*, which comes from the suppression of double occupancy. These processes are contained in the second and the third term of Eq. (30). The central result is that for momenta \mathbf{k} laying at (and near) the Fermi surface, $\gamma_{c0}(\mathbf{k}, \mathbf{q}, \omega = 0)$ has a strong *forward scattering peak* at $\mathbf{q} = 0$, which is very pronounced for lower doping $\delta (\ll 1)$. On the other hand, the backward (at large \mathbf{q}) scattering is substantially suppressed, see Fig. 4a. Such a behavior of the vertex function means that a quasiparticle moving in the strongly correlated medium digs up a *giant correlation hole* with the radius $\xi_{ch} \approx a/\delta$, where a is the lattice constant. The effect of the J -term is small, since γ_c is determined by charge fluctuations which are spread over the whole bare bandwidth $W_B \sim zt_0 \gg J_0$.

We stress that γ_{c0} in Fig. 4a is calculated in the *adiabatic approximation*, i.e. for $\omega = 0$ in $\gamma_{c0}(\mathbf{k}, \mathbf{q}, \omega)$. However, in the *nonadiabatic regime* $\omega > \mathbf{q} \cdot \mathbf{v}_F(\mathbf{q})$ the vertex function reaches its maximal value $\gamma_c(\mathbf{k}_F, \mathbf{q} = \mathbf{0}, \omega) = 1$, see Fig. 4b. This nonadiabaticity occurs whenever the phase velocity (ω/q) of charge excitations is larger than the Fermi velocity. This effect is realized in case of high

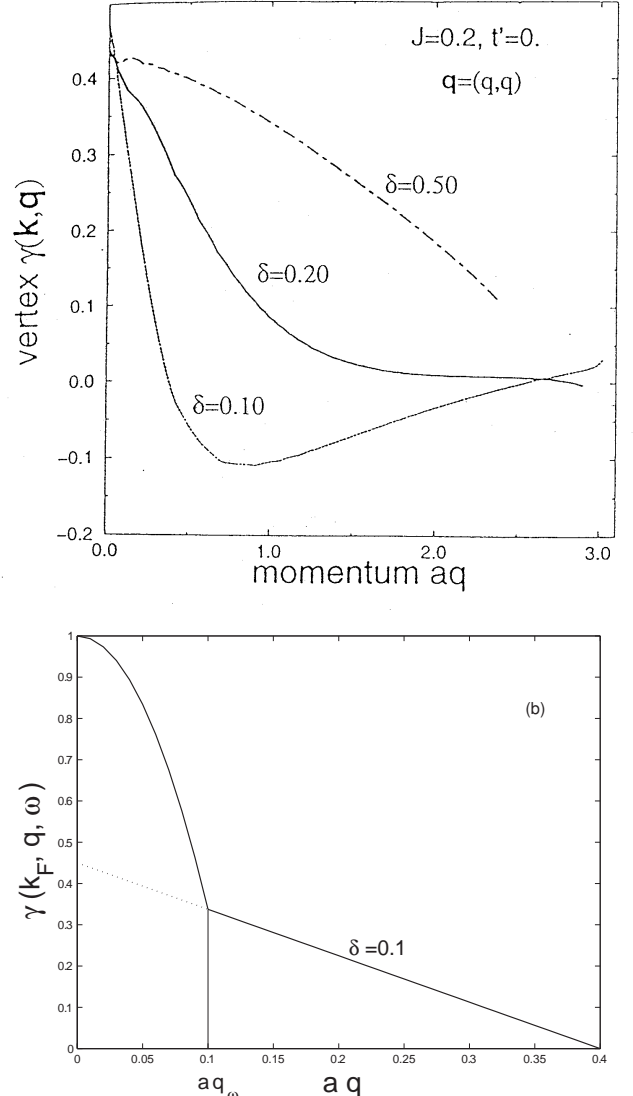


FIG. 4: (a) Adiabatic ($\omega = 0$) vertex function $\gamma(\mathbf{k}_F, \mathbf{q})$ of the t - J model as a function of the momentum aq with $\mathbf{q} = (q, q)$ for three different doping levels δ . From Ref. [32]. (b) Non-adiabatic ($\omega \neq 0$) vertex function $\gamma(\mathbf{k}_F, \mathbf{q}, \omega)$ schematically with $q\omega = \omega/v_F$.

energy phonons. This means that due to nonadiabatic effects strong correlations do not suppress the EPI coupling with optical phonons at $q = 0$, in contrast to a number of claims [62] that they do.

Since the real physics is characterized by $N = 2$ one can ask - how *reliable* are the calculations of $\gamma_c(\mathbf{k}_F, \mathbf{q})$ by the $1/N$ expansion method and in the limit $N \rightarrow \infty$. Here let us mention that VL (Ginzburg) used to paraphrase a Landau's remark "that the many-body theory is an experimental science". This means that the correctness of the theory is tested by experiments. In this respect, the exact diagonalization of charge correlation function $N(\mathbf{q}, \omega)$ in the t - J model [60] shows clearly that low-energy charge scattering processes at large momenta

$|\mathbf{q}| \approx 2k_F$ are strongly suppressed compared to scattering at small transferred momenta ($|\mathbf{q}| \ll 2k_F$). This unambiguously confirms the results obtained by the X-method in [30], [31], [32] on the suppression of backward scattering in the vertex. Second, very recent Monte Carlo (numerical) calculations of the vertex function $\gamma_c(\mathbf{k}_F, \mathbf{q})$ in the Hubbard model with finite U [62] show clear development of the forward scattering peak in $\gamma_c(\mathbf{k}_F, \mathbf{q})$, that is more pronounced for larger U . This result definitely confirms the predictions of appearance of the forward scattering peak in $\gamma_c(\mathbf{k}_F, \mathbf{q})$ in Refs. [30], [31], [32], [7]. For analytical theories numerical calculations in some models play the role of an experiment, then the above theory of strong correlations and EPI is in that sense confirmed experimentally in accord with the Landau remark.

Finally, it is possible to calculate the contribution of *covalent EPI* coupling \hat{H}_{EP}^{cov} to the self-energy. In this case, the vertex renormalization by strong correlations is determined by the four-point *vertex function* $\gamma_t(1, 2; 3, 4)$. The latter is an important ingredient of EPI not only in HTSC cuprates but also in heavy fermion systems. The calculations in [11] show that γ_t differs from that obtained by the mean-field approximation SB model, what implies that the previous studies of EPI in heavy fermion materials, in which the "covalent" coupling $\sim \gamma_t$ dominates, should be reconsidered by using the correct form of γ_t .

D. Pairing and transport EPI coupling constants

Depending on the symmetry of superconducting order parameter $\Delta(\mathbf{k}, \omega)$ (*s*-, *d*-wave pairing) various averages (over the Fermi surface) of $\alpha^2 F(\mathbf{k}, \mathbf{k}', \omega)$ enter the Eliashberg equations. Assuming that the superconducting order parameter transforms according to the representation Γ_i ($i = 1, 3, 5$) of the point group C_{4v} of a square lattice (in the CuO_2 planes), the appropriate symmetry-projected spectral function is given by

$$\begin{aligned} \alpha^2 F_i(\tilde{\mathbf{k}}, \tilde{\mathbf{k}}', \omega) &= \frac{N_{sc}(0)}{8} \sum_{\nu, j} |g_{0,scr}(\tilde{\mathbf{k}}, \tilde{\mathbf{k}} - T_j \tilde{\mathbf{k}}', \nu)|^2 \times \\ &\times \delta(\omega - \omega_\nu(\tilde{\mathbf{k}} - T_j \tilde{\mathbf{k}}')) |\gamma_c(\tilde{\mathbf{k}}, \tilde{\mathbf{k}} - T_j \tilde{\mathbf{k}}')|^2 D_i(j), \quad (31) \end{aligned}$$

where $\tilde{\mathbf{k}}$ and $\tilde{\mathbf{k}}'$ are the momenta on the Fermi line in the irreducible Brillouin zone which is equal to 1/8 of the total Brillouin zone. Here, $g_{0,scr}(\mathbf{k}, \mathbf{p}, \nu)$ is the EPI coupling constant for the ν -the mode, where the screening by long-range Coulomb interaction is included, i.e. $g_{0,scr}(\mathbf{k}, \mathbf{p}, \nu) = g_0(\mathbf{k}, \mathbf{p}, \nu)/\varepsilon_e(\mathbf{p})$. The density of states $N_{sc}(0)$ is renormalized by strong correlations, where $N_{sc}(0) = N_0(0)/q_0$ and $q_0 = \delta/2$ in the $t-t'$ model ($J = 0$). In the $t - J$ model $N_{sc}(0)$ has another form which does not diverge for $\delta \rightarrow 0$, but one has $N_{sc}(0)(\sim 1/J_0) > N_0(0)$, where the bare density

of states $N_0(0)$ is calculated, for instance by the *LDA* scheme. T_j , where $j = 1,..8$, denotes the eight point-group transformations that form the symmetry group of the square lattice. This group has five irreducible representations which we distinguish by the label $i = 1, 2, \dots, 5$. In the following the representations $i = 1$ and $i = 3$, which correspond to the *s*- and *d*-wave symmetry of the full rotation group, respectively, will be of importance. $D_i(j)$ is the representation matrix of the j -th transformation for the representation i . For each symmetry one obtains the corresponding spectral function $\alpha^2 F_i(\omega) = \langle \langle \alpha^2 F_i(\tilde{\mathbf{k}}, \tilde{\mathbf{k}}', \omega) \rangle \rangle_{\tilde{\mathbf{k}}}$, which (in the first approximation) determines the transition temperature for the order parameter with the symmetry Γ_i . In the case $i = 3$ the electron-phonon spectral function $\alpha^2 F_3(\omega)$ in the *d-channel* is responsible for *d*-wave superconductivity represented by the irreducible representation Γ_3 (or sometimes labelled as B_{1g}).

Performing similar calculations (as above) for the phonon-limited resistivity one finds that the latter is related to the *transport spectral function* $\alpha^2 F_{tr}(\omega) = \langle \langle \alpha^2 F(\mathbf{k}, \mathbf{k}', \omega) [\mathbf{v}(\mathbf{k}) - \mathbf{v}(\mathbf{k}')]^2 \rangle \rangle_{\mathbf{k}} / 2 \langle \langle \mathbf{v}^2(\mathbf{k}) \rangle \rangle_{\mathbf{k}'}$, where $\mathbf{v}(\mathbf{k})$ is the Fermi velocity. The effect of strong correlations on EPI was discussed in [30] and more extensively in [31], [32] within the model where the phonon frequencies $\omega(\tilde{\mathbf{k}} - \tilde{\mathbf{k}}')$ and $g_{0,scr}(\mathbf{k}, \mathbf{p}, \lambda)$ are weakly momentum dependent. In order to illustrate the effect of strong correlations on $\alpha^2 F_i(\omega)$ we consider the latter functions at zero frequency ($\omega = 0$) which are then reduced to the (so called) "enhancement" functions

$$\Lambda_i = \frac{N_{sc}(0)}{8N_0(0)} \sum_{j=1}^8 \langle \langle |\gamma_c(\tilde{\mathbf{k}}, \tilde{\mathbf{k}} - T_j \tilde{\mathbf{k}}')|^2 \rangle \rangle_{\tilde{\mathbf{k}}} D_i(j). \quad (32)$$

Note that in the case $J = 0$ one has $N_{sc}(0)/N_0(0) = q_0^{-1}$, where q_0 is related to the doping concentration, i.e. $q_0 = \delta/2$. Similarly, the correlation effects on the resistivity $\rho(T)(\sim \Lambda_{tr})$ renormalize the transport coupling constant Λ_{tr} (similarly to Λ_i it is defined via $\alpha^2 F_{tr}(\omega)$). Note that for quasiparticles with an isotropic band the absence of correlations implies that $\Lambda_1 = \Lambda_{tr} = 1$, $\Lambda_i = 0$ for $i > 1$. The averages in Λ_1 , Λ_3 and Λ_{tr} , shown in Fig. 5, were performed numerically in [31] by using a realistic anisotropic band dispersion in the $t-t'$ -J model and the corresponding charge vertex. The three curves are multiplied by a common factor so that Λ_1 approaches 1 in the empty-band limit $\delta \rightarrow 1$, when strong correlations are absent. Note that T_c in the weak-coupling limit and in the i -th channel scales like $T_c^{(i)} \approx \langle \omega \rangle \exp(-1/(\Lambda_i - \mu_i^*))$, where μ_i^* is the Coulomb pseudopotential in the i -th channel and $\langle \omega \rangle$ is the averaged phonon frequency.

Several interesting results, which are shown in Fig. 5, should be stressed. *First*, in the empty-band limit $\delta \rightarrow 1$ the *d*-wave coupling constant Λ_3 is much smaller than the *s*-wave coupling constant Λ_1 , i.e. $\Lambda_3 \ll \Lambda_1$. Furthermore, the totally symmetric function Λ_1 decreases with decreased doping. *Second*, in both models Λ_1 and Λ_3 approach one another at some small doping $\delta \approx 0.1 - 0.2$,

where $\Lambda_1 \approx \Lambda_3$ but still $\Lambda_1 > \Lambda_3$. By taking into account residual Coulomb repulsion of quasiparticles which usually have $\mu_d^* \ll \mu_s^*$ one finds that the s-wave superconductivity (which is governed by the coupling constant Λ_1) is strongly suppressed by μ_s^* , while the d-wave superconductivity (governed by Λ_3) is only weakly affected by μ_d^* . In that case the d-wave superconductivity due to EPI becomes more stable than the s-wave superconductivity at sufficiently small doping δ , i.e. $T_c^{(d)} > T_c^{(s)}$. Interference experiments [61] show that this occurs in underdoped, optimally doped and overdoped cuprates. This means, that EPI is responsible for the strength of pairing in cuprates, while the d-wave superconductivity is triggered by the residual Coulomb interaction (including also spin-fluctuation scattering). *Third*, in the nonadiabatic regime when the phonon frequency fulfills the condition $\omega_{ph} > \mathbf{q} \cdot \mathbf{v}_F(\mathbf{q})$ the enhancement function $\gamma_c^2(\mathbf{k}_F, \mathbf{p}, \omega_{ph})/q_0$ is substantially larger compared to the adiabatic one, which is shown in Fig. 5. This means that the strength of EPI coupling is differently affected by strong correlations for different phonons. For a given frequency the coupling to phonons with momenta $p < p_c = \omega/v_F$ is *enhanced*, while the coupling to those with $p > p_c = \omega/v_F$ is substantially reduced due to suppression of backward scattering by strong correlations. *Fourth*, the *transport coupling constant* Λ_{tr} (not properly normalized in Fig. 5 - see the correction in [32]) is reduced in the presence of strong correlations, especially for lower doping where one has approximately $\Lambda_{tr} < \Lambda/3$ [32]. This is an important result since it resolves the experimental puzzle - that λ_{tr} (which enters resistivity $\rho(T) \sim \lambda_{tr} T$) is *much smaller* than the coupling constant λ (which enters the self-energy Σ and T_c), i.e. $\lambda_{tr} \ll \lambda$. To remind the reader, $\lambda_{tr} \approx \lambda$ is realized in almost all LTSC. One of the important differences between LTSC and HTSC in cuprates lies in strong correlations present in cuprates which causes the forward scattering peak in charge scattering processes. *Fifth*, the forward scattering peak in EPI of strongly correlated systems is a general phenomenon *affecting electronic coupling to all phonons*. This means that the bare EPI coupling constant for each phono-mode (ν) must be multiplied by the vertex function, i.e. $g_\nu^0(\mathbf{k}, \mathbf{q}) \rightarrow \gamma(\mathbf{k}, \mathbf{q})g_\nu^0(\mathbf{k}, \mathbf{q})$.

As we already said, Monte Carlo (numerical) calculations of the Hubbard model at finite U - performed by Scalapino's group [62], show that the forward scattering peak in the EPI coupling constant (and the charge vertex) develops as U is increased. These numerical results prove the essential correctness of EPI theory based on the X method. The latter effect is more pronounced at lower doping. Results similar to Monte Carlo ones were obtained recently within the framework of Rückenstein-Kotliar (four slave-boson) model [63].

We stress that, contrary to the X-method where the systematic $1/N$ calculations of the EPI self-energy is uniquely done, this is still a problem for the *SB* method where an $1/N$ expansion of the partition function $Z(T, \mu)$ is usually performed [64]. The expression for the vertex

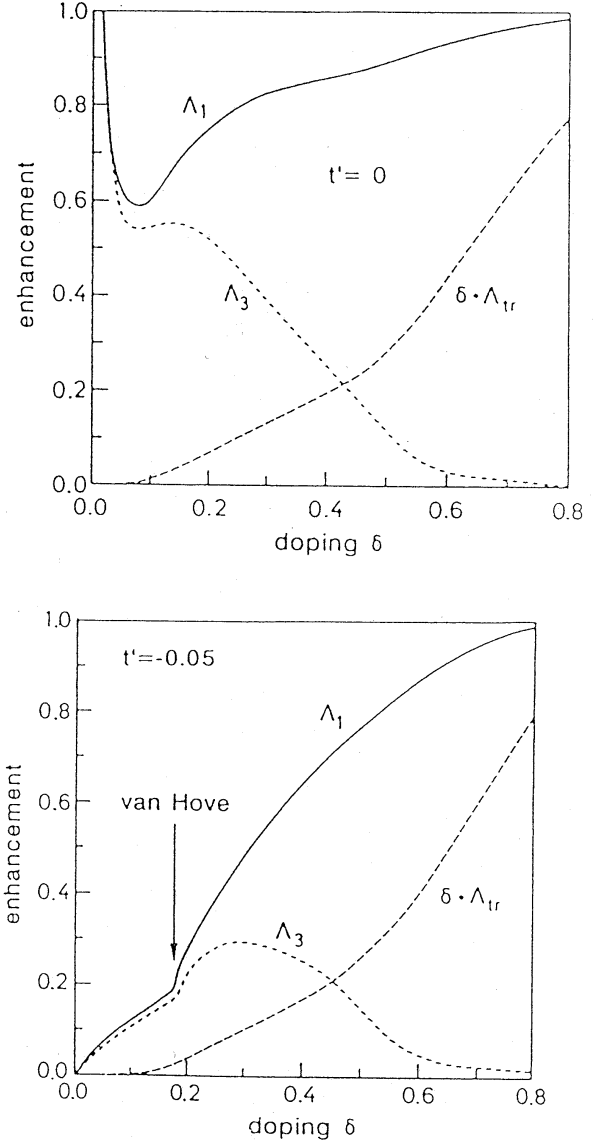


FIG. 5: (a) Normalized s-wave Λ_1 , d-wave Λ_3 and transport $\delta \cdot \Lambda_{tr}$ coupling constants as a function of doping δ for $t' = 0$ and $J = 0$. (b) Λ_1 and Λ_3 and $\delta \cdot \Lambda_{tr}$ as a function of doping δ for $t' = -0.05$ and $J = 0$. After Ref. [31].

function in the SB method is different from that in the X method [30], [31]. It seems that the existing SB treatment of EPI omits a class of diagrams which causes an incorrect dependence of the coupling constant λ on doping. As a result, the vertex function in the *SB* approach is peaked not at $q = 0$ but at some finite q_{\max} , where $q_{\max} = 0$ only for doping $\delta = 0$.

V. NOVEL EFFECTS DUE TO THE FORWARD SCATTERING PEAK IN EPI

There are a number of effects which are predicted by the theory with FSP in EPI and in nonmagnetic impurity scattering - the *FSP theory*. We have already explained the effects of the forward scattering peak on the EPI. We discuss briefly some other predictions of the FSP theory including aspects not covered in [7].

A. Theory of ARPES self-energy in cuprates

Recent ARPES experiments of the Shen group [20], [23], [50], [65] gave additional evidence that phonons are involved in pairing mechanism of cuprates. Furthermore, the clear isotope effect was found in the real part of the ARPES self-energy $\text{Re } \Sigma(\mathbf{k}, \omega)$ [24], which confirms the importance of EPI interaction in cuprates.

1. ARPES kink and non-shift puzzle

Recently, it was reported that in all metallic cuprates there is a *kink* in the quasiparticle dispersion $\omega(\xi_{\mathbf{k}})$ in the nodal direction (along the $(0, 0) - (\pi, \pi)$ line) at around $\omega_{ph}^{(70)} \sim (60 - 70) \text{ meV}$ [20], see the property (6_N) in Sec.II.F and Fig. 3. In the superconducting state this kink is not shifted (the property (3_S) in Sec. II.F) contrary to the standard Eliashberg theory - we call this the *ARPES non-shift puzzle*. In the case of the antinodal point $(\pi, 0)$ there is a kink at 40 meV in the normal state which is shifted by the maximal gap in the superconducting state (the property (4_S) [23], see Fig. 3. This means that any theory which aspires to explain the pairing in cuprates must solve the *non-shift puzzle*. It is worth mentioning that in spite of the apparent existence of the non-shift puzzle since 2001, practically there have been no publications that treat this problem except the paper [37] where a plausible theory was given. The approach in [37] is based on the *FSP theory* for EPI and other charge scattering processes, which is discussed above. In order to explain the non-shift puzzle by the FSP theory the following simplifications are made: (i) electron-phonon interaction is dominant in HTSC, and its spectral function $\alpha^2 F(\mathbf{k}, \mathbf{k}', \Omega) \approx \alpha^2 F(\varphi, \varphi', \Omega)$ (φ is the angle on the Fermi surface) has a pronounced forward scattering peak due to strong correlations. Its width is very narrow $|\mathbf{k} - \mathbf{k}'|_c \ll k_F$ even in overdoped systems [30], [31], [32]. To the leading order, one can put $\alpha^2 F(\varphi, \varphi', \Omega) \sim \delta(\varphi - \varphi')$; (ii) for simplicity the slightly broadened Einstein spectrum is assumed; (iii) the dynamic part (beyond the Hartree-Fock) of the Coulomb interaction is characterized by the spectral function $S_C(\mathbf{k}, \mathbf{k}', \Omega)$. The ARPES non-shift puzzle implies that S_C is either peaked at small transfer momenta $|\mathbf{k} - \mathbf{k}'|$, or it is so small that the shift is weak and beyond the experimental resolution of ARPES. We

assume that the former case is realized, although this is not crucial because ARPES indicates that electron-phonon coupling is much larger than the Coulomb coupling, i.e. $\lambda_{ph} \gg \lambda_C$; (iv) The scattering potential from non-magnetic impurities has pronounced forward scattering peak, which is also due to strong correlations [30], [31], [32]. The latter is characterized by two rates $\gamma_{1(2)}$. The case $\gamma_1 = \gamma_2$ mimics the extreme forward impurity scattering. In this case, d-wave pairing is unaffected by impurities [7] - the *Anderson theorem for unconventional pairing*. On the other hand the case $\gamma_2 = 0$ describes the isotropic exchange scattering - see discussion in [37].

The Green's function is given by

$$G_k = -\frac{i\tilde{\omega}_k + \xi_{\mathbf{k}}}{\tilde{\omega}_k^2 + \xi_{\mathbf{k}}^2 + \tilde{\Delta}_k^2} \quad (33)$$

where $k = (\mathbf{k}, \omega)$. In the FSP theory the equations for $\tilde{\omega}_k$ and $\tilde{\Delta}_k$ are local on the Fermi surface, i.e. in \mathbf{k} space and [37]

$$\tilde{\omega}_{n,\varphi} = \omega_n + \pi T \sum_m \frac{\lambda_{1,\varphi}(n-m)\tilde{\omega}_{m,\varphi}}{\sqrt{\tilde{\omega}_{m,\varphi}^2 + \tilde{\Delta}_{m,\varphi}^2}} + \Sigma_{n,\varphi}^C, \quad (34)$$

$$\tilde{\Delta}_{n,\varphi} = \pi T \sum_m \frac{\lambda_{2,\varphi}(n-m)\tilde{\Delta}_{m,\varphi}}{\sqrt{\tilde{\omega}_{m,\varphi}^2 + \tilde{\Delta}_{m,\varphi}^2}} + \tilde{\Delta}_{n,\varphi}^C, \quad (35)$$

where $\lambda_{1(2),\varphi}$ is given by

$$\begin{aligned} \lambda_{1(2),\varphi}(n-m) &= \lambda_{ph,\varphi}(n-m) + \delta_{mn}\gamma_{1(2),\varphi} & (36) \\ \lambda_{ph,\varphi}(n) &= 2 \int_0^\infty d\Omega \frac{\alpha_{ph,\varphi}^2 F_\varphi(\Omega)\Omega}{(\Omega^2 + \omega_n^2)} \end{aligned}$$

with the electron-phonon coupling function $\lambda_{ph,\varphi}(n)$. Since EPI and $\Sigma_{n,\varphi}^C$ in Eq. (34-35) has a *local form* as a function of the angle φ due to FSP, then the equation for $\tilde{\omega}_{n,\varphi}$ has also a local form. This means that different points on the Fermi surface are decoupled. In that case $\tilde{\omega}_{n,\varphi}$ depends on the local value (on the Fermi surface) of the gap $\tilde{\Delta}_{n,\varphi} \approx \Delta_0 \cos 2\varphi$. *This property alone is important in solving the ARPES non-shift puzzle*. So, at the *nodal point* ($\varphi = \pi/4$) one has $\tilde{\Delta}_{n,\varphi} = 0$ and the quasiparticle spectrum given by

$$E - \xi_{\mathbf{k}} - \Sigma_k(E, \tilde{\Delta}_{n,\varphi} = 0) = 0 \quad (37)$$

is *unaffected* by superconductivity, i.e. the kink is not-shifted in the superconducting state, as shown in Fig. 6a. This is exactly what is seen in the experiment of the Shen group [20], [66] - see Fig. 3. The FSP theory also predicts: (1) that $\Sigma_2 (\equiv \text{Im } \Sigma)$ has a knee-like shape for $\omega < \omega_{ph}^{(70)}$, see Fig. 6b, exactly as seen recently by ARPES [20], [66]; (2) that for $\omega > \omega_{ph}^{(70)}$ the EPI contribution to Σ_2 is constant while its slope in this region is determined by the Coulomb scattering giving a small coupling constant

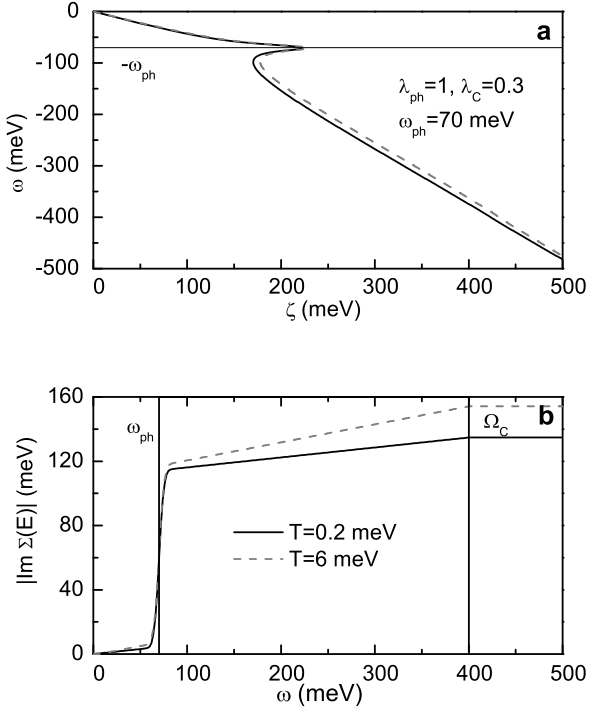


FIG. 6: Nodal direction: (a) The quasiparticle-spectrum $\omega(\xi_k)$ and (b) the imaginary self-energy $Im\Sigma(\xi = 0, \omega)$ in the nodal direction ($\varphi = \pi/4$) in the superconducting ($T = 0.2$ meV) and normal ($T = 6$ meV) state. $\Omega_C = 400$ meV is the cutoff in S_C . After Ref. [37].

$\lambda_C < 0.4$. Such a behavior is just what has been observed in ARPES spectra [20], [66], thus confirming the correctness of the FSP theory. Let us point out that the experimental ARPES curves for Σ_1 and Σ_2 are smoother than (our) theoretical curves, since we study the problem in the very simplified model with the slightly broadened Einstein spectrum. Since the tunnelling and ARPES experiments indicate that the broad spectrum of phonons contribute to EPI, then the quantitative analysis must rely on the realistic Eliashberg spectral function which is at present unknown.

In the case of *antinodal point* ($\varphi \approx \pi/2$) the calculations show, that there is a singularity at 40 meV ($E_{\sin g}$) in the quasiparticle spectrum in the normal state - see Fig. 7. The analytic and numeric calculations of Eq. (34) show that this singularity is *shifted* by Δ_0 in the superconducting state, i.e. $E_{\sin g} \rightarrow E_{\sin g} + \Delta_0$. This is exactly what is seen in the recent experiment on BSCCO [23] - see Fig. 3, where the singularity of the normal state spectrum at 40 meV is shifted to (65 – 70) meV in the superconducting state, since $\Delta_0 \approx (25 – 30)$ meV. We stress that the coupling constants λ_{ph} (> 1) and λ_C (~ 0.4) were estimated from $Re\Sigma$ by knowing that $Re\Sigma = -(\lambda_{ph} + \lambda_C)\omega$ for $\omega \ll \omega_{ph}^{\max}$ and $Re\Sigma = -\lambda_C\omega$ for $\omega_{ph}^{\max} \ll \omega < W$ (the

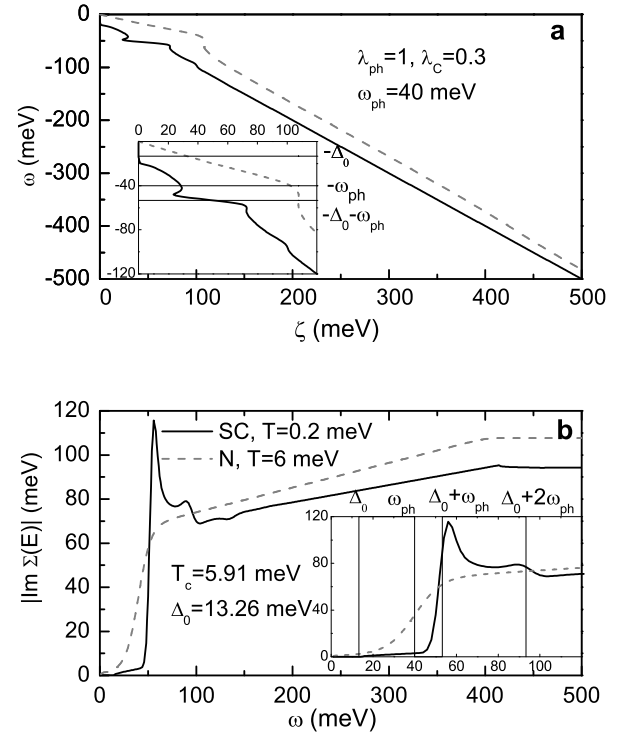


FIG. 7: Anti-nodal point: (a) The quasiparticle-spectrum $\omega(\xi_k)$ and (b) the imaginary self-energy $Im\Sigma(\xi = 0, \omega)$ in the anti-nodal direction ($\varphi = 0; \pi/2$) in the superconducting ($T = 0.2$ meV) and normal ($T = 6$ meV) state. After Ref. [37].

band width). The FSP theory explains in the natural way also the *peak-dip-hump structure* in $A(\mathbf{k}, \omega)$ if $\lambda_{ph} > 1$, as observed experimentally- see more in [37].

In conclusion, the different behavior of the nodal and the anti-nodal kinks in the superconducting state can be consistently described by the existence of the forward scattering peak in EPI and other charge scattering processes. We stress that the FSP theory is up to now the only one that succeeded in resolving the non-shift.

2. ARPES isotope effect

Recent ARPES spectra in the optimally doped Bi2212 taken near the nodal and the anti-nodal points [24] show after oxygen isotope substitution $^{16}O \rightarrow ^{18}O$ a pronounced isotope effect in the real part of the quasiparticle self-energy. This result, if confirmed, will be a crucial evidence for the importance of EPI in cuprates.

A. Isotope effect along the nodal direction. The ARPES results for the isotope effect in optimally doped Bi2212 samples are as follows [24]: (1) there is a kink in the quasiparticle spectrum at $\omega_{k,70} \simeq 70$ meV which

is unshifted in the SC state; (2) there is a red shift $\delta\omega_{k,70} \sim -(10-15) \text{ meV}$ of the kink for the $^{16}\text{O} \rightarrow ^{18}\text{O}$ substitution; (3) the isotope shift of the self-energy is more pronounced at large energies $\omega = 100-300 \text{ meV}$.

The results (1)-(2) can be explained by the EPI theory with FSP in a natural way. As it is already discussed, the theory predicts that the kink in the superconducting state is non-shifted with respect to that in the normal state, what is due to the FSP in the EPI. Related to the isotope effect, the theory predicts [67] that in the *nodal direction* after the substitution $^{16}\text{O} \rightarrow ^{18}\text{O}$ ($\omega_{O^{16}} = \omega_{kink} \sim 70 \text{ meV}$) there is a red-shift of $\text{Re}\Sigma(\mathbf{k}, \omega)$ in the normal and superconducting state, due to the isotope dependence of the maximum of $\text{Re}\Sigma(\mathbf{k}, \omega)$ at $\omega \approx \omega_{kink}$. The isotope effect is more pronounced at higher energies. This is shown in Fig. 8 for the Debye model with the spectral function $\alpha^2 F(\omega) = \lambda(\omega/\omega_O)^2$ with $\omega_O = (k/M_O)^{1/2}$ (M_O is the oxygen mass) - see the left panels in Fig. 8.

The pronounced isotope effect is also present in the quasiparticle dispersion $\omega(k)$ with the read shift of the kink energy upon the substitution $^{16}\text{O} \rightarrow ^{18}\text{O}$. This is shown in the right panels of Fig. 9. The property (3) is difficult to explain by the Eliashberg-like theory we have used above. Some speculations that the pronounced isotope effect at high energies is of polaronic origin wait for further theoretical elaborations.

B. Isotope effect near the anti-nodal point. The main experimental results for the ARPES isotope effect near the *anti-nodal* point $\mathbf{k}_{AN} \approx (0, \pi)$ are [24]: (1) there is a kink in the quasiparticle spectrum around $\omega_{k,40} \approx 40 \text{ meV}$ which is shifted in the SC state by $\Delta(\mathbf{k}_{AN}, \omega) \approx 30 \text{ meV}$; (2) there is a red shift of the kink in the SC state with the energy change $\delta\omega_k \sim -5 \text{ meV}$ at $T = 25 \text{ K}$, which is smaller than the corresponding one in the nodal direction; (3) there is an inverse IE at higher energies $\omega > \omega_{k,40}$, i.e. $\omega(\xi_k; ^{18}\text{O}) > \omega_O(\xi_k; ^{16}\text{O})$; (4) in the normal state at $T = 100 \text{ K}$ there is practically no red shift for the $^{16}\text{O} \rightarrow ^{18}\text{O}$ substitution.

Theoretical calculations of the self-energy in the *anti-nodal* region have been done for the Debye spectrum [67], only. Since the density of states near the anti-nodal point is higher than at the nodal point, we assume a larger (than in the nodal case) EPI coupling constant $\lambda_{ep, \mathbf{k}_{AN}} = 2$. In Fig. 10 (top) it is seen that in the *SC* state (at $T = 25 \text{ K}$) the kink in the quasiparticle energy is shifted by the gap $\Delta(\mathbf{k}_{AN})$ and that there is a moderate red-shift ($\sim -(5-8) \text{ meV}$) of the kink for the $^{16}\text{O} \rightarrow ^{18}\text{O}$ substitution. Note that this value is only accidentally in agreement with the experimental one ($\sim -5 \text{ meV}$). However, the theory predicts smaller (compared to experiments) inverse isotope effect ($\omega(\xi_k; ^{18}\text{O}) > \omega_O(\xi_k; ^{16}\text{O})$) which occurs at higher energies. It seems that the origin of this behavior lies in the smaller gap value $\Delta(\mathbf{k}_{AN})$ of ^{18}O (dashed line in Fig. 10) than of ^{16}O (bold line). In spite of the fact that these results resemble qualitatively the experimental results (1)-(3) there is quantitative difference between the theory and experiment at

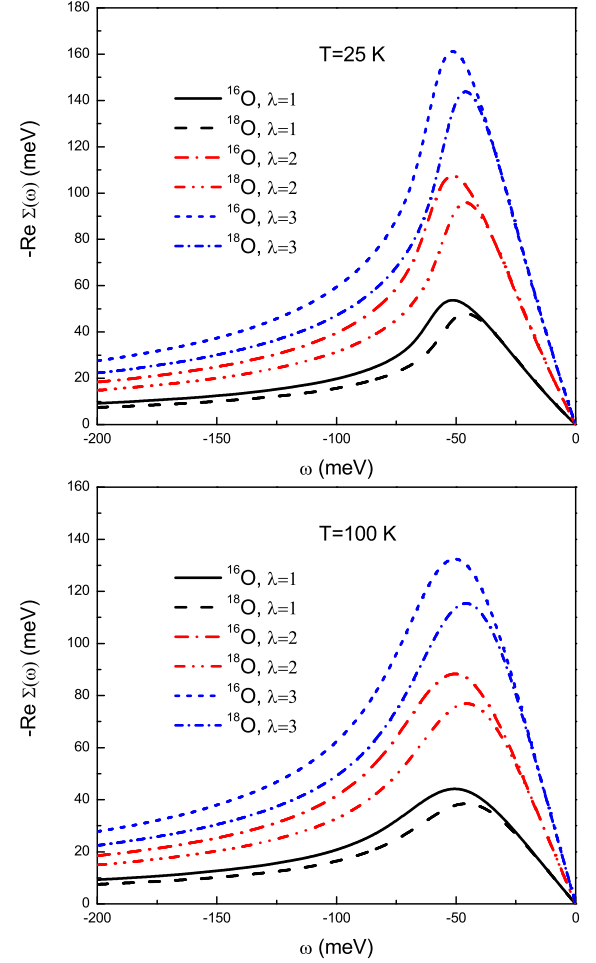


FIG. 8: The shift of $\text{Re}\Sigma(\mathbf{k}, \omega)$ in the nodal direction upon the isotope substitution $^{16}\text{O} \rightarrow ^{18}\text{O}$ calculated using the Debye model with $\omega_{O^{16}} = 60 \text{ meV}$ for various EPI coupling constants λ at $T = 25 \text{ K}$ (top) and $T = 100 \text{ K}$ (bottom). From Ref. [67].

high energies, the origin of which is unknown at present.

The FSP theory predicts that the isotope effect at the anti-nodal point is much less pronounced in the normal state (at 100 K) as shown in Fig. 10. These results resemble qualitatively the experimental results in [24]. The origin of the small shift of the kink in the normal state lies in the lower antinodal kink energy and in the smearing effects at higher temperatures.

3. Collapse of the anti-nodal elastic scattering in the superconducting state

A number of ARPES experiments on optimally doped Bi-2212 give evidence for the significant elastic scattering which varies along the Fermi surface, being the smallest

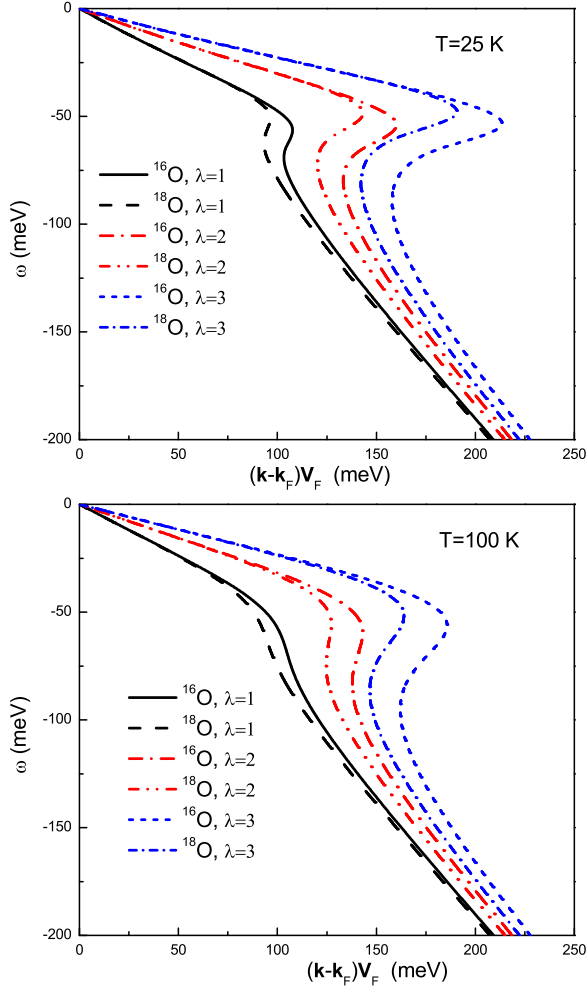


FIG. 9: The quasiparticle energy $\omega(k - k_F)$ in the nodal direction upon the isotope substitution $^{16}O \rightarrow ^{18}O$ calculated using the Debye model with $\omega_{O^{16}} = 60$ meV for various EPI coupling constants λ at $T = 25$ K (top) and $T = 100$ K (bottom). From Ref. [67].

along the nodal direction and the largest near the anti-nodal point, see [21] and references therein. The experiments indicate that the quasiparticle spectral function $A(\mathbf{k}, \omega)$ at the anti-nodal point is broad in the normal state and strongly sharpens in the superconducting state. On the other side, at the nodal point $A(\mathbf{k}, \omega)$ has a standard Lorentzian form which is almost unchanged in the superconducting state.

This dramatic sharpening of the spectral function near the anti-nodal point $(\pi, 0)$ at $T < T_c$ can be explained by assuming that there is a forward scattering peak in the elastic impurity scattering as it was done in [37]. It is easy to see from Eq. (34-35), which describe the extreme forward scattering, that in the case of the FSP in impurity potential one has $\gamma_1 = \gamma_2$. As a result,

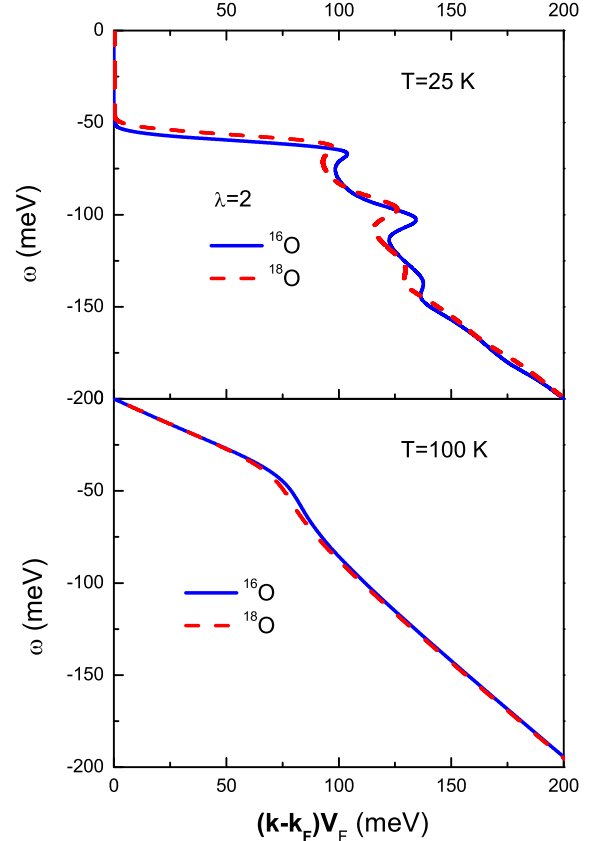


FIG. 10: The quasiparticle energy $\omega(k - k_F)$ in the *anti-nodal region* under the isotope substitution $^{16}O \rightarrow ^{18}O$ in the Debye model with $\omega_{O^{16}} = 40$ meV for the EPI coupling constants $\lambda_{ep, k_{AN}} = 2$ at $T = 25$ K (top) and $T = 100$ K (bottom). k_F and v_F are the Fermi momentum and velocity, respectively.

one finds that the impurity scattering rate $\Gamma_{imp}(\mathbf{k}, \omega) = \Gamma_n(\mathbf{k}, \omega) + \Gamma_a(\mathbf{k}, \omega) = 0$ for $|\omega| < \Delta_0$ for any kind of pairing (s- p- d-wave etc.) since the normal (Γ_n) and the anomalous (Γ_a) scattering rates compensate each other in the superconducting state - the *collapse of the elastic scattering rate*. This result is a consequence of the Anderson theorem [68]-[69]. In such a case d-wave pairing is unaffected by impurities - there is a negligible reduction in T_c , as was first elaborated in [68] and [69], and further studied in [72]. The physics behind this result is rather simple. Forward scattering means that electrons scatter into a very small region in the \mathbf{k} -space, so that at the most part of the Fermi surface there is no mixing of states with different signs of the order parameter $\Delta(\mathbf{k})$, and the detrimental effect of impurities is reduced. Only for states near the nodal points there is mixing but since $\Delta(\mathbf{k})$ is a small there is only small reduction in T_c [33]. The collapse of the elastic scattering rate in the ARPES spectra was recently considered in [70], where a

number of interesting results are reported.

The idea of the forward scattering peak in the non-magnetic impurity scattering was applied recently in [71] in the study of the anomalous temperature dependence of the Hall angle in optimally doped HTSC. By taking into account (besides the inelastic scattering) also the small-angle elastic scattering on non-magnetic impurities in [71] it was explained the experimental finding in $YBa_2Cu_{3-x}Zn_xO_{7-\delta}$ that $\cot\Theta_H(T) = \sigma_{xx}/\sigma_{xy} \sim T^2$ (Θ_H is the Hall angle, H is the applied magnetic field) for $100K < T < 300K$. This is contrary to the expected linear behavior (for $\cot\Theta_H(T)$), since in that temperature interval one has $\rho(T) \sim T$.

In conclusion, in order to explain ARPES results in cuprates it is necessary to take into account: (1) EPI interaction, since it dominates in the quasiparticle scattering in the frequency region responsible for pairing in cuprates; (2) effects of elastic nonmagnetic impurities with FSP; (3) the Coulomb interaction which dominates at higher energies $\omega > \omega_{ph}$. In this respect, the presence of ARPES kink and the knee-like shape of the spectral width are the *smoking-gun experiments* that strongly constraint possible theories.

B. Nonmagnetic impurities and robustness of d-wave pairing

In the presence of strong correlations the impurity potential is also renormalized, as it is mentioned above, and the effective potential in the Born approximation is given by $u_i^2(\mathbf{q}) = \gamma_c^2(k_F, \mathbf{q})u_{i,0}^2(\mathbf{q})$, where $u_{i,0}(\mathbf{q})$ is the single impurity scattering potential in the absence of strong correlations. This was proved first in [30] and elaborated quantitatively in [68] and [69]. Since the charge vertex $\gamma_c(\mathbf{p}_F, \mathbf{q})$ is peaked at $\mathbf{q} = \mathbf{0}$ the potential $u_i(\mathbf{q})$ is also peaked at $\mathbf{q} = \mathbf{0}$. This means that the scattering amplitude contains not only the s-channel (as usually assumed in studying impurity effects in cuprates), but also the d-channel, etc. Based on this property the FSP theory succeeded in explaining some experimental facts, such as: (i) suppression of the residual resistivity ρ_i [30], [31]. This effect was observed in optimally doped $YBCO$, where the resistivity $\rho(T)$ at $T = 0K$ has a rather small value $< 10 \mu\Omega\text{cm.}$; (ii) robustness of d-wave pairing [68], [69] in the presence of impurities and other defects in CuO_2 planes, such as Zn, Ga, O defects, etc., see [74].

Early theories of the effect of nonmagnetic impurities on T_c in cuprates [73] always assumed that $u_i(\mathbf{q}) = \text{const.}$, i.e. that only the s-wave scattering channel is present. Such a theory predicts that $T_c(\rho_{i,c}) = 0$ at a much smaller residual resistivity $\rho_{i,c}^{(s)} \sim 50 \mu\Omega\text{cm}$, while the experimental range is $200 \mu\Omega\text{cm} < \rho_{i,c}^{\text{exp}} < 1500 \mu\Omega\text{cm}$ [74]. The latter experimental fact means that d-wave pairing in HTSC is *much more robust* than what the standard theory predicts, and it is one of the smoking gun experiments in testing the concept of FSP in the charge scattering potential. It is worth mentioning that in a number of pa-

pers the pair-breaking effect of non-magnetic impurities in HTSC was analyzed in terms of the impurity concentration n_i , i.e. the dependence $T_c(n_i)$. However, n_i is not the parameter which governs this pair-breaking effect. The more appropriate parameter for discussing the robustness of d-wave pairing is the impurity scattering amplitude $\Gamma(\theta, \theta')$, which can be related to the measured residual resistivity ρ_i and to $T_c(\rho_i)$. The robustness of d-wave pairing in HTSC can be revealed only by studying the experimental curve $T_c(\rho_i)$, as was first recognized experimentally in [74] and theoretically in [30], [68].

The robustness of d-wave pairing in HTSC was explained first in [68], where the FSP theory [30], [31] was applied to this problem. We shall not go into details - see [68], [7] - but just give here the general formula for the $T_c(\rho_i)$ dependence in anisotropic (including unconventional) superconductors. We assume that in an unconventional (anisotropic) superconductor the order parameter has the form $\Delta(\theta) = \Delta_0 Y(\theta)$ and generally one has $\langle Y(\theta) \rangle \neq 0$ ($\langle Y^*(\theta)Y(\theta) \rangle = 1$). In the case of FSP, the momentum dependent impurity scattering amplitude is given by $\Gamma(\theta, \theta') = \Gamma_s(\theta, \theta') + \Gamma_d Y_d(\theta)Y_d(\theta') + \dots$ and the critical temperature T_c by

$$\ln \frac{T_c}{T_{c0}} = \Psi\left(\frac{1}{2}\right) - \Psi\left(\frac{1}{2} + (1 - \beta)x\right) - \langle Y(\theta) \rangle^2 \left[\Psi\left(\frac{1}{2}\right) - \Psi\left(x + \frac{1}{2}\right) \right]. \quad (38)$$

Here, T_{c0} is the bare critical temperature in the absence of impurities, $x = \Gamma_s/4\pi T_{c0}$, $\beta = \Gamma_d/\Gamma_s$ and $\langle Y(\theta) \rangle$ means averaging over the Fermi surface. If one takes into account that the inelastic scattering, which is characterized by the coupling constant λ_Z , screens the impurity scattering, then the parameter x in Eq. (38) should be replaced by $x/(1 + \lambda_Z)$. Note that Eq. (38) holds independently on the scattering strength Γ_s , Γ_d , i.e. it holds in the Born limit as well as in the unitary limit. The residual resistivity ρ_i can be related to the transport scattering rate by $\rho_i = 4\pi\Gamma_{tr}/\omega_{pl}^2$, while the s-wave amplitude is related to Γ_{tr} by $\Gamma_s = p\Gamma_{tr}$. The parameter $p > 1$ can be obtained from the microscopic model (in the t-J model $p \approx 2 - 3$) or can be treated as a fitting parameter, see more in [7]. In the case of an unconventional pairing in the tetragonal lattice one has $\langle Y(\theta) \rangle = 0$ and the last term drops. For the s-scattering only ($\Gamma_d = 0$) one has $\beta = 0$ and $T_c(\rho_i)$ should be suppressed very strongly contrary to the experimental results [74], see Fig. 11.

The FSP theory of impurity scattering in the t-J model [68] gives that the s-channel and d-channel almost equally contribute to the impurity scattering amplitude, since $\beta \approx 0.75 - 0.85$ for doping $\delta \approx 0.1 - 0.2$. The dependence of $\beta(\delta)$ has been calculated for the t-J model, see [68], [7]. Since the d-channel in scattering is not detrimental for d-wave pairing the FSP theory predicts that $T_c(\rho_i)$ vanishes at much larger $\rho_{i,c}$, i.e. $\rho_{i,c}^{(\text{FSP})} \gg \rho_{i,c}^{(s)}$, in good agreement with experiments, as shown in Fig. 11. In

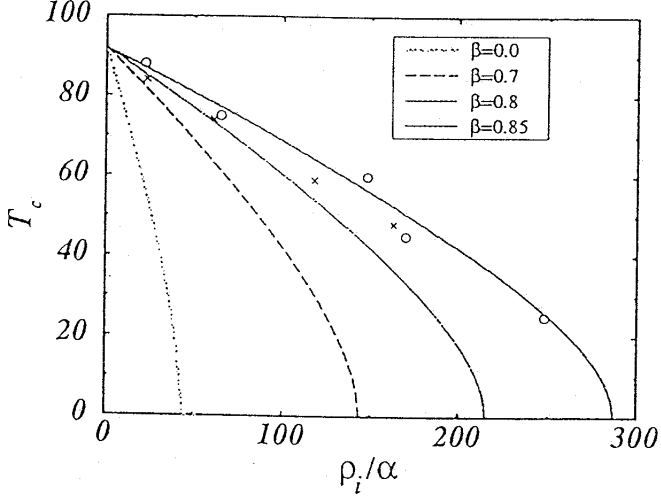


FIG. 11: The critical temperature T_c [K] of a d-wave superconductor as a function of the experimental parameter ρ_i/α_c [K], where ρ_i is the residual resistivity and $\alpha = 8\pi^2\lambda_{tr}/\omega_{pl}^2$. The case $\beta = 0$ corresponds to the prediction of the standard d-wave theory with isotropic scattering [73]. The experimental data [74] are indicated by crosses for $YBa_2(Cu_{1-x}Zn_x)_3O_{7-\delta}$, and by circles for $Y_{1-y}Pr_yBa_2Cu_3O_{7-\delta}$. From Ref. [68].

the extreme forward scattering limit, T_{c0} would be unrenormalized, i.e. the Anderson theorem holds also for unconventional superconductors. In this case impurity scattering does not mix superconducting states with different sites of $\Delta(\mathbf{k})$.

Here, we have studied the effects of impurities and other defects placed in the CuO_2 planes. The corresponding experiments can be explained by FSP in the impurity potential, which is due to strong correlations. In the case when impurities are placed out of these planes their effect is weaker and also there is a forward scattering peak due to weak screening along the c -axis. The proposed theory in [68], [69] and Eq.(38) holds for both cases equally.

C. Nonadiabatic corrections of T_c

Cuprates are characterized not only by strong correlations but also by the relatively small Fermi energy E_F , which is not much larger than the characteristic (maximal) phonon frequency ω_{ph}^{\max} , i.e. $E_F \simeq 0.1 - 0.3$ eV, $\omega_{ph}^{\max} \simeq 80$ meV. The situation is even more pronounced in *fullerene compounds* A_3C_{60} , with $T_c = 20 - 35$ K, where $E_F \simeq 0.2$ eV and $\omega_{ph}^{\max} \simeq 0.16$ eV. This fact implies a possible breakdown of the Migdal's theorem [75], which asserts that the relevant vertex corrections due to the $E - P$ interaction are small if $(\omega_D/E_F) \ll 1$. In that respect a comparison of the intercalated graphite KC_8 and the fullerene A_3C_{60} compounds, given in [76], is very

instructive, because both compounds have a number of similar properties. However, the main difference in these systems lies in the ratio ω_D/E_F , since $(\omega_D/E_F) \ll 1$ in KC_8 , while it is rather large $(\omega_D/E_F) \sim 1$ in A_3C_{60} . Since the ratio ω_D/E_F is not negligible in the fullerene compounds and in cuprates it is necessary to correct the Migdal-Eliashberg theory by *vertex corrections due to EPI*. It is known that these vertex corrections lower T_c in systems with isotropic EPI. However, in systems with FSP and with the cut-off $q_c \ll k_F$ in the pairing potential these vertex corrections cause an appreciable increase in T_c . The calculations by the Pietronero group [76] provided two important results: (1) there is a drastic increase of T_c by lowering $Q_c = q_c/2k_F$, for instance $T_c(Q_c = 0.1) \approx 4T_c(Q_c = 1)$; (2) Even small values of $\lambda < 1$ can give large T_c . The latter results open a new possibility in reaching high T_c in systems with appreciable ratio ω_D/E_F and with FSP. The difference between the Migdal-Eliashberg and non-Migdal theories can be explained qualitatively in the framework of an approximative McMillan formula for T_c (for not too large λ) which reads $T_c \approx \langle \omega \rangle e^{-1/[\tilde{\lambda} - \mu^*]}$. The Migdal-Eliashberg theory predicts $\tilde{\lambda}_{ME} \approx \lambda/(1 + \lambda)$ while the non-Migdal theory [76] gives $\tilde{\lambda}_{nM} \approx \lambda(1 + \lambda)$. For instance $T_c \sim 100$ K in cuprates can be explained by the Migdal-Eliashberg theory if $\lambda \sim 2$, while in the non-Migdal theory much smaller coupling constant is needed, i.e. $\lambda \sim 0.5$.

VI. PSEUDOGAP AND THE ELECTRON-PHONON INTERACTION

The pseudogap (PG) problem is a very intriguing one and it is not surprising that a variety of theoretical models have been proposed to explain it. We are not going to discuss all these in detail but only mention some that may have experimental support. The *first* one is based on the assumption that the PG phase represents the state with *pre-formed pairs* [77], where the true critical temperature T_c is smaller than the mean-field one T_c^{MF} . In the region $T_c < T < T_c^{MF}$ pre-formed pairs give rise to a dip in the density of states $N(\omega)$. This approach is physically plausible having in mind that cuprates are characterized by a short coherence length, quasi-two dimensionality and proximity to the Mott-Hubbard insulating state. As we already discussed the latter gives rise to small phase stiffness K_s^0 of the superconducting order parameter $\Delta = |\Delta| e^{i\varphi}$. In 2D systems the Berezinskii-Kosterlitz-Thouless transition temperature, $T_c = (\pi/2)K_s^0(T_c)$ ($\sim \delta$ for small doping), can be much smaller than T_c^{MF} . From the experimental side there is some support for this approach, at least in not very broad temperature region close to T_c . For instance, the specific heat measurements [78] (with smaller jumps at T_c) point to a *non-mean field* character of the superconducting phase transition, particularly for underdoped compounds. As we have already mentioned in the Introduction, ARPES measurements show that for $T_c < T < T^*$

PG is d-wave like $\Delta_{pg}(\mathbf{k}) \approx \Delta_{pg,0}(\cos k_x - \cos k_y)$, like the superconducting gap, and that $\Delta_{pg,0}$ increases at lower doping.

The *second* approach assumes that PG is due to existence of an additional competing order, but usually without the true long-range order. For instance, the "spin-density wave" alias for strong antiferromagnetic fluctuations can also produce dip in $N(\omega)$ [79]. Related approaches are based on RVB, orbital currents, d-wave order, etc., which are not discussed here.

We would like to pay attention to two possible effects, which are due to FSP, that can also give rise to PG in the density of states. The first is related to EPI interaction with FSP that can produce a dip in $N(\omega)$ for $\omega < \Omega$, where Ω is the characteristic phonon frequency. The second is related to a novel type of fluctuations - internal Cooper pair fluctuations, due to the long-range pairing forces (alias for FSP) - due to EPI with FSP.

1. Pseudogap due to phonons

The EPI, in the Einstein model with the phonon frequency Ω , was also studied in the extreme limit of FSP [80], where in leading order the spectral function is *singular*, i.e. $\alpha^2 F(\mathbf{k}, \mathbf{k}', \omega) \sim \delta(\mathbf{k} - \mathbf{k}')\delta(\omega - \Omega)$. In such a singular case besides renormalization of frequency ($\omega \rightarrow Z(\mathbf{k}, \omega)\omega$) there is also significant renormalization of the quasiparticle energy ($\xi_{\mathbf{k}} \rightarrow \chi(\mathbf{k}, \omega)\xi_{\mathbf{k}}$) in the Eliashberg equations, giving a very interesting behavior of the *density of states* $N(\omega)$ [80]. *First*, there is an increase of $N(\omega = 0)(> N_{bare}(\omega = 0))$ at $\omega = 0$, where $N_{bare}(\omega = 0)$ is the bare density of states in the absence of EPI, see Fig. 12a. This fact is mainly due to renormalization of the quasiparticle energy ($\xi_{\mathbf{k}} \rightarrow \chi(\mathbf{k}, \omega)\xi_{\mathbf{k}}$).

In such a case there is a pseudogap feature in the region $(\Omega/5) < \omega \leq \Omega$, where $N(\omega) < N_{bare}(\omega)$. This pseudogap feature disappears at temperature comparable to the phonon energy Ω . Note that the usual isotropic and short-ranged EPI does not renormalize the density of states in the normal state, i.e. $N(\omega) = N_{bare}(\omega)$.

It is interesting that without renormalization of the quasiparticle energy ($\xi_{\mathbf{k}} \rightarrow \xi_{\mathbf{k}}$, i.e. $\chi(\mathbf{k}, \omega) = 1$) there is also pseudogap behavior. The case $\chi = 1$ is probably realized in systems with finite width of FSP ($\delta k \ll k_F$) and with *particle-hole symmetry*. In such a case one has $N(\omega = 0) < N_{bare}(\omega = 0)$ and the pseudogap exist for $\omega < \Omega$, as it is seen in Fig. 12b.

Let us mention that for $\chi(\mathbf{k}, \omega) \neq 1$ the transport properties are very peculiar due to the pseudogap behavior of $N(\omega)$ and the existence of peak at $N(\omega = 0)$. For instance, the resistivity $\rho(T)$ is linear in T starting at very low temperatures, i.e. $\rho(T) \sim T$ for $(\Omega/30) \leq T$ and this linearity extends up to several Ω . The dynamic conductivity $\sigma_1(\omega)$ shows the (extended) Drude-like behavior with the Drude width $\Gamma_{tr} \sim T$, for $\omega < T$. The above numbered properties are in a qualitative agreement with experimental results in cuprates - see more in [80], [7].

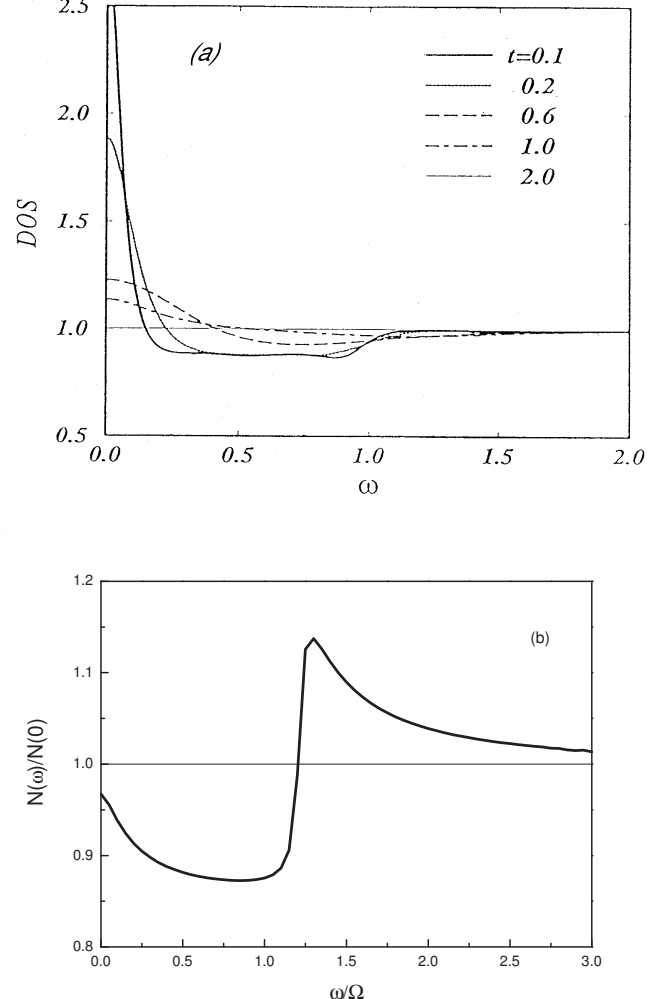


FIG. 12: (a) The density of states $N(\omega)$ in the FSP model for EPI with the dimensionless coupling $l (= V_{EP}/\pi\Omega) = 0.1$ for various $t (= \pi T/\Omega)$ - case $\xi_{\mathbf{k}, \omega} = \chi(\mathbf{k}, \omega)\xi_{\mathbf{k}}$. (b) $N(\omega)$ for the same parameter 1 but for $\xi_{\mathbf{k}, \omega} = \xi_{\mathbf{k}}$. From Ref. [80].

In this extreme FSP limit one can also calculate the mean-field critical temperature T_{c0}^{MF} . In leading order of $\Omega/T_{c0}^{MF} (\gg 1)$ one has $T_{c0}^{MF} \approx N(0)V_{EP} = \lambda N(0)/4$, where $\lambda = N(0)V_{EP}$. In this case the maximal superconducting gap is given by $\Delta_0 = 2T_{c0}^{MF}$ which is reached on the Fermi surface, while away from it the gap decreases, i.e. $\Delta_{\mathbf{k}} = \Delta_0 \sqrt{1 - (\xi_{\mathbf{k}}/\Delta_0)^2}$. The expression for T_{c0}^{MF} tells us that it can be large even for $\lambda < 0.1$, since in cuprates the bare density of states is $N_{bare}(0) \sim 1$ states/eV. It is apparent that in this order *there is no isotope effect* in T_{c0}^{MF} since $\alpha = 0$. However, such an extreme limit is never realized in nature, but for a qualitative understanding of the self-energy it is a good starting point, since the effects of the finite width (k_c) of $\alpha^2 F(\mathbf{k}, \mathbf{k}', \omega)$, whenever $k_c \ll k_F$, change mostly the quantitative picture - see [80]. In case of finite width of FSP when $k_c v_F \ll \Omega$ the reduction of T_c is given by

$T_c^{MF} = T_{c0}^{MF}(1 - 7\zeta(3)k_c v_F / 4\pi^2 T_{c0}^{MF})$. There is also reduction of T_c^{MF} due to retardation effects giving rise to finite isotope effect $\alpha \neq 0$. [80]. Such a singular model has repercussions on other properties. For, instance interesting calculations within more realistic FSP theory with the finite width k_c , but $k_c \ll k_F$, were done in [81], where the FSP theory for EPI and the SFI theory (based on spin-fluctuation mechanism of pairing) were compared. It was shown in this interesting paper that the FSP theory can explain the appreciable increase of anisotropy gap-ratio $R \equiv \Delta(\pi, 0)/\Delta(\pi/2, \pi/2)$ when $T \rightarrow T_c$, while the SFI theory fails. Furthermore, the FSP theory of EPI can explain the pronounced effect of orthorhombicity ($a \neq b$) in $YBCO$ on the gap ratio Δ_a/Δ_b , the anisotropy of penetration depth λ_a^2/λ_b^2 and the supercurrent ratio in the c-axis Pb-YBCO junction. On the other hand, the SFI theory is ineffective here, since it predicts at least one order of magnitude smaller effects [81], [7].

2. Pseudogap due to internal Cooper pair fluctuations

As it is stated above, the FSP theory also predicts existence of a long-range pairing force due to the renormalization of EPI by strong correlations. This opens an additional possibility for PG. Due to FSP in EPI, the mean-field critical temperature has a non-BCS dependence, i.e. $T_c^{MF} = V_{EP}/4$ and it is inevitably reduced by *phase and internal Cooper pair fluctuations*. The latter are always present in systems with long-range attractive forces, i.e. with FSP, as it was pointed out first in [82]. It was shown there that such a long-ranged superconductor exhibits an additional class of fluctuations in which the internal structure of Cooper pair is soft. This leads to PG behavior in which the actual transition temperature T_c is greatly depressed from its mean-field value T_c^{MF} . We stress that these fluctuations are not the standard phase fluctuations in superconductors. Because of the importance, as well as due to internal beauty, of the approach given in [82] we summarize briefly its main results.

In the following the weak coupling limit for the pairing Hamiltonian is assumed

$$\hat{H} = \sum_{\sigma} \int d\mathbf{x} \hat{\psi}_{\sigma}^{\dagger}(\mathbf{x}) \xi(\hat{\mathbf{p}}) \hat{\psi}_{\sigma}(\mathbf{x}) - \int d\mathbf{x} d\mathbf{x}' V(\mathbf{x} - \mathbf{x}') \hat{\psi}_{\uparrow}^{\dagger}(\mathbf{x}) \hat{\psi}_{\downarrow}^{\dagger}(\mathbf{x}') \hat{\psi}_{\downarrow}(\mathbf{x}') \hat{\psi}_{\uparrow}(\mathbf{x}). \quad (39)$$

In the mean-field approximation (MFA) the order parameter $\Delta(\mathbf{x}, \mathbf{x}')$ is given by $\Delta(\mathbf{x}, \mathbf{x}') = V(\mathbf{x} - \mathbf{x}') \langle \hat{\psi}_{\downarrow}(\mathbf{x}') \hat{\psi}_{\uparrow}(\mathbf{x}) \rangle$, which depends in fact on the internal coordinate $\mathbf{r} = \mathbf{x} - \mathbf{x}'$ and the center of mass $\mathbf{R} = (\mathbf{x} + \mathbf{x}')/2$, i.e. $\Delta(\mathbf{x}, \mathbf{x}') = \Delta(\mathbf{r}, \mathbf{R})$. In standard superconductors (LTSC) with a *short-range pairing potential* $V_{sr}(\mathbf{x} - \mathbf{x}') \approx V_0 \delta(\mathbf{x} - \mathbf{x}')$ one has $\Delta(\mathbf{r}, \mathbf{R}) = \Delta(\mathbf{R})$ and in that case only the spatial (\mathbf{R}) fluctuations of the order parameter might be pronounced. In the case of

long-range pairing potential there are additional fluctuations of the internal degrees of freedom (\mathbf{r}). In the following we sketch the analysis given in [82]. When the range of pairing potential is large, i.e. $r_c > \xi$ (the superconducting coherence length), fluctuations of the internal Cooper pair wave-function are important since they give rise to a large reduction of the mean-field quantities. In order to understand the physics of internal wave-function fluctuations we study a much simpler Hamiltonian - the so called reduced BCS Hamiltonian,

$$\hat{H}_{BCS} = \sum_{\mathbf{k}\sigma} \xi_{\mathbf{k}} \hat{c}_{\mathbf{k}\sigma}^{\dagger} \hat{c}_{\mathbf{k}\sigma} - \sum_{\mathbf{k}, \mathbf{k}'} V_{\mathbf{k}-\mathbf{k}'} \hat{c}_{\mathbf{k}\uparrow}^{\dagger} \hat{c}_{-\mathbf{k}\downarrow}^{\dagger} \hat{c}_{-\mathbf{k}'\downarrow} \hat{c}_{\mathbf{k}'\uparrow}. \quad (40)$$

Since we shall study excitations around the ground state we assume that there are no unpaired electrons which allows us to study the problem in the *pseudo-spin Hamiltonian* (see [82] and references therein)

$$\begin{aligned} \hat{H}_{ps} &= \sum_{\mathbf{k}\sigma} 2\xi_{\mathbf{k}} \hat{S}_{\mathbf{k}\sigma}^z - \frac{1}{2} \sum_{\mathbf{k}, \mathbf{k}'} V_{\mathbf{k}-\mathbf{k}'} (\hat{S}_{\mathbf{k}}^+ \hat{S}_{\mathbf{k}'}^- + \hat{S}_{\mathbf{k}'}^+ \hat{S}_{\mathbf{k}}^-) \\ &= \sum_{\mathbf{k}\sigma} 2\xi_{\mathbf{k}} \hat{S}_{\mathbf{k}\sigma}^z - \sum_{\mathbf{k}, \mathbf{k}'} V_{\mathbf{k}-\mathbf{k}'} (\hat{S}_{\mathbf{k}}^x \hat{S}_{\mathbf{k}'}^x + \hat{S}_{\mathbf{k}'}^y \hat{S}_{\mathbf{k}}^y), \end{aligned} \quad (41)$$

where the pseudo-spin 1/2 operators $\hat{S}_{\mathbf{k}\sigma}^z$, $\hat{S}_{\mathbf{k}\sigma}^+ = (\hat{S}_{\mathbf{k}\sigma}^z)^{\dagger}$ are given by

$$\begin{aligned} \hat{S}_{\mathbf{k}\sigma}^z &= \frac{1}{2} (\hat{c}_{\mathbf{k}\uparrow}^{\dagger} \hat{c}_{\mathbf{k}\uparrow} - \hat{c}_{-\mathbf{k}\downarrow}^{\dagger} \hat{c}_{-\mathbf{k}\downarrow} - 1), \\ \hat{S}_{\mathbf{k}\sigma}^+ &= \hat{c}_{\mathbf{k}\uparrow}^{\dagger} \hat{c}_{-\mathbf{k}\downarrow}^{\dagger}. \end{aligned} \quad (42)$$

We see that Eq. (41) belongs to the class of *Heisenberg ferromagnetic Hamiltonians* (since $V_{\mathbf{k}-\mathbf{k}'} > 0$) with the lattice in the Brillouin zone. It is well-known for the Heisenberg model that in the case of long-range forces $V_{\mathbf{k}-\mathbf{k}'} = \text{const}$ in a large part of the \mathbf{k} -space, then the phase fluctuations are negligible and thermodynamic properties are well described in MFA

$$\hat{H}_{MFA} = - \sum_k \mathbf{h}_{\mathbf{k}} \hat{\mathbf{S}}_{\mathbf{k}} \quad (43)$$

with the mean-field $\mathbf{h}_{\mathbf{k}}$ given by

$$\mathbf{h}_{\mathbf{k}} = -2\xi_{\mathbf{k}} \mathbf{z} + \sum_{\mathbf{k}'} V_{\mathbf{k}-\mathbf{k}'} \langle \hat{S}_{\mathbf{k}'}^x \mathbf{x} + \hat{S}_{\mathbf{k}'}^y \mathbf{y} \rangle, \quad (44)$$

where \mathbf{x}, \mathbf{y} and \mathbf{z} are unit vectors. Since x - and y -axis are equivalent one can look for $\mathbf{h}_{\mathbf{k}}$ in the form $\mathbf{h}_{\mathbf{k}} = -2\xi_{\mathbf{k}} \mathbf{z} + 2\Delta_{\mathbf{k}} \mathbf{x}$, where the order parameter $\Delta_{\mathbf{k}}$ is the solution of equation

$$\Delta_{\mathbf{k}} = \sum_{\mathbf{k}'} V_{\mathbf{k}-\mathbf{k}'} \langle \hat{S}_{\mathbf{k}'}^x \rangle = \sum_{\mathbf{k}'} \frac{V_{\mathbf{k}-\mathbf{k}'} \Delta_{\mathbf{k}'}}{2E_{\mathbf{k}'}} \tanh \frac{\beta E_{\mathbf{k}'}}{2}, \quad (45)$$

with $E_{\mathbf{k}} = \sqrt{\xi_{\mathbf{k}}^2 + \Delta_{\mathbf{k}}^2}$. We stress that the long-range force ($V_{\mathbf{k}-\mathbf{k}'} = \text{const}$) in the \mathbf{k} -space produces in the

real space *short-range BCS-like force* $V_{BCS}(\mathbf{x} - \mathbf{x}') \approx V_0 \delta(\mathbf{x} - \mathbf{x}')$. This situation is realized in LTSC superconductors where the metallic screening makes the pairing potential short-ranged.

For the *long-range attractive forces* the function $V_{\mathbf{k}-\mathbf{k}'}$ is sharply peaked at $|\mathbf{k} - \mathbf{k}'| = 0$, for instance in the extreme FSP case (see Section 6.2) one has $V_{\mathbf{k}-\mathbf{k}'} = V_0 \delta(\mathbf{k} - \mathbf{k}')$. In such a case we deal with the short-range Heisenberg model in the \mathbf{k} -space. It is well known that in such a system low-lying excitations, such as the Goldstone magnons, tend to destroy the long-range order, i.e. in these systems one has $T_c \ll T_c^{MF}$. In fact these fluctuations correspond to the internal Cooper pair fluctuations

In the following we analyze s-wave pairing only, where the solution of Eq. (45) gives $T_c^{MF} = V_0/4$ and $\Delta_0 = 2T_c^{MF}$. (Note, that in the BCS case one has $\Delta_0 = 1.76 T_c^{MF}$). The coherence length is defined by $\xi = v_F/\pi\Delta_0$. As we said, the important fact is that in the case of long-ranged superconductors the Heisenberg-like Hamiltonian in the momentum space is short-ranged giving rise to low-lying spin-wave spectrum. The latter spectrum are in fact the low-energy bound states (excitons) which loosely correspond to the low-energy collective modes (in the true many-body theory based on Eq. (39)). This problem was studied in [82] for the long-range (but finite) potential $V(r) = V_0 \exp\{-r^2/2r_c^2\}$ (its Fourier transform is $V_k = (2\pi r_c^2) V_0 \exp\{-k^2 r_c^2/2\}$), and it was found that a large number $N_{cm} \sim \pi k_F r_c / 6\xi$ (for $r_c \gg \xi$) of the excitonic like collective modes ω_{mn}^{exc} exist at zero momentum. These excitonic modes lie between the ground state and the two-particle continuum, i.e. their energies are $\omega < 2\Delta_0$. Note that since we assume that $\Delta_0 \ll E_F$, the system is far from the Bose-Einstein condensation limit.

The above analysis in terms of the pseudo-spins is useful for physical understanding, but the full many-body fluctuation problem, which is based on the Hamiltonian in Eq. (39), is studied in [82] where the Ginzburg-Landau (G-L) equation is derived for the long-ranged superconductor. Due to fluctuations of the internal wavefunction the G-L free-energy functional $F\{\Delta(\mathbf{R}, \mathbf{k})\}$ for the order parameter $\Delta(\mathbf{R}, \mathbf{k}) = \int d\mathbf{r} \Delta(\mathbf{R} - \mathbf{r}/2, \mathbf{R} + \mathbf{r}/2) \exp\{-i\mathbf{k}\mathbf{r}\}$ has a more complicated form

$$F\{\Delta(\mathbf{R}, \mathbf{k})\} = \sum_k \int d\mathbf{R} \{ A_{\mathbf{k}} |\Delta(\mathbf{R}, \mathbf{k})|^2 + B_{\mathbf{k}} |\Delta(\mathbf{R}, \mathbf{k})|^2 \}$$

$$+ \frac{1}{2M} |\partial_{\mathbf{k}} \Delta(\mathbf{R}, \mathbf{k})|^2 + \frac{1}{2m_{\mathbf{k}}} |\partial_{\mathbf{R}} \Delta(\mathbf{R}, \mathbf{k})|^2 \}, \quad (46)$$

where $M = r_c^2 V_0$ and

$$A_{\mathbf{k}} = \frac{1}{V_0} - \frac{\tanh(\beta\xi_{\mathbf{k}}/2)}{2\xi_{\mathbf{k}}}$$

$$\frac{1}{2m_{\mathbf{k}}} = \frac{\beta^2 v_F^2 \sinh(\beta\xi_{\mathbf{k}}/2)}{32\xi_{\mathbf{k}} \cosh^3(\beta\xi_{\mathbf{k}}/2)}$$

$$B_{\mathbf{k}} = \frac{\tanh(\beta\xi_{\mathbf{k}}/2)}{8\xi_{\mathbf{k}}^3} - \frac{\beta}{16\xi_{\mathbf{k}}^2 \cosh^3(\beta\xi_{\mathbf{k}}/2)}. \quad (47)$$

The term with the partial derivative $\partial_{\mathbf{k}}$ is a direct consequence of the long-ranged pairing potential, and it describes fluctuations of the internal Cooper pair wavefunction. The effect of these fluctuations, described by the free-energy functional in Eq. (46), was studied in the Hartree-Fock approximation in the limit $r_c \gg \xi$, and a large reduction of the mean-field critical temperature is found

$$T_c \sim \frac{T_c^{MF}}{(r_c/\xi)}. \quad (48)$$

The latter result means that T_c in the long-range superconductors is *controlled by thermal fluctuations of collective modes* which is in contrast with the 3D short-range (BCS-like) superconductivity, where phase fluctuations dominate but only slightly suppress T_c^{MF} . In the temperature interval $T_c < T < T_c^{MF}$, the system with long-range pairing force is in PG regime where the electrons are paired but there is *no long-range phase coherence*. The latter sets in only at $T < T_c$. We shall not further discuss this interesting approach but only stress that it can be generalized by including repulsive interactions, for instance due to spin fluctuations and residual Coulomb interaction. This will be studied elsewhere [83].

In conclusion, FSP in EPI gives rise to the long-range pairing (in real space) which produces internal fluctuations of Cooper pairs. These are soft excitonic modes of the internal Cooper wave function which may reduce T_c strongly. In the region $T_c < T < T_c^{MF}$ PG phase is realized. In this approach PG possess the same symmetry as the superconducting gap. Since the cuprates are systems near the Mott-Hubbard insulating state due to strong correlations, this is responsible for very small phase stiffness and strong phase fluctuations. Additionally, strong correlations (in conjunction with the long-range Madelung interaction due to ionic-metallic structure of cuprates) make EPI long-ranged, which causes strong internal fluctuations of Cooper pairs. In a realistic theory both type of fluctuations must be taken into account [83].

VII. SUMMARY AND CONCLUSIONS

A number of experiments, such as optics (IR and Raman), transport, tunnelling, ARPES, neutron scattering, etc. give convincing evidence that EPI in cuprates is sufficiently strong and contributes to pairing. The ARPES experiments made a breakthrough in the physics of cuprates, since they allowed a direct study of quasi-particle properties, such as self-energy effects. These experiments also give evidence for the presence of strong correlations which modify EPI not only quantitatively but also qualitatively. The most spectacular result of

the EPI theory in strongly correlated systems is the appearance of FSP in EPI, as well as in other charge scattering processes such as the residual Coulomb interaction, scattering on non-magnetic impurities - the *FSP theory* [30], [31], [32], [7]. FSP is especially pronounced at lower doping δ . This fundamental result allows us to resolve at least qualitatively a number of experimental facts which can not be explained by the old theory based on isotropic Migdal-Eliashberg equations for EPI. The most *important predictions of the FSP theory of EPI* and other charge scattering processes are: (1) the transport coupling constant λ_{tr} (entering the resistivity, $\varrho \sim \lambda_{tr}T$) is *much smaller* than the pairing λ , i.e. $\lambda_{tr} < \lambda/3$; (2) the strength of pairing in cuprates is basically *due to EPI*, while the residual Coulomb repulsion (including spin-fluctuations) *triggers* d-wave pairing; (3) d-wave pairing is very *robust* in presence of non-magnetic impurities with FSP; (4) the nodal kink in the quasiparticle spectrum is *not-shifted* in the superconducting state, while the anti-nodal singularity is shifted by the maximal superconducting gap; (5) there is a collapse of the elastic impurity scattering rate in the superconducting state at the anti-nodal point giving rise to sharpening of the ARPES features; (6) internal fluctuations of Cooper pairs, due to the long-ranged scattering potential, can additionally increase the temperature range of the PG effect.

We point out the following two facts that stem from the theoretical analysis: (i) FSP in EPI of strongly correlated systems is a general phenomenon and it *affects electron coupling to all phonons*; (ii) the existence of FSP in EPI is confirmed numerically by Monte Carlo calculations for the Hubbard-Holstein model with finite U [62], by exact diagonalization [60], as well as by some other methods [63]. Thanks to these numerical results which confirm the correctness of the FSP theory [30], [31], [32], [7], a number of new results were recently reported [84], which are in favor of strong EPI interaction and the FSP theory.

We would like to stress that the calculation of the momentum dependent EPI coupling constant $\lambda_{\mathbf{k}}$ in cuprates is a big challenge for the theory. The latter must include properly: (a) *ionic-metallic coupling* due to the long-range Madelung energy as well as *covalent coupling*, and (b) *strong electronic correlations*. From this point of view, one can say that we still do not have a quantitative microscopic theory of pairing in cuprates.

In the last several years a large number of papers has been devoted to the study of spin-fluctuation interaction as a mechanism of pairing in cuprates. In spite of much effort led by the greatest authorities in the field, which have opened some new research directions in the theory of electron magnetism, there is no theoretical evidence for the effectiveness of non-phononic mechanism of pairing. Moreover, recent numerical calculations [14] show that probably there is no high-temperature superconductivity in the t-J model. If it exists at all, its T_c is extremely low. Finally, numerical calculations in the Hubbard model [13] show that the repulsive Hubbard interaction is unfavorable for high-temperature superconductivity, contrary to the attractive interaction which favors it.

In conclusion, we would like to stress again: in order to explain the high critical temperature in cuprates, it is necessary to include EPI which is renormalized by strong electronic correlations. We hope that in the future such projects will be supported much more.

Acknowledgement. I express my deep gratitude and respect to Vitalii Lazarevich Ginzburg for his support over many years, for sharing his deep understanding of physics generously with us - his students, collaborators and friends. I am thankful to Oleg V. Dolgov and Evgenii G. Maksimov for collaboration and numerous elucidating discussions on superconductivity theory. I am thankful to Ivan Božović for valuable discussions on optical properties of oxides, for his scientific support, for careful reading of the paper and useful comments.

[1] The members of the Ginzburg group, by including the present author as well as many others, used to call Vitalii Lazarevich Ginzburg simply VL. This is a way of expressing our love, devotion and respect to him. Some of us (probably most of us) by calling him VL have been expressing our wish to be closer friends of this great and remarkable man.

[2] *High Temperature Superconductivity*, eds. V. L. Ginzburg and D. A. Kirzhnitz, Consultant Bureau, New York, London, 1982

[3] J. G. Bednorz, K. A. Müller, Z. Phys. **B 64**, 189 (1986)

[4] M. L. Cohen, P. W. Anderson, *Superconductivity in d and f band metals*, AIP Conference Proceedings (ed. D. H. Douglass) New York, p.17 (1972)

[5] D. A. Kirzhnitz, in *High Temperature Superconductivity*, eds. V. L. Ginzburg and D. Kirzhnitz, Consultant Bureau New York, London, 1982

[6] O. V. Dolgov, D. A. Kirzhnitz, E. G. Maksimov, Rev. Mod. Phys. **53**, 81 (1981)

[7] M. L. Kulić, Phys. Reports **338**, 1-264 (2000)

[8] E. G. Maksimov, Uspekhi Fiz. Nauk **170**, 1033 (2000); V. L. Ginzburg, E. G. Maksimov, Physica C **235-240**, 193 (1994); Superconductivity (in Russian) **5**, 1505 (1992)

[9] I. Božović, Phys. Rev. **B 42**, 1969 (1990)

[10] P. A. Lee, N. Nagaosa, C.-G. Wen, Rev. Mod. Phys. **78**, 17 (2006)

[11] M. L. Kulić, *AIP Conference Proceedings Volume 715*, 75 (2004), Lectures On The Physics Of Highly Correlated Electron Systems; M. L. Kulić, O. V. Dolgov, phys. stat. solidi (b) **242**, 151 (2005)

[12] A. J. Millis, H. Monien, D. Pines, Phys. Rev. **B 42**, 167 (1990); P. Monthoux and D. Pines, Phys. Rev. Lett. **69**, 961 (1992); Phys. Rev. B **47**, 6069 (1993); R. J. Radtke, K. Levin, H. -B. Schüttler and M. R. Norman, Phys. Rev. B **48**, 15957 (1993); D. Pines, preprint CNSL Newsletter, LALP-97-010, No. 138, June 1997; Physica **B 163**, 78

(1990)

[13] D. J. Scalapino, S. R. White, S. C. Zhang, Phys. Rev. Lett. **68**, 2830 (1992)

[14] L. Pryadko, S. Kivelson, O. Zachar, Phys. Rev. Lett. **92**, 067002 (2004)

[15] D. J. Scalapino, Physics Reports **250**, 329 (1995)

[16] J. F. Franck, in *Physical Properties of High Temperature Superconductors V*, ed. D. M. Ginsberg, (World Scientific, Singapore, 1994); Physica **C 282-287**, 198 (1997)

[17] S. I. Vedeneev, A. G. M. Jansen, A. A. Tsvetkov, P. Wyder, Phys. Rev. **B 51**, 16380 (1995); C. C. Tsuei, J.R. Kirtley, C. C. Chi, L. S. Yu-Jahnes, A. Gupta, T. Shaw, J. Z. Sun, M. B. Ketchen, Phys. Rev. Lett., **73**, 593 (1994); C. C. Tsuei, J. R. Kirtley, M. Rupp, A. Gupta, J. Z. Sun, T. Shaw, M. B. Ketchen, C. Wang, Z. F. Ren, J. H. Wang, M. Bhushan Science **27**, 329 (1996); C. C. Tsuei, J. R. Kirtley, J. Low Temp. Phys., **107**, 445 (1997); C. C. Tsuei, J. R. Kirtley, Z. F. Ren, J. H. Wang, H. Raffy, Z. Z. Li, Nature **387**, 481 (1998); C. C. Tsuei et al., cond-mat/0402655 (2004)

[18] K. McElroy, R. W. Simmonds, J. E. Hoffman, D. H. Lee, K. M. Lang, J. Orenstein, H. Eisaki, S. Uchida, J. C. Davis, Nature **422**, 592 (2003); J. Lee et al., Bull. Am. Phys. Soc. **50**, 299 (2005); J. C. Davis et al., Bull. Am. Phys. Soc. **50**, 1223 (2005)

[19] J. Hofer, K. Conder, T. Sasagawa, Guo-meng Zhao, M. Willemin, H. Keller, and K. Kishio, Phys. Rev. Lett. **84**, 4192 (2000); J. Hofer, K. Conder, T. Sasagawa, Guo-meng Zhao, T. Schneider, J. Karpinski, M. Willemin, H. Keller, and K. Kishio, J. Supercond. **13**, 963 (2000); T. Schneider, phys. stat. sol. (b) **242**, 58 (2005)

[20] A. Lanzara et al., Nature **412**, 510 (2001)

[21] A. Damascelli, Z. Hussain, Z. -X. Shen, Rev. Mod. Phys. **75**, 473 (2003); J. C. Campuzano, M. R. Norman, M. Randeria, cond-mat/0209476 (2002)

[22] A. Bansil, M. Lindros, Phys. Rev. Lett. **83**, 5154 (1999)

[23] T. Cuk et al., Phys. Rev. Lett. **93**, 117003 (2004)

[24] G.-H. Gweon et al., Nature **430**, 187 (2004)

[25] H. Krakauer, W. E. Picket, R. E. Cohen, Phys. Rev. **B 47**, 1002 (1993)

[26] G. L. Zhao et al., Phys. Rev. **B 50**, 9511 (1994)

[27] C. Falter, M. Klenner, G. A. Hoffmann, Phys. Rev. **B 55**, 3308 (1997); Phys. Stat. Sol. (b) **209**, 235 (1998); Phys. Rev. **B 57**, 14 444 (1998)

[28] H. J. Kaufmann, O. V. Dolgov, E. K. Salje, Phys. Rev. **B 58**, 9479 (1998)

[29] P. Samuely, N. L. Bobrov, A. G. N. Jansen, P. Wyder, S. N. Barilo, S. V. Shiryaev, Phys. Rev. **B 48**, 13904 (1993); P. Samuely, P. Szabo, A. G. N. Jansen, P. Wyder, J. Marcus, C. Escribe-Filippini, M. Afronte, Physica **B 194-196**, 1747 (1994)

[30] M. L. Kulić, R. Zeyher, Phys. Rev. **B 49**, 4395 (1994); Physica **C 199-200**, 358 (1994); Physica **C 235-240**, 358 (1994)

[31] R. Zeyher, M. L. Kulić, Phys. Rev. **B 53**, 2850 (1996)

[32] R. Zeyher, M. L. Kulić, Phys. Rev. **B 54**, 8985 (1996); M. L. Kulić and R. Zeyher, Mod. Phys. Lett. **B 11**, 333 (1997)

[33] A. I. Lichtenstein, M. L. Kulić, Physica **C 245**, 186 (1995)

[34] Ph. Bourges, in *The Gap Symmetry and Fluctuations in High Temperature Superconductors*, J. Bok, G. Deutscher, D. Pavuna, S. A. Wolf, Eds. (Plenum, New York, 1998), pp. 349-371; preprint cond-mat/9901333 (1999)

[35] H. -Y. Kee, S. Kivelson, G. Aeppli, Phys. Rev. Lett. **88**, 257002 (2002)

[36] M. L. Kulić, I. M. Kulić, Physica **C 391**, 42 (2003)

[37] M. L. Kulić, O. V. Dolgov, Phys. Rev. **B 71**, 092505 (2005)

[38] O. V. Dolgov, E. G. Maksimov, S. V. Shulga, in *Electron-Phonon Interaction in Oxide Superconductors*, World Scien., p.30 (1991)

[39] S. V. Shulga, O. V. Dolgov, E. G. Maksimov, Physica **C 178**, 266 (1989)

[40] E. G. Maksimov, D. Y. Savrasov, S. Y. Savrasov, Physics - Uspekhi **40**, 337 (1997)

[41] H. J. Kaufmann, Ph. D. Thesis, Uni. Cambridge, February 1999

[42] E. Schachinger, J. P. Carbotte, Phys. Rev. **B 64**, 094501 (2001)

[43] A. V. Puchkov, D. N. Basov, T. Timusk, J. Phys.: Condens. Matter **8**, 10049 (1996); J. Hwang, T. Timusk, G. D. Gu, Nature **427**, 714 (2004); M. Norman, Nature **427**, 692 (2004).

[44] A. V. Boris et al., Science **304**, 708 (2004).

[45] A. E. Karakozov, E. G. Maksimov, O. V. Dolgov, Sol. St. Comm. **124**, 119 (2002)

[46] I. Božović, J. H. Kim, J. S. Harris, Jr., C. B. Eom, J. M. Phillips, J. T. Cheung, Phys. Rev. Lett., **73**, 1436 (1995)

[47] S. N. Rashkeev and G. Wendin, Phys. Rev. **B 47**, 11603 (1993)

[48] Q. Huang, J. F. Zasadinski, N. Tralshawala, K. E. Gray, D. Hinks, J. L. Peng and R. L. Greene, Nature (London) **347**, 389 (1990)

[49] V. J. Emery, S. Kivelson, Nature (London) **374**, 434 (1995)

[50] X. J. Zhou et al., Phys. Rev. Lett. **95**, 117001 (2005)

[51] P. W. Anderson, Science **235**, 1196 (1987)

[52] A. E. Ruckenstein, S. Schmit-Rink, Phys. Rev. **B 38**, 7188 (1988); due to some subtle effect missed in this paper the $1/N$ expansion of the self-energy could not be proven. This was successfully done in [30], where the self-energy is expressed in terms of the charge- and spin-vertex functions. The latter functions obey $1/N$ expansion.

[53] F. Manchini, A. Avella, Advances in Physics, **53**, 537 (2004)

[54] A. Greco, R. Zeyher, Europh. Lett., **35**, 115 (1996); R. Zeyher, A. Greco, Z. Phys. **B 104**, 737 (1997)

[55] I. I. Mazin, S. Rashkeev, S. Y. Savrasov, Phys. Rev. **B 42**, 366 (1990)

[56] T. Jarlborg, Solid State Comm., **67**, 297 (1988); **71**, 669 (1989)

[57] S. Barišić, I. Batistić, Europhys. Lett. **8**, 765 (1989); R. Zeyher, Z. Phys. **B 80**, 187 (1990)

[58] W. Weber, Phys. Rev. Lett. **58**, 2154 (1987); W. Weber, L. F. Mattheiss, Phys. Rev. **B 37**, 599 (1988); A. Alligia, M. L. Kulić, V. Zlatić and K. H. Bennemann, Sol. State Comm. **65**, 501 (1988)

[59] A. A. Abrikosov, Physica **C 244**, 243 (1995); J. Ruvalds et al., Phys. Rev. B **51**, 3797 (1995); G. Santi, T. Jarlborg, M. Peter, M. Weger, J. of Supercond. **8**, 215 (1995); M. Weger, B. Barbelini, M. Peter, Z. Phys. **B 94**, 387 (1994); M. Weger, M. Peter, L. P. Pitaevskii, Z. Phys. **B 101**, 573 (1996); M. Weger, J. of Supercond. **10**, 435 (1997)

[60] T. Tohyama, P. Horsch and S. Maekawa, Phys. Rev. Lett. **74**, 980 (1995)

- [61] C. C. Tsuei, J. R. Kirtley, Rev. Mod. Phys. **72**, 969 (2000)
- [62] Z. B. Huang, W. Hanke, E. Arrigoni, D. J. Scalapino , Phys. Rev. **B 68**, 220507(R) (2003)
- [63] E. Cappelluti, B. Cerruti, L. Pietronero, Phys. Rev. **B 69**, 161101(R) (2004); E. Koch, R. Zeyher, Phys. Rev. **B 70**, 094510 (2004)
- [64] J. H. Kim and Z. Tešanović, Phys. Rev. Lett. **71**, 4218 (1993); Ju H. Kim, K. Levin, R. Wentzovitch and A. Aurbach, Phys. Rev. **B 44**, 5148 (1991); M. Grilli and C. Castellani, Phys. Rev. **B 50**, 16880 (1994); Phys. Rev. Lett. **74**, 1488 (1995)
- [65] W. Meevasana et al., cond-mat/0602508 (2006)
- [66] X. J. Zhou et al. , Nature (London) **423**, 398 (2003)
- [67] E. G. Maksimov, O. V. Dolgov, M. L. Kulić, Phys. Rev. **B 72**, 212505 (2005)
- [68] M. L. Kulić, V. Oudovenko, Solid State Comm. **104**, 731 (1997)
- [69] M. L. Kulić, O. V. Dolgov, Phys. Rev. **B**60, 13062(1999)
- [70] L. Zhu, P. J. Hirschfeld, D. J. Scalapino, Phys. Rev. **70**, 214503 (2004)
- [71] E. Abrahams, C. M. Varma, Proc. Natl. Acad. Sci. U.S.A. **97**, 5714 (2000)
- [72] H.-Y. Kee, Phys. Rev. **B** 64, 012506 (2001)
- [73] R. Ferenbacher, Phys. Rev. Lett. **77**, 1849 (1996); R. Ferenbacher, M. Norman, Phys. Rev. **B** 50, 3495 (1994)
- [74] S. K. Tolpygo et al., Phys. Rev. **B** 53, 12454 (1996); ibid 12462 (1996)
- [75] P.B. Allen, B. Mitrović, Solid State Physics, ed. H. Ehrenreich, F. Seitz, D. Turnbull, Academic, New York, **V 37**, p. 1, (1982)
- [76] C. Grimaldi, L. Pietronero, S. Sträßer, Phys. Rev. **B 52**, 10516 (1995); ibid **B 52**, 10530 (1995)
- [77] J. R. Engelbracht, M. Randeria, C. A. R. Sa de Melo, Phys. Rev. **B 55**, 15 153 (1997)
- [78] A. Junod, A. Erb, C. Renner, Physica **C 317**, 333 (1999)
- [79] M. V. Sadovskii, Physics-Uspekhi **44** (5), 515 (2001)
- [80] O. V. Danylenko, O. V. Dolgov, M. L. Kulić, V. Oudovenko, Europ. Phys. Jour. **B 9**, 201 (1999)
- [81] G. Varelogiannis, Phys. Rev. **B 57**, 13743 (1998); ibid **B 570**, 15974 (1994)
- [82] K. Yang, S. L. Sondhi, Phys. Rev. **B** **62**, 11 778 (2000)
- [83] M. L. Kulić, in preparation
- [84] A. W. Sandvik, D. J. Scalapino, N. E. Bickers, Phys. Rev. **B** **69**, 094523 (2004); P. Barone et al., Phys. Rev. **B** **73**, 085120 (2006); S. Fratini, S. Ciuchi, Phys. Rev. **B** **72**, 235107 (2005); S. Isihara, N. Nagaosa, Phys. Rev. **B** **69**, 144520 (2004)